Report No. 113-30
Part III

# TWO PHASE FLOW AND HEAT TRANSFER IN POROUS BEDS UNDER VARIABLE BODY FORCES



Final Report
Part III

By James V. French, Jr. and Harold R. Henry

Project Director:

Harold R. Henry, Ph.D.
Professor of Engineering Mechanics
University of Alabama

Submitted to

George C. Marshall Space Flight Center
National Aeronautics and Space Administration
Huntsville, Alabama

Contract No. NAS8-21143
University of Alabama No. 22-6560

November 1969
Bureau of Engineering Research
University of Alabama

Report No. 113-30
Part III

# TWO PHASE FLOW AND HEAT TRANSFER IN POROUS BEDS UNDER VARIABLE BODY FORCES

Final Report
Part III

By James V. French, Jr. and Harold R. Henry

Project Director:

Harold R. Henry, Ph.D.
Professor of Engineering Mechanics
University of Alabama

Submitted to

George C. Marshall Space Flight Center
National Aeronautics and Space Administration
Huntsville, Alabama

Contract No. NAS8-21143
University of Alabama No. 22-6560

November 1969
Bureau of Engineering Research
University of Alabama

TABLE OF CONTENTS

LIST OF FIGURES

## LIST OF SYMBOLS

| | | |
|---|---|---|
| a | Wave Amplitude | ft |
| A | Dimensionless Wave Amplitude | |
| b | Average Tube Radius | ft |
| B | Dimensionless Pressure Function | |
| c | Half Wavelength | ft |
| C | Dimensionless Half Wavelength | |
| E | Dimensionless Time Increment | |
| $f_r$ | Radial Body Force | $lb/ft^3$ |
| $f_z$ | Axial Body Force | $lb/ft^3$ |
| $F_z$ | Dimensionless Axial Body Force | |
| H | Dimensionless Grid Size | |
| p | Pressure | $lb/ft^2$ |
| P | Dimensionless Pressure | |
| Q | Volumetric Flowrate | $ft^3/sec$ |
| r | Radial Coordinate | ft |
| R | Dimensionless Radial Coordinate | |
| S | Dimensionless Stream Function | |
| t | Time | sec |
| T | Dimensionless Time | |
| u | Dimensionless Axial Velocity | |
| U | Average Axial Velocity | ft/sec |

| | | |
|---|---|---|
| $v$ | Dimensionless Radial Velocity | |
| $V_T$ | Dimensionless Bubble Velocity | |
| $v_r$ | Radial Velocity | ft/sec |
| $v_z$ | Axial Velocity | ft/sec |
| W | Dimensionless Vorticity | |
| X | Transformed Axial Coordinate | |
| Y | Transformed Radial Coordinate | |
| z | Axial Coordinate | ft |
| Z | Dimensionless Axial Coordinate | |
| RN | Reynolds Number | |
| WN | Weber Number | |
| $\alpha$ | Fraction of Grid Width | |
| $\beta$ | Fraction of Grid Width | |
| $\zeta$ | Vorticity | $sec^{-1}$ |
| $\theta$ | Slope of Bubble Surface | radians |
| $\lambda$ | Proportionality Constant | |
| $\mu$ | Dynamic Viscosity | $lb\text{-}sec/ft^2$ |
| $\nu$ | Kinematic Viscosity | $ft^2/sec$ |
| $\rho$ | Density | $lb\text{-}sec^2/ft^4$ |
| $\rho_1$ $\rho_2$ | Radii of Curvature | ft |
| $\sigma$ | Surface Tension | lb/ft |
| $\tau$ | Viscous Stress | $lb/ft^2$ |
| $\phi$ | Angular Coordinate | radians |
| $\psi$ | Stream Function | $ft^3/sec$ |
| $\omega$ | Relaxation Factor | |
| $\Omega$ | Pressure Function | $lb/ft^2$ |

# PREFACE

This is Part III of a seven part final report under contract No. NAS8-21143 between the George C. Marshall Space Flight Center and the University of Alabama. This report includes the results of analytical and computational work on an idealized geometrical and mathematical model of two-phase flow in porous media. The model consists of flow of a viscous liquid in which spherical gas bubbles are moving along the centerline of a wavy wall tube.

This analytic work was motivated by results obtained from the experimental pilot model channel and from the breadboard channel in which individual gas bubbles were observed by high speed photography to be moving through well defined, but tortuous, channels. The mathematical model used herein represents many of the features of the flow but cannot simulate the tortuosity of the flow channels experienced in the actual porous media.

This work is based on the fundamental equations of fluid mechanics which are expressed in dimensionless form by the proper use of reference variables.

These results show that a high speed digital computer can be used as a powerful tool in problems of this nature.

Results are plotted in the form of streamline flow patterns with Reynolds number ranging from near zero to fifty. The importance of the inertial effect is indicated by the eddy formation at the higher Reynolds numbers. The effect of the Weber number is also discussed.

The trends in pressure drop are similar to the experimental data but differ in magnitude because of difference in tortuosity of flow.

# I INTRODUCTION

## Motivation for Study

Computational fluid mechanics has emerged in recent years as a new tool which holds great promise for the study of all types of fluid phenomena. Although it can not be considered as a replacement for either purely analytical study or laboratory experimentation, it has increased the flexibility of fluid mechanics investigations. The principal appeal is that solutions to more complex flows can be obtained than with purely analytical methods while retaining complete control over the pertinent flow parameters. Beside the fact that the numerical solutions are of great value of themselves, they may also lead to greater insight to a given problem, which would result in more effective experimentation or to better analytical approaches.

In this study it is proposed to apply some of the techniques of computational fluid mechanics to a flow situation in which three fluid effects interact in a rather general way; viscosity, inertia and surface tension. Consider a flow in which a series of gas bubbles moves along the centerline of a tube in which a viscous liquid flows. The cross sectional area of the tube changes in a

smooth periodic fashion with distance along the centerline. The liquid is Newtonian and the bubble surface exhibits surface tension. The range of Reynolds numbers to be considered is such that the viscous and inertia effects in the liquid are of the same order of importance. Although it might be possible to find this situation in a significant physical system, this type of flow is proposed only as a model which is used to study the interaction of these fluid effects. However, it is hoped that the results of this work will lead to at least a better qualitative understanding of flows in which viscosity, inertia and surface tension are present. One such case, which provided the principal motivation for undertaking the study, is the two phase flow of gas and liquid in porous media. Experimental studies with which the author has been associated [13]*, [14] and other investigations show that fundamental knowledge is needed as to the motion of gas bubbles moving through a porous matrix with a viscous liquid. In this case the flow is governed by viscosity since solid boundaries are present. The tortuosity of the flow paths causes continual accelerations so that fluid inertia should be considered. Finally, the surface tension of the gas-liquid interface determines the bubble shapes.

---

*Numbers in square brackets refer to references listed at the end of the paper.

Even limited theoretical results would be of aid in planning and analyzing the laboratory experiments in this field.

The study of the motion of bubbles is a very broad subject since a variety of flow patterns may be produced depending on such considerations as the size of the bubbles, the magnitude of surface tension, the viscosity of the liquid and the presence of walls. Although, no reference has been found in the literature of work which considers the interaction of a bubble with a viscous liquid to the extent of this study or which uses finite differences for fluid dynamics problems involving surface tension, a summary is presented of some of the relevant papers concerning the motion of bubbles, along with others treating the numerical solution to incompressible, viscous flows.

## Related Work

The modern interest in the motion of bubbles can be said to have begun with the work of Davies and Taylor in 1949 [11] in which a combination of experimental and theoretical means was used to determine a relationship for the rise velocity of large spherical cap bubbles in infinite liquids. Haberman and Morton [17] in 1953 made an extensive experimental investigation of the rise of bubbles through various liquids of infinite extent. The papers of Saffman [31], Hartunian and Sears [23], and Davenport, et al. [10] were also concerned with the rise

of bubbles in infinite liquids. Walters and Davidson [34], [35] have studied the initial motion of gas bubbles in an inviscid liquid. Collins [9] collected experimental data for a large bubble rising in a cylindrical container and made an analysis based on irrotational flow about an axisymmetric doublet which is shown to agree with experimental data for limiting cases, but the results involve ratios of infinite series which are replaced with a semi-empirical expression based on experimental data.

In the area of purely analytical solutions to the motion of a bubble Rybczynski and Hadamard [3], independently of one another, found a solution for translation of a fluid sphere neglecting fluid inertia. Their results can be applied to spherical bubbles if the Reynolds numbers of the flow both outside and inside the bubble is very close to zero. Taylor and Acrivos [32] extended this work to include the effects of slight deformation from a sphere with small inertia forces. Their procedure was patterned after the one used by Proudman and Pearson [29] to extend the Stokes solution for flow about a sphere from zero to low Reynolds numbers.

In contrast to these works which assume small Reynolds numbers, Moore [26], [27] has considered the rise of gas bubbles by assuming that the flow is irrotational about the bubble except in a thin region near the surface in which the flow adjusts itself to a zero tangential stress at the surface. The principal restriction is that

the Reynolds number be large, yet still below the separated flow limit and that the Weber number be small. Moore also considered a similar problem for ellipsoidal bubbles [28]. Harper and Moore considered the effect of temperature gradients in a bubble surface [21] and later a spherical liquid drop moving in a fluid of comparable density and viscosity [22].

The purely analytical treatments described above are quite significant in the advancement of understanding, but most require rather involved order of magnitude arguments which are difficult to justify with experimental results due to the uncertainty caused by such factors as surface contaminants in the gas-liquid interface. The solution by numerical means of the problems considered in the above papers could serve the purpose of checking the order of magnitude assumptions without this uncertainty.

This situation is similar to the problems encountered in analytically extending Stokes' solution for zero Reynolds number flow about a solid sphere to higher Reynolds numbers. Early attempts by Whitehead and Oseen were unsatisfactory [3]. Only recently has such an analytical extension been carried out by Proudman and Pearson [29] by a matching of separate asymptotic solutions near and far from the body. Although this analysis is rather long and highly mathematical, it is still limited to very small Reynolds numbers in its range of applicability. However, this problem has been solved numerically, with good agreement to experimental

results, using finite difference approximations to the vorticity transport equations, for Reynolds numbers from zero up to 40, where separation occurs [24], [25], [30]. Purely analytical methods have yet to approach these Reynolds numbers for flow about a sphere.

Numerical methods of solution for the complete Navier-Stokes equations for incompressible, viscous flow have been vigorously applied by Fromm, Harlow and Welch of the University of California at Low Alamos, New Mexico. The problems studied by this group include the von Karman wake behind a rectangular cylinder and wave motion of a free surface. Some of the notable papers of this group as listed in the references are [15], [16], [18], [19], [20]. A large part of the work in this study has been adapted from the above papers and that of Thompson [33].

## Scope of Study

The present investigation considers three classes of problems of low Reynolds numbers flow in a tube with periodically varying cross-sectional area: (1) steady state flow of liquid only, (2) time-dependent flow of liquid only and (3) time-dependent flow with gas bubbles. The Reynolds number based on average velocity and average tube radius ranges from zero up to two hundred. The gas bubbles are restricted to maintain a constant volume

and to be equally apaced along the centerline of the tube with the distance between centers one wavelength of the tube.

The equations governing the flow of a liquid with arbitrarily shaped bubbles are developed. A coordinate transformation is used which simplifies the boundary geometry. Finite difference approximations to the transformed equations are used to obtain numerical solutions. Typical numerical results are presented for steady state flow of liquid only. Although numerical solutions for arbitrary bubble shapes were not obtained, results for the case of spherical bubbles are presented.

## II MATHEMATICAL STATEMENT OF THE PROBLEM

The fluid flow problem under consideration is a two phase flow consisting of a viscous liquid flowing inside a wavy wall tube and a series of gas bubbles moving along the centerline of the tube. In this chapter the equations of motion governing the flow along with appropriate boundary conditions and constraints will be stated.

### Physical Model

The term "wavy wall tube" as used in this paper means a tube which is circular in any given cross section but has its radius varying as a smooth periodic function of distance along the axis. Such a tube could be formed by revolving a periodic function about a line outside of the wave and parallel to its mean. See Figure 1 for a cross section view showing the tube geometry and location of typical bubbles. We will consider one wavelength of such a wavy wall tube which extends to infinity in each direction.

The liquid phase flowing in the tube is assumed to have a constant volumetric flow rate caused by some external source. The liquid is further assumed to be incompressible and Newtonian. The liquid velocity at the wall will be zero,

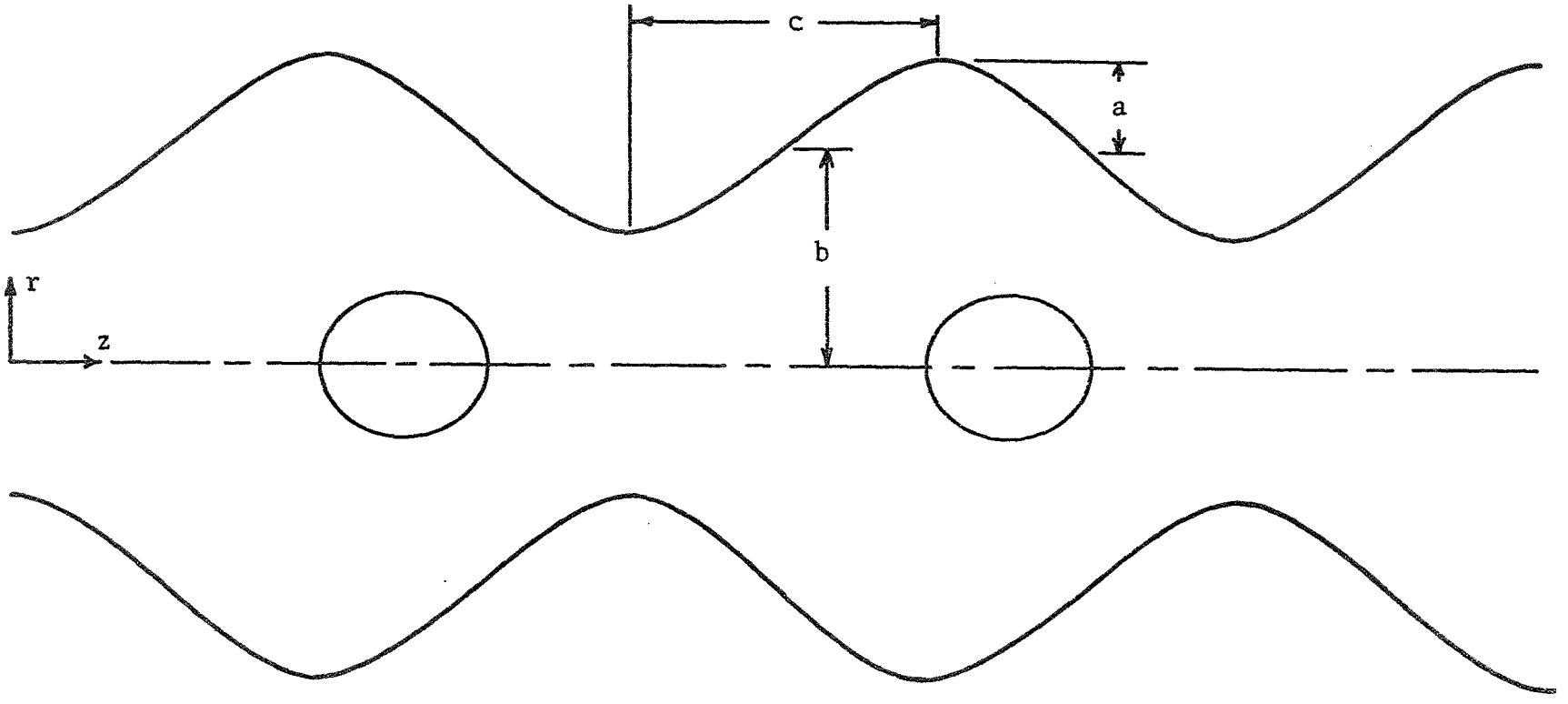


Figure 1. Cross Section of Wavy Wall Tube with Gas Bubbles along Centerline

The gas bubbles are restricted to be centered in the tube with the distance between bubble centers being one wavelength of the tube. In general, the bubbles' shape and velocity are functions of time and displacement, but all bubbles are identical at a given time due to the periodicity of the flow. The mass of gas contained in a bubble is constant so that no transfer of mass occurs across the bubble interface. The gas is assumed to have a constant volume for the range of pressure variations considered and gas body forces are neglected compared to those in the liquid. The problem is formulated with arbitrary bubble shapes, but numerical results were obtained only for spherical bubbles.

## Equations of Motion for the Liquid Phase

The flow regime considered is that of low Reynolds numbers, from zero to approximately two hundred. Except for zero Reynolds number, the viscous and inertia effects are of the same order of importance and the equations of motion are the full Navier-Stokes equations. Since the bubbles are centered and the tube is circular, the flow is assumed to axisymmetric. Using the cylindrical polar coordinates $r, \phi$, z with z along the tube axis and noting that under the assumption of axisymmetric flow, the velocity in the $\phi$-direction is zero and all partial derivatives with respect to $\phi$ are zero, the equations of motion for the radial and axial directions are [7]

$$\frac{\partial v_r}{\partial t} + v_r \frac{\partial v_r}{\partial r} + v_z \frac{\partial v_r}{\partial z} = \frac{1}{\rho} f_r - \frac{1}{\rho} \frac{\partial p}{\partial r} + \nu\left(\frac{\partial^2 v_r}{\partial r^2} + \frac{1}{r} \frac{\partial v_r}{\partial r} - \frac{v_r}{r^2} + \frac{\partial^2 v_r}{\partial z^2}\right), \tag{1}$$

$$\frac{\partial v_z}{\partial t} + v_r \frac{\partial v_z}{\partial r} + v_z \frac{\partial v_z}{\partial z} = \frac{1}{\rho} f_z - \frac{1}{\rho} \frac{\partial p}{\partial z} + \nu\left(\frac{\partial^2 v_z}{\partial r^2} + \frac{1}{r} \frac{\partial v_z}{\partial r} + \frac{\partial^2 v_z}{\partial z^2}\right), \tag{2}$$

where $v_r$ is the component of velocity in the r-direction, $v_z$ is the component of velocity in the z-direction, $\rho$ is density, $f_r$ and $f_z$ are components of body force per unit volume, p is pressure, $\nu$ is kinematic viscosity, and t is time. The body force in the radial direction will be taken to be zero here. To equations (1) and (2) we must add the equation of continuity of an incompressible fluid in axisymmetric flow,

$$\frac{\partial v_r}{\partial r} + \frac{v_r}{r} + \frac{\partial v_z}{\partial z} = 0. \tag{3}$$

The equation of continuity may be satisfied by introducing the stream function $\psi$, such that

$$v_r = -\frac{1}{r} \frac{\partial \psi}{\partial z}, \quad v_z = \frac{1}{r} \frac{\partial \psi}{\partial r}. \tag{4),(5}$$

Also we introduce the vorticity, $\zeta$, with

$$\zeta = \frac{\partial v_r}{\partial r} - \frac{\partial v_z}{\partial r}. \tag{6}$$

We consider the vorticity to be a scalar since the flow is axisymmetric and only the magnitude of $\zeta$ is important. By differentiating equation (1) with respect to z and equation (2) with respect to r and subtracting the results and putting in $\zeta$ and $\psi$ we are left with

$$\frac{\partial \zeta}{\partial t} - \frac{\partial \psi}{\partial z}\frac{\partial}{\partial r}\left(\frac{\zeta}{r}\right) + \frac{1}{r}\frac{\partial \psi}{\partial r}\frac{\partial \zeta}{\partial z} = \nu\left[\frac{\partial^2 \zeta}{\partial r^2} + \frac{\partial}{\partial r}\left(\frac{\zeta}{r}\right) + \frac{\partial^2 \zeta}{\partial z^2}\right], \qquad (7)$$

and from equation (6)

$$\zeta = -\frac{1}{r}\left(\frac{\partial^2 \psi}{\partial r^2} - \frac{1}{r}\frac{\partial \psi}{\partial r} + \frac{\partial^2 \psi}{\partial z^2}\right), \qquad (8)$$

where it is assumed in the development of equation (7) that $f_z$ is not a function of the radius, r. Equation (7) is the usual vorticity transport equation and has the form of a modified diffusion equation [7]. Equation (8) is the definition of vorticity in terms of stream function. The two equations could easily be combined to form a single fourth order equation involving both $\psi$ and $\zeta$. However, due to the nonlinearity of equation (7) it is necessary to use approximate methods to obtain solutions. In this work finite difference techniques were found to be well suited. With this method it is better to have the equations in the form given by (7) and (8) rather than as a fourth order equation, since increasing the order of the differential equations increases the coupling of the difference equations. The nonlinear character of equation (7) is inherent in the equations of motion for the regime of flow and would appear in any form of the equations.

Once the stream function and vorticity are known from the solutions to (7) and (8), the velocity may be found from the definition of the stream function. The pressure gradients may then be determined from the Navier-Stokes equations

(1) and (2) and then integrated to find the pressure throughout the incompressible phase, within an additive arbitrary constant. However, for computer calculation, a slightly different procedure may be used. Starting with the Navier-Stokes equations, (1) and (2), multiply (1) by r, take the partial derivative with respect to r, divide by r and add this to the partial derivative of equation (2) with respect to z. Then by use of the continuity equation, we obtain

$$\frac{1}{\rho}\left(\frac{\partial^2\Omega}{\partial r^2} + \frac{1}{r}\frac{\partial\Omega}{\partial r} + \frac{\partial^2\Omega}{\partial z^2}\right) = -\left[\left(\frac{\partial v_r}{\partial r}\right)^2 + \left(\frac{v_r}{r}\right)^2 + 2\frac{\partial v_z}{\partial r}\frac{\partial v_r}{\partial z} + \left(\frac{\partial v_z}{\partial z}\right)^2\right], \tag{9}$$

where

$$\Omega = p - f_z z .$$

Using the definition of the stream function to eliminate the velocities from (9), we obtain

$$\frac{1}{\rho}\left(\frac{\partial^2\Omega}{\partial r^2} + \frac{1}{r}\frac{\partial\Omega}{\partial r} + \frac{\partial^2\Omega}{\partial z^2}\right) = -\left[\frac{\partial}{\partial r}\left(\frac{1}{r}\frac{\partial\psi}{\partial z}\right)\right]^2 - \left[\frac{1}{r^2}\frac{\partial\psi}{\partial z}\right]^2 + 2\frac{\partial}{\partial r}\left(\frac{1}{r}\frac{\partial\psi}{\partial r}\right)\frac{\partial}{\partial z}\left(\frac{1}{r}\frac{\partial\psi}{\partial z}\right) - \left[\frac{\partial}{\partial z}\left(\frac{1}{r}\frac{\partial\psi}{\partial r}\right)\right]^2 . \tag{10}$$

Once the solution for the stream function is known, the right-hand side of equation (10) is completely known. It

may then be considered as a Poisson's equation for the pressure field. The advantages of using this equation are that the viscous terms and time derivatives do not appear as they would in solving for the pressure gradients from the equations of motion directly. Also, numerically it is easier to apply the point iteration solution of (10) than a series of line integrations if the geometry is complex.

For generality equations (7), (8) and (10) will be nondimensionalized by the following substitutions:

$$Z = z/b \ , \ R = r/b \ , \ T = Ut/b$$

$$S = \psi/b^2U \ , \ W = \zeta b/U \tag{11}$$

$$B = \Omega/\rho U^2 \ , \ F_z = bf_z/\rho U^2 ,$$

where b is the average radius of the wavy wall tube, $\rho$ is the density of the liquid and U is the average velocity, that is, the velocity required to yield the flow rate if a rectangular velocity profile existed at the average tube radius. The Reynolds number, RN, is taken to be

$$RN = Ub/\nu . \tag{12}$$

The nondimensional forms of (7), (8) and (10) respectively are

$$\frac{\partial W}{\partial T} - \frac{\partial S}{\partial Z}\frac{\partial}{\partial R}\left(\frac{W}{R}\right) + \frac{1}{R}\frac{\partial S}{\partial R}\frac{\partial W}{\partial Z} = \frac{1}{RN}\left[\frac{\partial^2 W}{\partial R^2} + \frac{\partial}{\partial R}\left(\frac{W}{R}\right) + \frac{\partial^2 W}{\partial Z^2}\right], \tag{13}$$

$$W = -\frac{1}{R}\left(\frac{\partial^2 S}{\partial R^2} - \frac{1}{R}\frac{\partial S}{\partial R} + \frac{\partial^2 S}{\partial Z^2}\right), \tag{14}$$

$$\frac{\partial^2 B}{\partial R^2} + \frac{1}{R}\frac{\partial B}{\partial R} + \frac{\partial^2 B}{\partial Z^2} = -\left[\frac{\partial}{\partial R}\left(\frac{1}{R}\frac{\partial S}{\partial Z}\right)\right]^2 - \left[\frac{1}{R^2}\frac{\partial S}{\partial Z}\right]^2$$

$$+ 2\,\frac{\partial}{\partial R}\left(\frac{1}{R}\frac{\partial S}{\partial R}\right)\frac{\partial}{\partial Z}\left(\frac{1}{R}\frac{\partial S}{\partial Z}\right) - \left[\frac{\partial}{\partial Z}\left(\frac{1}{R}\frac{\partial S}{\partial Z}\right)\right]^2 \tag{15}$$

The coordinates R and Z do not conform to the shape of the tube wall or to the shape of the bubbles. This type of disparity would cause the application of the boundary conditions at the wall and bubble interface to be very cumbersome. However, this undesirable situation can be eliminated by the following coordinate transformation. Let the periodic function which describes the tube wall be given by FW(Z), and the bubble shape be given by FB(Z), both in non-dimensional form. FB(Z) will be defined to be zero for any Z outside the bubble. Let

$$R = [FW(Z) - FB(Z)]Y + FB(Z)$$

$$Z = X \tag{16}$$

Then

$$Y = \frac{R - FB(Z)}{FW(Z) - FB(Z)}$$

$$X = Z \tag{17}$$

In order to transform equations (13), (14) and (15), we need expressions for derivatives with respect to R and Z in terms of Y and X. For convenience, let

$$FD(Z) = FW(Z) - FB(Z)$$

The partial derivative with respect to R may be written as

$$\frac{\partial}{\partial R} = \frac{\partial Y}{\partial R}\frac{\partial}{\partial Y} + \frac{\partial X}{\partial R}\frac{\partial}{\partial X}$$

and from (17) we get

$$\frac{\partial}{\partial R} = \frac{1}{FD(X)}\frac{\partial}{\partial Y} \tag{18}$$

For the partial derivative with respect to Z, we have

$$\begin{aligned} \frac{\partial}{\partial Z} &= \frac{\partial X}{\partial Z}\frac{\partial}{\partial X} + \frac{\partial Y}{\partial Z}\frac{\partial}{\partial Y} \\ \frac{\partial}{\partial Z} &= \frac{\partial}{\partial X} + G(X,Y)\frac{\partial}{\partial Y} \end{aligned} \tag{19}$$

where

$$\begin{aligned} G(X,Y) &= \frac{-FD(X)FB'(X) - [R-FB(X)]\ FD'(X)}{FD^2(X)} \\ G(X,Y) &= -\frac{FB'(X) + Y\ FD'(X)}{FD(X)} \end{aligned} \tag{20}$$

and the primes indicate derivatives with respect to X. Similarly, expressions for higher derivatives can be found. Collecting all of these in a group we have

$$\begin{aligned} \frac{\partial}{\partial R} &= \frac{1}{FD(X)}\frac{\partial}{\partial Y}\,, \\ \frac{\partial^2}{\partial R^2} &= \frac{1}{FD^2(X)}\frac{\partial^2}{\partial Y^2}\,, \end{aligned} \tag{21}$$

$$\frac{\partial}{\partial Z} = \frac{\partial}{\partial X} + G(X,Y)\frac{\partial}{\partial Y} \quad ,$$

$$\frac{\partial^2}{\partial Z^2} = \frac{\partial^2}{\partial X^2} + \left[\frac{\partial G(X,Y)}{\partial X} + G(X,Y)\frac{\partial G(X,Y)}{\partial Y}\right]\frac{\partial}{\partial Y} + 2\,G(X,Y)\frac{\partial^2}{\partial X \partial Y} + G^2(X,Y)\frac{\partial^2}{\partial Y^2} \tag{21}$$

$$\frac{\partial^2}{\partial R \partial Z} = \frac{1}{FD(X)}\left[\frac{\partial^2}{\partial X \partial Y} + \frac{\partial G(X,Y)}{\partial Y}\,\frac{\partial}{\partial Y} + G(X,Y)\frac{\partial^2}{\partial Y^2}\right] \quad ,$$

with

$$G(X,Y) = -\frac{FB'(X) + Y\,FD'(X)}{FD(X)}$$

$$\frac{\partial G(X,Y)}{\partial Y} = -\frac{FD'(X)}{FD(X)}$$

$$\frac{\partial G(X,Y)}{\partial X} = -\frac{[FB''(X)+Y\,FD''(X)+G(X,Y)FD'(X)]}{FD(X)}$$

Under this transformation the tube wall is transformed to Y = 1 and the centerline is transformed to Y = 0 with the bubble boundary going to a segment of Y = 0. The region of interest in the X,Y plane is therefore rectangular with the boundaries conforming to the coordinate lines. See Figure 2 for the transformed tube geometry. For ease of notation let

$$G = G(X,Y) \quad ,$$

$$G_X = \frac{\partial G(X,Y)}{\partial X} \quad ,$$

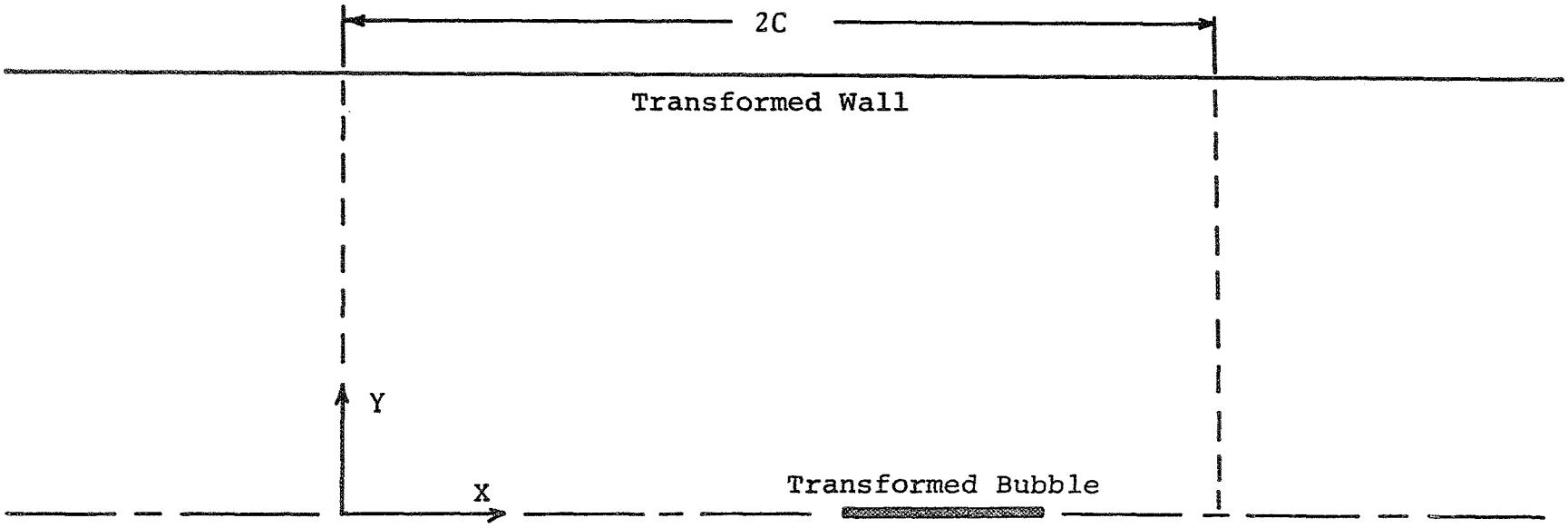


Figure 2. Wavy Wall Tube after Transforming to Y,X Coordinates

$$Y = \frac{R - FB(X)}{FW(X) - FB(X)}$$

FW(X) describes the shape of the wall in dimensionless form

FB(X) describes the shape of the bubbles in dimensionless form

$$G_Y = \frac{\partial G(X,Y)}{\partial Y}$$

Equations (13), (14) and (15) now become

$$\begin{aligned}
&\frac{\partial W}{\partial T} - \frac{1}{FD(X)}\left(\frac{\partial S}{\partial X} + G\frac{\partial S}{\partial Y}\right)\frac{\partial}{\partial Y}\left[\frac{W}{FD(X)Y+FB(X)}\right] \\
&+ \frac{1}{FD(X)\left[FD(X)Y+FB(X)\right]}\frac{\partial S}{\partial Y}\left[\frac{\partial W}{\partial X} + G\frac{\partial W}{\partial Y}\right] \\
&= \frac{1}{RN}\left\{\frac{1}{FD^2(X)}\frac{\partial^2 W}{\partial Y^2} + \frac{1}{FD(X)}\frac{\partial}{\partial Y}\left[\frac{W}{FD(X)Y+FB(X)}\right]\right. \\
&\left. + \frac{\partial^2 W}{\partial X^2} + (G_X+GG_Y)\frac{\partial W}{\partial Y} + 2G\frac{\partial^2 W}{\partial X \partial Y} + G^2\frac{\partial^2 W}{\partial Y^2}\right\} ,
\end{aligned} \tag{22}$$

$$\begin{aligned}
W = &- \frac{1}{FD(X)Y+FB(X)}\left\{\frac{1}{FD^2(X)}\frac{\partial^2 S}{\partial Y^2} - \frac{1}{FD(X)\left[FD(X)Y+FB(X)\right]}\frac{\partial S}{\partial Y}\right. \\
&\left. + \frac{\partial^2 S}{\partial X^2} + (G_X+GG_Y)\frac{\partial S}{\partial Y} + 2G\frac{\partial^2 S}{\partial Y \partial X} + G^2\frac{\partial^2 S}{\partial Y^2}\right\} ,
\end{aligned} \tag{23}$$

$$\begin{aligned}
&\frac{1}{FD^2(X)}\frac{\partial^2 B}{\partial Y^2} + \frac{1}{FD(X)\left[FD(X)Y+FB(X)\right]}\frac{\partial B}{\partial Y} + \frac{\partial^2 B}{\partial X^2} \\
&+ (G_X+GG_Y)\frac{\partial B}{\partial Y} + 2G\frac{\partial^2 B}{\partial X \partial Y} + G^2\frac{\partial^2 B}{\partial Y^2} \\
&+ \frac{2}{\left[FD(X)Y+FB(X)\right]^4}\left(\frac{\partial S}{\partial Z}\right)^2 + \\
&- \frac{2}{FD(X)\left[FD(X)Y+FB(X)\right]^3}\frac{\partial S}{\partial Z}\frac{\partial^2 S}{\partial Y \partial Z} \\
&+ \frac{2}{FD^2(X)\left[FD(X)Y+FB(X)\right]^2}\frac{\partial^2 S}{\partial Y \partial Z} \\
&+ \frac{2}{FD(X)\left[FD(X)Y+FB(X)\right]^3}\frac{\partial S}{\partial Y}\frac{\partial^2 S}{\partial Z^2} \\
&- \frac{2}{FD^2(X)\left[FD(X)Y+FB(X)\right]^2}\frac{\partial^2 S}{\partial Y^2}\frac{\partial^2 S}{\partial Z^2} = 0 ,
\end{aligned} \tag{24}$$

where the partial derivatives with respect to Z are given by the expression (21).

The mathematical effect of the above transformation is to shift the complication of irregular boundaries to the internal field equations. But since it is already conceded that the possibility of analytical solutions is very remote and numerical methods will have to be used, this complication in the field equations is of little consequence when compared to the simplicity of the transformed geometry.

Boundary Conditions for the Liquid Phase

The physical requirements that the liquid flowing in the tube must meet are that the flow be axisymmetric, the total velocity at the wall be zero, and that the flow field be periodic in one wavelength of the tube. These constraints will be translated into mathematical boundary conditions for the equations of motion.

In axisymmetric flow the radial component of velocity must be zero at the centerline along with the partial derivative of the axial component with respect to the radius. Denoting the nondimensional axial component of velocity by u and the radial component by v, these conditions are

$$\text{at } R = 0,\ v = 0 \text{ and } \frac{\partial u}{\partial R} = 0. \tag{25}$$

The first condition above means that the centerline is a stream line with a constant value of S. We can arbitrarily set the value of S along this boundary to zero since only

differences and derivatives of stream function are significant. Using the fact that the value of u must be finite at the centerline and the two conditions above, the following conditions on S and W at the centerline result

$$\text{at } R = 0, \quad S = 0, \quad W = 0$$
$$\frac{\partial S}{\partial R} = 0, \quad \frac{\partial^3 S}{\partial R^3} = 0. \tag{26}$$

Since the flow field must be periodic over one wavelength of the tube, the corresponding conditions on S and W and their derivatives are that they are periodic along with their derivatives with respect to Z.

$$\begin{aligned} S(R,0) &= S(R,2C), \\ W(R,0) &= W(R,2C), \\ \left.\frac{\partial S}{\partial Z}\right|_{Z=0} &= \left.\frac{\partial S}{\partial Z}\right|_{Z=2C} \\ \left.\frac{\partial W}{\partial Z}\right|_{Z=0} &= \left.\frac{\partial W}{\partial Z}\right|_{Z=2C} \end{aligned} \tag{27}$$

where C is the dimensionless half wavelength of the tube, equal to the physical half wavelength divided by the average tube radius, b.

Since the total velocity at the wall is zero, the partial derivatives of S with respect to R and Z are both zero and the value of S is constant along the wall. Since the value of S has been set equal to zero along the centerline

the value at the wall is determined by the volumetric flow rate. The volumetric flow rate, Q, is

$$Q = \int_0^{\text{wall}} 2\pi r v_z dr.$$

Using the definition of the stream function $\psi$ from equation (5) and the fact that $\psi$ is zero at the centerline, Q becomes

$$Q = 2\pi \psi_{\text{wall}}$$

but from the way that U, the average velocity was defined, Q is also

$$Q = \pi b^2 U .$$

Therefore, relating $\psi$ to S, we have that

$$S_{\text{wall}} = 1/2$$

In the transformed coordinates Y and X

$$\text{at } Y = 1, \quad S = 1/2$$

$$\frac{\partial S}{\partial Y} = 0$$

$$W = - \frac{1}{FW(X)} \left(\frac{1}{FW^2(X)} + G^2\right) \frac{\partial^2 S}{\partial Y^2} \tag{28}$$

In order to solve for the pressure field using equation (24), the boundary values of P must be established. Since only pressure gradients and differences are of interest, an arbitrary constant pressure may be assumed to exist on the centerline at the beginning of the section of interest. The expressions for the pressure gradients

along the centerline, the wall and across the two ends of the section can be obtained from the Navier-Stokes equations, (1) and (2). Starting from the fixed pressure point, these expressions can be integrated along the boundaries of the region to provide the boundary values for equation (24).

Along the centerline, noting that $v_r$ and $\frac{\partial v_z}{\partial z}$ are both zero, from equation (2) we obtain

$$\frac{\partial p}{\partial z} = -\rho \frac{\partial v_z}{\partial t} - \rho v_z \frac{\partial v_z}{\partial z} + F_z + \mu[2 \frac{\partial v_z}{\partial r^2} \quad \frac{\partial^2 v_z}{\partial z^2}] . \qquad (29)$$

In order to simplify the expression in square brackets on the right side in the above equation, consider

$$\frac{\partial \zeta}{\partial r} = \frac{\partial}{\partial r}[\frac{\partial v_r}{\partial z} - \frac{\partial v_z}{\partial r}]$$

$$= \frac{\partial^2 v_r}{\partial r \partial z} - \frac{\partial^2 v_z}{\partial r^2}$$

Using the equation of continuity which along the centerline is

$$2 \frac{\partial v_r}{\partial r} + \frac{\partial v_z}{\partial z} = 0$$

so that

$$\frac{\partial \zeta}{\partial r} = \frac{\partial}{\partial z}(- \frac{1}{2} \frac{\partial v_z}{\partial z}) - \frac{\partial^2 v_z}{\partial r^2}$$

$$= - \frac{1}{2} \frac{\partial^2 v_z}{\partial z^2} - \frac{\partial^2 v_z}{\partial r^2}$$

Since at the centerline

$$v_z = \frac{\partial^2 \psi}{\partial r^2}$$

equation (29) now becomes

$$\frac{\partial p}{\partial z} = F_z - \rho \frac{\partial}{\partial t}\left(\frac{\partial^2 \psi}{\partial r^2}\right) - \frac{1}{2} \rho \frac{\partial}{\partial z}\left(\frac{\partial^2 \psi}{\partial r^2}\right)^2 - 2 \mu \frac{\partial \zeta}{\partial z}$$

Nondimensionalizing and transforming to Y and Z as before

$$\frac{\partial P}{\partial Z} = F_z - \frac{1}{FD^2(X)} \frac{\partial}{\partial T}\left(\frac{\partial^2 S}{\partial Y^2}\right) - \frac{1}{2FD^4(X)} \frac{\partial}{\partial X}\left(\frac{\partial^2 S}{\partial Y^2}\right)^2 - \frac{2}{RN \cdot FD(X)} \frac{\partial W}{\partial Y} . \tag{30}$$

At the wall both velocity components are zero and again from equation (2) the pressure gradient in the axial direction is

$$\frac{\partial p}{\partial z} = F_z + \mu\left[\frac{\partial^2 v_z}{\partial r^2} + \frac{1}{r} \frac{\partial v_z}{\partial r} + \frac{\partial^2 v_z}{\partial z^2}\right] . \tag{31}$$

Equation (31) may be written

$$\frac{\partial p}{\partial z} = F_z - \frac{\mu}{r} \frac{\partial}{\partial r}(r\zeta) .$$

In nondimensional form this is

$$\frac{\partial P}{\partial z} = F_z - \frac{1}{(R)(RN)} \frac{\partial}{\partial R} (RW) \tag{32}$$

and after transformation, we have

$$\frac{\partial P}{\partial X} + G \frac{\partial P}{\partial Y} = F_z - \frac{1}{(R)(RN)} \frac{\partial}{\partial R}(RW). \tag{33}$$

But from equation (1) we can obtain an expression for the partial of P with respect to R as

$$\frac{\partial P}{\partial R} = \frac{1}{RN} \frac{\partial W}{\partial Z} . \tag{34}$$

After transformation this becomes

$$\frac{\partial P}{\partial Y} = \frac{FD(X)}{RN} \left(\frac{\partial W}{\partial X} + G\frac{\partial W}{\partial Y}\right). \tag{35}$$

Combining (33) and (35) we have

$$\begin{aligned} \frac{\partial P}{\partial X} &= F_z - G \frac{FD(X)}{RN} \left(\frac{\partial W}{\partial X} + G \frac{\partial W}{\partial Y}\right) \\ &- \frac{1}{(RN)FD(X)[FD(X)Y+FB(X)]} \frac{\partial}{\partial Y}\{[FD(X)Y+FB(X)]W\} . \end{aligned} \tag{36}$$

Equation (36) is an expression which may be integrated to give the pressure along the wall in the X,Y plane.

At the two ends of the section, Z = 0 and Z = 2C, the radial pressure gradient is needed. From equation (1) we find, recalling that $f_r$ is zero,

$$\begin{aligned} \frac{\partial p}{\partial r} = &- \rho\frac{\partial v_r}{\partial t} - \rho v_r \frac{\partial v_r}{\partial r} - \rho\, v_z \frac{\partial v_z}{\partial z} \\ &+ \mu\left[\frac{\partial^2 v_r}{\partial r^2} + \frac{1}{r}\frac{\partial v_r}{\partial r} - \frac{v_r}{r^2} + \frac{\partial^2 v_r}{\partial z^2}\right]. \end{aligned} \tag{37}$$

The viscous terms above may also be simplified using the vorticity.

$$\frac{\partial \zeta}{\partial z} = \frac{\partial}{\partial z}\left[\frac{\partial v_r}{\partial z} - \frac{\partial v_z}{\partial r}\right]$$

$$= \frac{\partial^2 v_r}{\partial z^2} - \frac{\partial}{\partial r}\left(-\frac{v_r}{r} - \frac{\partial v_r}{\partial r}\right)$$

$$= \frac{\partial^2 v_r}{\partial z^2} - \frac{v_r}{r^2} + \frac{1}{r}\frac{\partial v_r}{\partial r} + \frac{\partial^2 v_r}{\partial r^2} .$$

Making the above simplification and then nondimensionalizing and transforming to Y and X, equation (37) becomes

$$\frac{\partial P}{\partial Y} = \frac{FD(X)}{FD(X)Y+FB(X)}\frac{\partial^2 S}{\partial T \partial Z} + \frac{FD(X)}{[FD(X)Y+FB(X)]^3}\left(\frac{\partial S}{\partial Z}\right)^2$$

$$- \frac{1}{[FD(X)Y+FB(X)]^2}\frac{\partial S}{\partial Z}\frac{\partial^2 S}{\partial Y \partial Z} \qquad (38)$$

$$+ \frac{1}{[FD(X)Y+FB(X)]^2}\frac{\partial S}{\partial Y}\frac{\partial^2 S}{\partial Z^2} + \frac{FD(X)}{RN}\frac{\partial W}{\partial Z}$$

where the derivatives with respect to Z are given by (21).

Bubble Conditions

Since the flow in the physical model has been restricted to be periodic, it is sufficient to consider only the bubble located in a typical wavelength of the tube. The bubble is of constant mass and it is further assumed that the gas inside is not compressed so that the volume is also constant. This assumption is made to insure that the

bubble pattern in the entire tube remain periodic. If the volume of the bubbles were allowed to vary with pressure, the bubbles would have different volumes for the same mass due to the pressure gradient in the tube. This assumption is not a serious limitation on the study since the change in pressure over the distances moved by the bubble in a typical calculation can be made negligible compared to the absolute pressure in the tube, simply by raising the overall pressure level. The motion of the gas inside the bubble will be neglected in comparison to other effects. Since the gas body forces are neglected, this means that the pressure inside the bubble is everywhere the same at a given instant. This assumption also means that the bubble cannot support any shearing stress at the interface with the liquid. Finally, it is assumed that the fluid particles composing the gas-liquid interface remain always in the interface. This means that in order to follow the motion of the bubble all that is required is to keep track of particles at the interface.

The boundary conditions that must be satisfied on the bubble surface are that there must be equilibrium among inside and outside pressure, surface tension, and normal viscous stress at the bubble surface and that the shearing stress in the liquid at the bubble surface must be zero.

Since the bubble is symmetric with respect to the z axis, the normal to the surface lies in a r,z plane with

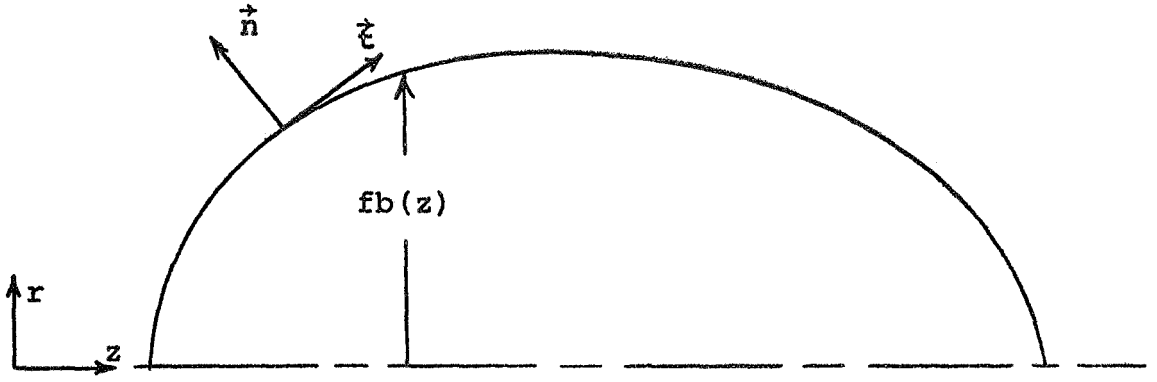


Bubble Cross Section

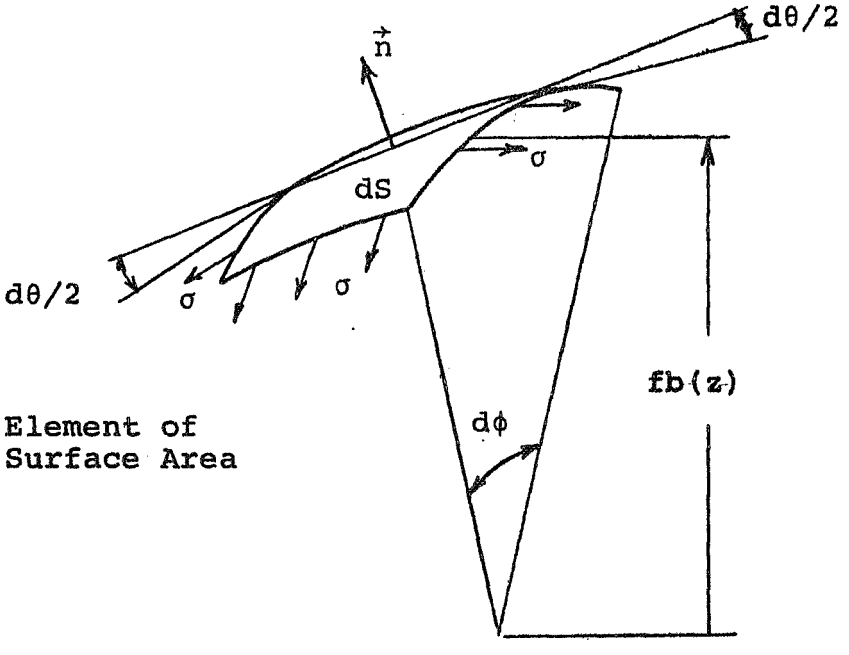


Figure 3. Bubble Geometry

components given by

$$n_z = \frac{-\frac{dfb}{dz}}{\sqrt{1 + \left(\frac{dfb}{dz}\right)^2}} \, , \quad n_r = \frac{1}{\sqrt{1 + \left(\frac{dfb}{dz}\right)^2}} \tag{39}$$

where fb(z) is the function which describes the bubble surface in the r,z plane. See Figure 3 for a sketch of the bubble geometry and an element of surface area, dS.

Denoting the differential force on dS due to the normal viscous stress by $dF_v$ and assuming positive in the direction of the outward normal to the bubble,

$$dF_v = \tau_{ij} \, n_i \, n_j \, dS \tag{40}$$

where $\tau_{ij}$ are the components of the viscous stress tensor in cylindrical polar coordinates. From Aris[1] for axisymmetric flow, the non-zero components are

$$\begin{aligned} \tau_{rr} &= 2\mu \frac{\partial v_r}{\partial r} \, , \quad \tau_{\phi\phi} = 2\mu \frac{v_r}{r} \\ \tau_{rz} &= \mu \left(\frac{\partial v_z}{\partial r} + \frac{\partial v_r}{\partial z}\right) \, , \quad \tau_{zz} = 2\mu \, \frac{\partial v_z}{\partial z} \, . \end{aligned} \tag{41}$$

Then, we have

$$dF_v = \left\{ \frac{2\mu \, \frac{\partial v_r}{\partial r}}{1 + \left(\frac{dfb}{dz}\right)^2} - \frac{2\mu \left(\frac{\partial v_z}{\partial r} \quad \frac{\partial v_r}{\partial z}\right) \frac{dfb}{dz}}{1 + \left(\frac{dfb}{dz}\right)^2} \, \frac{dfb}{dz} \quad + \right. \tag{42}$$

$$+ \frac{2\mu \frac{\partial v_z}{\partial z}}{1 + (\frac{dfb}{dz})^2} (\frac{dfb}{dz})^2 \Bigg\} \qquad (42)$$

Let $dF_{st}$ be the contribution of the surface tension forces in the gas-liquid interface. These forces are composed of the surface tension $\sigma$, multiplied by the length of an edge of dS times the cosine of the angle between the normal to dS and the surface tension forces along the edge in question.

$$dF_{st} = - 2\sigma(fb)(d\phi)(\frac{d\theta}{2}) - 2\sigma(\frac{d\theta}{2}) \frac{\sqrt{1 + (\frac{dfb}{dz})^2}}{\sqrt{1 + (\frac{dfb}{dz})^2}} \qquad (43)$$

But

$$|d\theta| = - \frac{d\theta}{dz} dz ,$$

$$\theta = \tan^{-1}\left(\frac{dfb}{dz}\right)$$

$$\frac{d\theta}{dz} = \frac{\frac{d^2fb}{dz^2}}{1 + (\frac{dfb}{dz})^2}$$

therefore,

$$dF_{st} = - \sigma \left\{ \frac{- \frac{d^2fb}{dz^2}}{[1 + (\frac{dfb}{dz})^2]^{3/2}} + \frac{1}{(fb)\sqrt{1 + (\frac{dfb}{dz})^2}} \right\},$$

$$\left[ (fb)\ d\phi \sqrt{1 + (\frac{dfb}{dz})^2}\ dz \right]$$

Since

$$dS = (fb)(d\phi)\sqrt{1 + (\frac{dfb}{dz})^2}\, dz \ ,$$

equation (43) becomes

$$dF_{st} = -\sigma \left\{ \frac{-\frac{d^2fb}{dz^2}}{[1+(\frac{dfb}{dz})^2]^{3/2}} + \frac{1}{(fb)\sqrt{1+(\frac{dfb}{dz})^2}} \right\} dS \qquad (44)$$

The two terms in brackets may be recognized to be the reciprocals of the curvature of the bubble surface, the first is the reciprocal of the radius in the r,z plane and the second is the reciprocal of the radius in the plane containing $\vec{n}$ and lying perpendicular to the r,z plane.

Combining (42) and (44) and adding in the internal and external pressures, the condition for the equilibrium of normal forces at the bubble surface becomes

$$P_{out} = P_{in} - \sigma \left\{ \frac{-\frac{d^2fb}{dz^2}}{[1+(\frac{dfb}{dz})^2]^{3/2}} + \frac{}{(fb)\sqrt{1+(\frac{dfb}{dz})^2}} \right\} \qquad (45)$$

$$+ \frac{2\mu}{1+(\frac{dfb}{dz})^2} \left[ \frac{\partial v_r}{\partial r} - (\frac{\partial v_z}{\partial r} + \frac{\partial v_r}{\partial z})\frac{dfb}{dz} + \frac{\partial v_z}{\partial z}(\frac{dfb}{dz})^2 \right] .$$

Replacing the velocity components with the stream function, nondimensionalizing and transforming to X,Y coordinates

yields:

$$P_{out} = P_{in} - \frac{1}{WN}\left[\frac{1}{\rho_1} + \frac{1}{\rho_2}\right] +$$

$$\frac{1}{RN\left[1+\left(\frac{dFB}{dZ}\right)^2\right]}\left\{\frac{2}{[FD(X)Y+FB(X)]}\left(\frac{\partial S}{\partial X} + G\,\frac{\partial S}{\partial Y}\right)\right.$$

$$- \frac{2}{FB(X)FD(X)}\left[\frac{\partial^2 S}{\partial Y \partial X} + G_y\,\frac{\partial S}{\partial Y} + G\,\frac{\partial^2 S}{\partial Y^2}\right]\left[1 - \left(\frac{dFB}{dZ}\right)^2\right] \qquad (46)$$

$$-\left[-\frac{1}{FD(X)FB^2(X)}\,\frac{\partial S}{\partial Y} + \frac{1}{FB(X)FD^2(X)}\,\frac{\partial^2 S}{\partial Y^2} -\right.$$

$$\left.\left.\frac{1}{FB(X)}\left(\frac{\partial^2 S}{\partial X^2} + (G_x + GG_y)\frac{\partial S}{\partial Y} + 2G\,\frac{\partial^2 S}{\partial Y \partial X} + G^2\,\frac{\partial^2 S}{\partial Y^2}\right)\right]\frac{dFB}{dZ}\right\},$$

where

$$\frac{1}{\rho_1} = \frac{-\frac{d^2FB}{dX^2}}{\left[1 + \left(\frac{dFB}{dX}\right)^2\right]^{3/2}}$$

$$\frac{1}{\rho_2} = \frac{1}{FB(X)\sqrt{1 + \left(\frac{dFB}{dX}\right)^2}}$$

where WN is the Weber number,

$$WN = \rho b U^2/\sigma$$

Referring to Figure 3, the tangent to the bubble surface will be assumed to be positive if the angle between $\vec{t}$

and the z axis is between -90 and 90 degrees.

$$t_r = \frac{1}{\sqrt{1 + (\frac{dfb}{dz})^2}}, \quad t_z = \frac{1}{\sqrt{1 + (\frac{dfb}{dz})^2}} \tag{47}$$

The tangential shearing stress at the bubble surface in the r,z plane is denoted by $\tau_{nt}$ and may be written

$$\tau_{nt} = \tau_{ij}\, n_i\, t_j \tag{48}$$

The components $\tau_{n\phi}$ are identically zero since the flow is axisymmetric. Using equations (41), (39) and (47) the above expression may be written out explicitly,

$$\tau_{nt} = 2\mu \frac{\partial v_r}{\partial r} \frac{\frac{dfb}{dz}}{1+(\frac{dfb}{dz})^2} + \mu(\frac{\partial v_z}{\partial r} + \frac{\partial v_r}{\partial z}) \frac{1}{1+(\frac{dfb}{dz})^2}$$

$$+ \mu(\frac{\partial v_z}{\partial r} + \frac{\partial v_r}{\partial z}) \frac{-(\frac{dfb}{dz})^2}{1+(\frac{dfb}{dz})^2} + 2\mu \frac{\partial v_z}{\partial z} \frac{-\frac{dfb}{dz}}{1+(\frac{dfb}{dz})^2} . \tag{49}$$

After the stream function is substituted into equation (49) for velocity, and the shearing stress set to zero, the nondimensional boundary condition in the X,Y plane becomes

$$\left\{\frac{4}{FD(X)}\left(\frac{\partial^2 S}{\partial Y \partial X} + G_y \frac{\partial S}{\partial Y} + G \frac{\partial^2 S}{\partial Y^2}\right)\right.$$

$$\left. - \frac{1}{FB(X)}\left(\frac{\partial S}{\partial X} + G \frac{\partial S}{\partial Y}\right)\right\} \frac{dFB}{dX} +$$

$$- \left\{\frac{1}{FD(X)} \frac{\partial^2 S}{\partial Y^2} - \frac{1}{FB(X)FD(X)} \frac{\partial S}{\partial Y} - \frac{\partial^2 S}{\partial X^2}\right. \tag{50}$$

$$\left. -(G_x + GG_y)\frac{\partial S}{\partial Y} - 2G \frac{\partial^2 S}{\partial Y \partial X} - G^2 \frac{\partial^2 S}{\partial Y^2}\right\}\left\{1 - \left(\frac{dFB}{dX}\right)^2\right\} = 0.$$

If the surface tension forces become very large compared to the other forces acting at the bubble surface, the Weber number may be taken to be zero and a bubble will be spherical at all times. Equation (46) in its present form is not suitable to be used as a boundary condition for the bubble. However, the requirement that the bubble not change shape may be used to develop a condition on the velocity distribution along the bubble surface and therefore a condition on the stream function distribution. Let $v_{r/b}$ and $v_{z/b}$ be velocity components at the bubble surface relative to the bubble center. If the bubble is not to change shape the normal velocity at the surface relative to the bubble center must be zero. This requires that

$$v_{z/b} = \frac{v_{r/b}}{\frac{dfb}{dz}} \tag{51}$$

where $\frac{dfb}{dz}$ is the slope of the bubble surface. This condition would apply for any shaped body which is not changing shape. If the bubble center is moving with a velocity $v_T$ in the axial direction, relative to a fixed observer, the velocity components, $v_r$ and $v_z$, at the surface, relative to a fixed observer become

$$v_z = v_T + \frac{v_{r/b}}{\frac{dfb}{dz}} \tag{52}$$

$$v_r = v_{r/b} \, . \tag{53}$$

From (52) one obtains

$$v_T = v_z - \frac{v_r}{\frac{dfb}{dz}} \, .$$

Let $V_T$ be the dimensionless translational velocity and using the dimensionless stream function, the above equation becomes

$$V_T = \frac{1}{R} \frac{\partial S}{\partial R} + \frac{\frac{\partial S}{\partial Z}}{R \frac{dFB}{dZ}} \, . \tag{54}$$

Transforming this to X and Y coordinates yields:

$$V_T = \frac{1}{FB(X)FD(X)} \frac{\partial S}{\partial Y} + \frac{\frac{\partial S}{\partial X} + G\frac{\partial S}{\partial Y}}{FB(X) \frac{dFB}{dX}} \, . \tag{55}$$

But on the bubble surface

$$G = - \frac{\frac{dFB}{dX}}{FD(X)} ,$$

so that equation (55) reduces to

$$V_T = \frac{\frac{\partial S}{\partial X}}{FB(X) \frac{dFB}{dX}}$$

or

$$\frac{\partial S}{\partial X} = FB(X) \frac{dFB}{dX} V_T \qquad (56)$$

Since S=0 at each end of the bubble on the centerline, the stream function distribution on the surface may be determined in terms of $V_T$ by integrating equation (56). However, since $V_T$ is unknown an iteration procedure will have to be used between $V_T$ and the liquid field equations to determine $V_T$ at each time step.

Initial Conditions

Equation (22) is time dependent and since the three equations (22), (23) and (24) are coupled, the variables describing the flow field will in general be a function of time. Therefore, initial conditions must be supplied for the solution of the field equations.

One possible initial condition for the flow is to let the fluid be at rest for times less than zero and at time zero require that the flow rate be a constant. This amounts to an impulsive start and requires theoretically infinite pressure gradients and velocity gradients at the wall. However, this type of start-up can be approximated numerically, although it is not well suited for the case of flow with bubbles with a pressure boundary condition since the resulting numerical approximations to the pressure gradients become very large. This initial condition is appropriate when it is desired to study the development of flow patterns with time, starting from rest. The technique is to set the initial vorticity to zero in the interior and solve for the corresponding stream function from equation (23). Application of the boundary conditions at time zero will result in a region of concentrated vorticity due to the large velocity gradients near the wall. This start-up flow corresponds to a potential flow field with a viscous boundary layer near the wall.

A method for starting the solution which is better suited to flows with bubbles is to use an initial guess which is close to a fully developed viscous flow and which is constrained to satisfy the bubble boundary conditions. In the case of a bubble with a pressure boundary condition this avoids the large pressure gradients associated with

the impulsive start. Also, since the motion of bubbles in a developed viscous flow is of most interest, the time for the liquid flow to become fully developed is decreased. The initial guess used was an adaptation of Hadamard's [3] solution with the stream function referenced to the fixed wall and adjusted so that the liquid boundary conditions at the wall were satisfied.

# III NUMERICAL METHODS

The field equations and accompanying boundary conditions presented in Chapter II are hardly amenable to analytical solutions. The flow is a function of three independent variables, two spatial coordinates and time, and the partial differential equations are nonlinear and coupled. Under these conditions it is proper to seek approximate solutions.

Since the flow regime of interest is that of Reynolds numbers from zero up to approximately two hundred, based on average tube radius and average axial velocity, simplification of the equations on physical considerations such as is done for potential flow, viscous boundary layers and creeping flow is notipossible. Therefore, it is necessary to use other approximation methods.

During the course of the investigation, considerable effort was directed toward use of Galerkin's method or some other integral technique such as the so-called local potential concept [2], [6]. These approaches have the appeal that they consider the flow field as a whole rather than point wise and yield an approximate solution based on minimization of a scalar variable which is defined in terms of integrals over the independent variables.

Unfortunately, such a scalar may not always have true physical significance. It was found that the use of the integral techniques investigated for this problem led to a great deal of complexity in the evaluation of integrals and application of boundary conditions. In fact, a suitable integral formulation for the bubble boundary conditions was never found. Even if this difficulty could have been overcome, it seemed that the mathematical complications involved in trying to apply this particular method almost completely obscured, rather than illuminated, the mechanics of the flow. For these reasons this attack was abandoned.

Finite Difference Approximations

A method which is quite different in concept from the above integral techniques is the method of finite difference approximations. This method replaces the continuous flow field with a set of discrete points and seeks to satisfy a set of algebraic equations at each point which are derived from the differential equations. The approximation premise is that the true solution to the differential equations may be approached as closely as desired by taking the discrete points sufficiently close together. This premise is intuitively reasonable and can be mathematically proved for linear and some nonlinear partial differential equations, but for most nonlinear equations has not been proved [8].

To apply finite difference approximations, a square network of mesh size H is superimposed on the section of the transformed tube shown in Figure 2; bounded by the centerline, the wall and the two dotted lines at each end of the section. The dimensions were chosen to be an integer multiple of H with the number of node points in the Y direction being M and the number in the X direction being N. Consider a typical point i,j as shown in Figure 4. If S(Y,X) is a continuous function of Y and X having continu- first and second derivatives in the region of interest, using Taylor series expansions, it may be easily shown [4] that

$$\frac{\partial S}{\partial Y} = \frac{S_{i+1,j} - S_{i-1,j}}{2H} + 0(H^2)$$

$$\frac{\partial^2 S}{\partial Y^2} = \frac{S_{i+1,j} + S_{i-1,j} - 2S_{i,j}}{H^2} + 0(H^2)$$

$$\frac{\partial S}{\partial X} = \frac{S_{i,j+1} - S_{i,j-1}}{2H} + 0(H^2) \qquad (57)$$

$$\frac{\partial^2 S}{\partial X^2} = \frac{S_{i,j+1} + S_{i,j-1} - 2S_{i,j}}{H^2} + 0(H^2) \ ,$$

where $0(H^2)$ indicates that the terms not written out are of the order H squared. By truncating the second order terms in the equations (51), the well known central difference approximations to first and second derivatives are obtained [4].

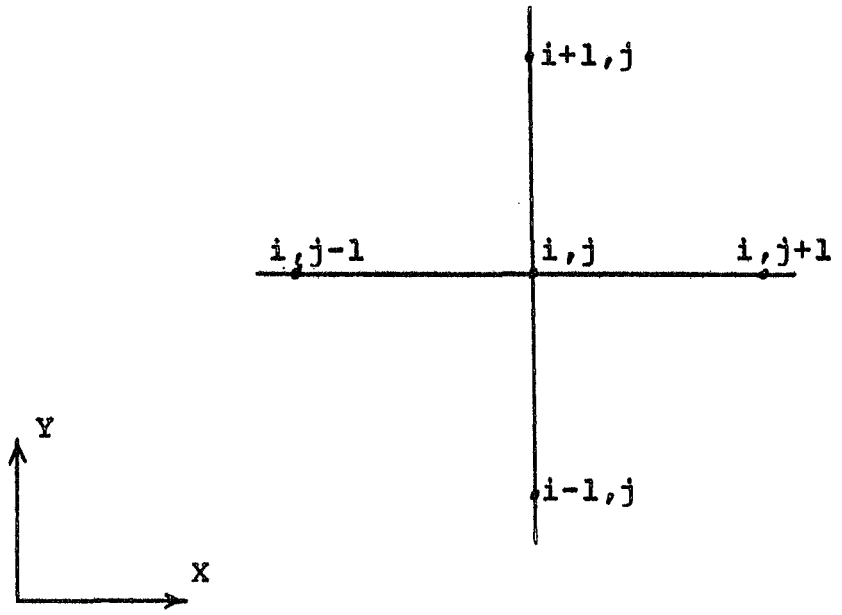


Figure 4. Typical Finite Difference Grid Point

In some cases central difference approximations cannot be used since some of the required points fall outside the boundaries of the problem. One method of dealing with this is the use of reflection points outside the boundaries. Another technique is to use one-sided differences. The backward difference approximations of error order H squared are

$$\frac{\partial S}{\partial Y} = \frac{3S_{i,j} - 4S_{i-1,j} + S_{i-2,j}}{2H} + 0(H^2)$$

$$\frac{\partial^2 S}{\partial Y^2} = \frac{2S_{i,j} - 5S_{i-1,j} + 4S_{i-2,j} - S_{i-3,j}}{H^2} + 0(H^2) \tag{58}$$

and the forward difference expressions of the same error are

$$\frac{\partial S}{\partial Y} = \frac{-3S_{i,j} + 4S_{i+1,j} - S_{i+2,j}}{2H} + 0(H^2)$$

$$\frac{\partial^2 S}{\partial Y^2} = \frac{2S_{i,j} - 5S_{i+1,j} + 4S_{i+2,j} - S_{i+3,j}}{H^2} + 0(H^2) \tag{59}$$

with derivatives with respect to X given by analogous expressions [4].

Difference Equations for Steady State Solutions

For flow of a liquid only in a wavy wall tube, a steady state flow pattern may be produced for a certain range of flows. In order to investigate such a flow, the

first term is dropped from equation (22) so that time no longer appears in the equations (22) and (23) or their associated boundary conditions. In the absence of any bubbles, FB(X) is identically zero along with its first and second derivatives and

$$FD(X) = FW(X)$$

The expressions for G(X,Y) and its derivatives in (21) in the absence of bubbles are simplified to

$$G(X,Y) = - Y \frac{FW'(X)}{FW(X)}$$

$$\frac{\partial G(X,Y)}{\partial Y} = - \frac{FW'(X)}{FW(X)} \tag{60}$$

$$\frac{\partial G(X,Y)}{\partial X} = - \frac{YFW''(X) + G(X,Y)FW'(X)}{FW(X)} .$$

The transformed equations of motion for steady state flow may be written

$$[\frac{1}{FW^2(X)} + G^2]\frac{\partial^2 W}{\partial Y^2} + \frac{\partial^2 W}{\partial X^2} + (G_X + GG_Y)\frac{\partial W}{\partial Y} + 2G \frac{\partial^2 W}{\partial X \partial Y}$$

$$+ \frac{1}{FW^2(X)} \frac{\partial}{\partial Y}[\frac{W}{YFW(X)}] + \frac{RN}{FW^2(X)} \frac{\partial}{\partial Y}[\frac{W}{YFW(X)}](\frac{\partial S}{\partial X} + G\frac{\partial S}{\partial Y}) \tag{61}$$

$$- \frac{RN}{YFW^2(X)} \frac{\partial S}{\partial Y}(\frac{\partial W}{\partial X} + G \frac{\partial W}{\partial Y}) = 0 ,$$

$$W = \frac{-1}{YFW(X)} \left\{ \left[ \frac{1}{FW^2(X)} + G^2 \right] \frac{\partial^2 S}{\partial Y^2} + \frac{\partial^2 S}{\partial X^2} \right.$$

$$\left. + \left[ G_x + GG_y - \frac{1}{YFW^2(X)} \right] \frac{\partial S}{\partial Y} + 2G \frac{\partial^2 S}{\partial X \partial Y} \right\}. \tag{62}$$

Central difference approximations may be used to form the difference equations from (61) and (62).

$$\frac{1}{H^2}\left[\frac{1}{FW^2(X)} + G^2\right](W_{i+1,j} + W_{i-1,j} - 2W_{i,j})$$

$$+ \frac{1}{H^2}(W_{i,j+1} + W_{i,j-1} - 2W_{i,j}) + \frac{1}{2H}(G_x + GG_y) \cdot$$

$$(W_{i+1,j} - W_{i-1,j}) + \frac{G}{2H^2}(W_{i+1,j+1} - W_{i+1,j-1}$$

$$- W_{i-1,j+1} + W_{i-1,j-1}) + \frac{WDY}{2H\ FW^2(X)} \tag{63}$$

$$+ \frac{RN}{4H^2 FW^2(X)} WDY[S_{i,j+1} - S_{i,j-1} + G(S_{i+1,j} - S_{i-1,j})]$$

$$- \frac{RN}{4H^2 Y\ FW^2(X)} (S_{i+1,j} - S_{i-1,j})[W_{i,j+1} - W_{i,j-1}$$

$$+ G(W_{i+1,j} - W_{i-1,j})] = 0,$$

where

$$WDY = \frac{W_{i+1,j}}{Y+H} - \frac{W_{i-1,j}}{Y-H} ,$$

and from (62) we have

$$\begin{aligned} -Y\ FW(X)\ W_{i,j} &= \frac{1}{H}\left[\frac{1}{FW^2(X)} + G^2\right](S_{i+1,j}+S_{i-1,j}-2S_{i,j}) \\ &+ \frac{1}{2H}\left[G_x + GG_y - \frac{1}{Y\ FW^2(X)}\right](S_{i+1,j}-S_{i-1,j}) \\ &+ \frac{1}{H^2}(S_{i,j+1}+S_{i,j-1}-2S_{i,j}) + \frac{1}{2H^2}\,G(S_{i+1,j+1}-S_{i+1,j-1} \\ &-S_{i-1,j+1}+S_{i-1,j-1}) . \end{aligned} \tag{64}$$

Equations (63) and (64) represent $2(M-2)(N-2)$ algebraic equations for $S_{i,j}$ and $W_{i,j}$ at each internal node point. With the availability of high speed digital computers, the most efficient method of solving such a large number of equations is iteration. To put (53) and (64) in suitable form for iteration, equation (63) is solved for $W_{i,j}$ and equation (64) for $S_{i,j}$. This is not the approach suggested by the differential equation, but is used since $S_{i,j}$ does not appear explicitly in equation (63), but $W_{i,j}$ does. The iteration equations are

$$2\left[\frac{1}{FW^2(X)} + G^2 + 1\right] W_{i,j} = \left[\frac{1}{FW^2(X)} + G^2\right] \cdot$$

$$(W_{i+1,j} + W_{i-1,j}) + W_{i,j+1} + W_{i,j-1} + \frac{H}{2}(G_x + GG_y) \cdot$$

$$\cdot(W_{i+1,j} - W_{i-1,j}) + \tfrac{1}{2} G(W_{i+1,j+1} - W_{i+1,j-1}$$

$$- W_{i-1,j+1} + W_{i+1,j+1}) + \frac{H \cdot WDY}{2FW^2(X)} + \frac{(RN)(WDY)}{4FW^2(X)}$$

$$\cdot[S_{i,j+1} - S_{i,j-1} + G(S_{i+1,j} - S_{i-1,j})]$$

$$- \frac{RN}{4Y\ FW^2(X)}(S_{i+1,j} - S_{i-1,j}) \cdot$$

$$\cdot[W_{i,j+1} + W_{i,j-1} + G(W_{i+1,j} - W_{i-1,j})] , \qquad (65)$$

$$2\left[\frac{1}{FW^2(X)} + G^2 + 1\right] S_{i,j} = \left[\frac{1}{FW^2(X)} + G^2\right](S_{i+1,j} + S_{i-1,j})$$

$$+ \frac{H}{2}\left[G_x + GG_y - \frac{1}{Y\ FW^2(X)}\right] + S_{i,j+1} + S_{i,j-1}$$

$$+ \tfrac{1}{2} G(S_{i+1,j+1} - S_{i-1,j+1} - S_{i+1,j-1} + S_{i-1,j-1})$$

$$+ Y\ H^2\ FW(X)\ W_{i,j} . \qquad (66)$$

The iteration procedure was the Gauss-Seidel method with a relaxation parameter [8]. The Gauss-Seidel method uses improved values for the unknowns at the node points in the iteration scheme whenever they become available. That is, if the field is being swept in the direction of increasing i and j, then at a point i,j, for the k-th iteration, the values used at i-1,j and i,j-1 are from the k-th iteration and the values used at i+1,j and i,j+1 are from the (k-1)-th iteration. The use of a relaxation parameter means that if $S^*_{i,j}$ is the value at k,j from the k-th Gauss-Seidel iteration, then the value taken for $S^k_{i,j}$ is

$$S^k_{i,j} = \omega\, S^*_{i,j} + (1-\omega) S^{k-1}_{i,j} , \tag{67}$$

where $S^{k-1}_{i,j}$ is the previous values of $S_{i,j}$ and $\omega$ is the relaxation parameter. If $\omega$ is less than unity, the process is called under relaxation, if $\omega$ is greater than unity it is called over relaxation. Since the equations are nonlinear no attempt was made to determine $\omega$ analytically. The values used were determined by trial and error with short computer runs.

Difference Equations for Time-Dependent Solutions

If the first term of equation (22) is retained, it is necessary to make an approximation to the partial derivative of vorticity with respect to time. One method is

to use central differences with respect to the time steps so that

$$\left.\frac{\partial W}{\partial T}\right|_{i,j}^{p} \simeq \frac{W_{i,j}^{p+1} - W_{i,j}^{p-1}}{2E} \tag{68}$$

where the superscript indicates the number of the time step. The other terms in equation (22) could then be approximated by central differences with respect to the spatial variables, at the p-th time step. It would then be possible to solve for $W_{i,j}^{p+1}$ explicitly in the form

$$W_{i,j}^{p+1} = W_{i,j}^{p-1} + 2E\ \Gamma_{i,j}(S^{p},W^{p}) \tag{69}$$

where E is the size of the dimensionless time step, and $\Gamma_{i,j}(S^{p},W^{p})$ is a function of values of S and W at i,j and adjacent points. This procedure yields the values of vorticity at the (p+1)th time step based upon the values of vorticity at p-1 and p and S at p. The values of S at p+1 could then be determined from equation (66). It has been shown that in order for this explicit method of integration in time of parabolic types of equations to be stable, the maximum time step, is of the form

$$E_{max} = \lambda H^{2} \tag{70}$$

where $\lambda$ is a parameter which depends upon the exact form of the partial differential equations [15], [5]. This restriction means that in practice it would be necessary to take a time step smaller than $\lambda H^2$ in order to be conservative. This restriction is not a property of the partial differential equations directly, but occurs because the numerical approximation scheme is explicit with respect to time.

If an implicit method on time is used, the stability criterion is much less stringent and for some cases the method may be unconditionally stable. In fact, the optimum time step for an implicit method is approximately the same as the maximum time step in the explicit method [12]. Also, there is an indication that an implicit method can more truly reproduce the nonlinearities of the liquid flow [33].

An implicit method which was presented and used by Thompson [33] was used in this study. It has the advantage of being simple enough to be easily used for computer calculations and still retain the inherent advantages of implicit methods. For this case, we use a backward difference approximation to the partial derivative with respect to time which has an error of order $E^2$.

$$\frac{\partial W_{i,j}^{p}}{\partial T} \simeq \frac{3W_{i,j}^{p} - 4W_{i,j}^{p-1} + W_{i,j}^{p-2}}{2E} \tag{71}$$

Introducing the following abbreviations

$$FD(X)Y + FB(X) = DiY$$

$$FD(X) = DiD$$

$$FW(X) = DiV \tag{72}$$

$$FB(X) = DiB$$

and using central difference approximations to the spatial derivatives with G(X,Y) and its derivatives given by (21), equation (22) is approximated by

$$\frac{3W_{i,j} - 4W^{p-1}_{i,j} + W^{p-2}_{i,j}}{2E} - \frac{WDY}{4H^2DiD}[S_{i,j+1} - S_{i,j-1} +$$

$$G(S_{i+1,j} - S_{i-1,j})] + \frac{1}{4H^2(DiY)(DiD)}(S_{i+1,j} -$$

$$S_{i-1,j})\cdot[W_{i,j+1} - W_{i,j-1} + G(W_{i+1,j} - W_{i-1,j})] =$$

$$\frac{1}{H^2RN}\left\{[\frac{1}{DiD^2} + G^2](W_{i+1,j} + W_{i-1,j} - 2W_{i,j}) \right. \tag{73}$$

$$+ \frac{H\cdot WDY}{2\ DiD} + W_{i,j+1} + W_{i,j-1} - 2W_{i,j} + \frac{H}{2}(G_x+GG_y)\cdot$$

$$(W^p_{i+1,j} - W^p_{i-1,j}) + \frac{G}{2}(W_{i+1,j+1} - W_{i+1,j-1} - W_{i-1,j+1}$$

$$\left. + W_{i-1,j-1}\right)$$

where the quantities without superscripts are at the p-th time step. Solving this equation for $W_{i,j}$

$$[3 + \frac{4E}{H^2RN}(1 + \frac{1}{DiD^2} + G^2)]W_{i,j} = 4W_{i,j}^{p-1} - W_{i,j}^{p-2}$$

$$+ \frac{E \cdot WDY}{2H^2(DiD)}[S_{i,j+1} - S_{i,j-1} + G(S_{i+1,j} - S_{i-1,j})]$$

$$- \frac{E}{2H^2(DiY)(DiD)}(S_{i+1,j} - S_{i-1,j})[W_{i,j+1} - W_{i,j-1} +$$

$$+ G(W_{i+1,j} - W_{i-1,j})] + \frac{2E}{H^2RN}\left\{(\frac{1}{DiD^2} + G^2)(W_{i+1,j}+ \right. \quad (74)$$

$$W_{i-1,j}) + \frac{H \cdot WDY}{2\ DiD} + W_{i,j+1} + W_{i,j-1} + \frac{H}{2}(G_x+G_yG) \cdot$$

$$(W_{i+1,j} - W_{i-1,j}) + \frac{G}{2}(W_{i+1,j+1} - W_{i+1,j-1} - W_{i-1,j+1}$$

$$\left. +W_{i-1,j-1})\right\} .$$

From equation (74) it may be seen why this method is called implicit, the values of vorticity at i,j for the p-th time step depend upon the values at the two previous time steps and stream function and vorticity at the p-th step. Therefore, an iterative procedure on the time integration as well as the spatial is needed. Using central differences on equation (23) we find that

$$2(\frac{1}{DiD^2} + G^2 + 1)S_{i,j} = (\frac{1}{DiD^2} + G^2)(S_{i+1,j} + S_{i-1,j}) +$$

$$+ \frac{H}{2}\left[G_x + GG_y - \frac{1}{(DiD)(DiY)}\right](S_{i+1,j} - S_{i-1,j}) \qquad (75)$$

$$+ S_{i,j+1} + S_{i,j-1} + \frac{G}{2}(S_{i+1,j+1} - S_{i+1,j-1} - S_{i-1,j+1}$$

$$+ S_{i-1,j-1}) + H^2 \cdot DiY \cdot W_{i,j} \cdot$$

It should be noted that the equations of motion in this problem have been reduced to only one time-dependent equation and a coupled equation in which time does not appear explicitly. The incompressibility of the liquid flow made this possible. In other types of fluid flow, where such a simplification cannot be made, the implicit methods may not have the advantage that they do in this problem.

Difference Equations for Pressure Calculations

Equation (24) may be approximated also using central differences. Let

$$SY = S_{i+1,j} - S_{i-1,j}$$

$$SYY = S_{i+1,j} + S_{i-1,j} - 2S_{i,j}$$

$$SX = S_{i,j+1} - S_{i,j-1} \qquad (76)$$

$$SXX = S_{i,j+1} + S_{i,j-1} - 2S_{i,j}$$

$$SYX = S_{i+1,j+1} - S_{i+1,j-1} - S_{i-1,j+1} + S_{i-1,j-1}$$

$$SZ = SX + G \cdot SY$$

$$SZZ = SXX + \tfrac{1}{2} H(G_X + GG_Y)SY + \tfrac{1}{2} G \cdot SYX + G^2 SYY \qquad (76)$$

$$SYZ = SYX + 2HG_Y \cdot SY + 4G \cdot SYY$$

From equation (24) then we get

$$2\left(1 + \frac{1}{DiD^2} + G^2\right)B_{i,j} = \left(\frac{1}{DiD^2} + G^2\right)\left(B_{i+1,j} + B_{i-1,j}\right)$$

$$+ B_{i,j+1} + B_{i,j-1} + \frac{H}{2}\left(\frac{1}{DiD \cdot DiY} + G_X + GG_Y\right) \cdot$$

$$\left(B_{i+1,j} - B_{i-1,j}\right) + \tfrac{1}{2} G\left(B_{i+1,j+1} - B_{i+1,j-1}\right. \qquad (77)$$

$$\left. -B_{i-1,j+1} + B_{i-1,j-1}\right) + \frac{(SZ)^2}{2(DiY)^4} - \frac{(SZ)(SYZ)}{4H(DiD)(DiY)^3}$$

$$+ \frac{(SYZ)^2}{8H^2(DiY)^2(DiD)^2} + \frac{(SY)(SZZ)}{H(DiY)^3(DiD)} - \frac{2(SYY)(SZZ)}{H^2(DiY)^2(DiD)^2} \cdot$$

Finite Difference Form of Liquid Boundary Conditions

The boundary conditions for the liquid phase not adjacent to the bubble are the same for steady state and time-dependent solutions. In the X,Y plane

i = 1 at the centerline

i = M at wall

j = 1 at X = 0

j = N at X = 2C.

The numerical form of the conditions (26) in the X,Y plane become

$$S_{1,j} = 0 \quad , \quad W_{1,j} = 0$$
$$S_{0,j} = S_{2,j} \; , \quad S_{2,j} = \frac{1}{4} S_{3,j} \tag{78}$$

where the subscript 0 corresponds to an imaginary grid line a distance H below the centerline.

The periodic end conditions (27) are

$$S_{i,1} = S_{i,N}$$
$$W_{i,1} = W_{i,N}$$
$$S_{i,0} = S_{i,N-1} \; , \quad S_{i,N+1} = S_{i,2} \tag{79}$$
$$W_{i,0} = W_{i,N-1} \; , \quad W_{i,N+1} = W_{i,2}$$

where the subscripts 0 and N+1 correpond to imaginary grid lines a distance H past the end boundaries.

At the wall in the X,Y plane the finite difference forms of conditions (28) are

$$S_{M,j} = 0.5$$
$$S_{M+1,j} = S_{M-1,j} \tag{80}$$
$$W_{M,j} = - \frac{2}{H^2 DiV} \left( \frac{1}{DiV^2} + G^2 \right) (S_{M-1,j} - 0.5)$$

The values of pressure along the boundaries in the X,Y plane may be determined by numerically integrating the expressions (30), (36) and (38) and assuming an arbitrary fixed pressure at 0,0. From equation (30), for calculations along the centerline we get

$$\frac{\partial P}{\partial X} = F_Z - \frac{1}{EH^2(DiD)^2}(3S_{2,j} - 4S^{p-1}_{2,j} + S^{p-2}_{2,j})$$

$$- \frac{1}{4H^5(DiD)^4}[(S_{2,j+1})^2 - (S_{2,j-1})^2] \qquad (81)$$

$$- \frac{1}{(RN)(DiY)(DiD)}[2(DiD\cdot H+DiB)W_{2,j} - (DiD\cdot H+DiB)W_{3,j}].$$

For steady state solution, the second term will be identically zero. Along the wall, an approximation to (36) is needed.

$$\frac{\partial P}{\partial X} = F_Z - \frac{G\cdot DiD}{2H\ RN}[W_{i,j+1} - W_{i,j-1} +$$

$$G(3W_{M,j} - 4W_{M-1,j} + W_{M-2,j})] \qquad (82)$$

$$- \frac{1}{2H(RN)(DiD)(DiY)}\Big\{3\ DiV\ W_{M,j} - 4[DiD(1-H) + DiB]\cdot$$

$$W_{M-1,j} + [DiD(1-2H) + DiB]W_{M-2,j}\Big\}.$$

At the ends, X = 0 and X = 2C, some of the quantities in (76) must be redefined such that

$$SX = S_{i,2} - S_{i,N-1}$$

$$SXX = S_{i,2} + S_{i,N-1} - 2S_{i,j} \tag{83}$$

$$SYX = S_{i+1,2} - S_{i-1,2} - S_{i+1,N-1} + S_{i-1,N-1}$$

with the other quantities remaining the same. The finite difference approximation to equation (38) then may be written as

$$\frac{\partial P}{\partial Y} = \frac{DiD}{4HE\ DiY}\left\{3(S_{i,2} - S_{i,N-1}) - 4(S^{p-1}_{i,2} - S^{p-1}_{i,N-1})\right.$$

$$+ S^{p-2}_{i,2} - S^{p-2}_{i,N-1} + G[3(S_{i+1,j} - S_{i-1,j}) - 4(S^{p-1}_{i+1,j} -$$

$$\left. S^{p-1}_{i-1,j}) + S^{p-2}_{i+1,j} - S^{p-2}_{i-1,j}]\right\} + \frac{(DiD)(SZ)^2}{4H^2(DiY)^3} - \tag{84}$$

$$\frac{(SZ)(SYZ)}{8H^3(DiY)^2} + \frac{(SY)(SZZ)}{2H^3(DiY)^2} + \frac{DiD}{2HRN}[W_{i,2} - W_{i,N-1} +$$

$$G(W_{i+1,j} - W_{i-1,j})] \ .$$

Finite Difference Form of Bubble Boundary Conditions

Since in the X,Y plane, the bubble interface is a line segment on the X axis, it is convenient to redefine the symbols used in (76) as

$$SX = S_{i,j+1} - S_{i,j-1} \tag{85}$$

$$SXX = S_{i,j+1} + S_{i,j-1} - 2S_{i,j}$$

$$SY = -3S_{i,j} + 4S_{i+1,j} - S_{i+2,j}$$

$$SYY = 2S_{i,j} - 5S_{i+1,j} + 4S_{i+2,j} - S_{i+3,j}$$

$$SYX = -3(S_{i,j+1} - S_{i,j-1}) + 4(S_{i+1,j+1} - S_{i+1,j-1}) - (S_{i+2,j+1} - S_{i+2,j-1}) \tag{85}$$

$$SZ = SX + G \cdot SY$$

$$SZZ = SXX + \tfrac{1}{2} H(G_x + GG_y) SYS + \tfrac{1}{2} G \cdot SYX + G^2 SYY$$

$$SYZ = SYX + 2HG_y SY + 4G\, SYY$$

The finite difference form of equation (46) then is

$$P_{i,j} = P_{in} - \frac{1}{WN}\left[\frac{1}{\rho_1} + \frac{1}{\rho_2}\right] + \frac{1}{RN\left[1 + \left(\frac{dFB}{dX}\right)^2\right]} \left\{ \frac{SZ}{H(DiB)^2} - \frac{SYZ}{2H^2(DiD)(DiB)}\left[1 - \left(\frac{dFB}{dX}\right)^2\right] + 2\left[\frac{SY}{2H(DiY)^2(DiD)} - \frac{SYY}{H^2(DiD)^2(DiB)} + \frac{SZZ}{H^2(DiB)}\right]\frac{dFB}{dX} \right\}. \tag{86}$$

This equation yields the pressure in the liquid at the bubble surface.

Since equation (24) must also be satisfied at the bubble surface a finite difference form of this equation

can be used to solve for the stream function at the bubble surface. Forward difference approximations to derivatives with respect to Y must be used. Since the pressure at the bubble surface is determined at the surface by equation (86), a quadratic algebraic equation for $S_{i,j}$ results. See the appendix for development of this expression and forms for $A_1$, $B_1$ and $C_1$.

$$S_{1,j} = \frac{-B_1 + \sqrt{B_1^2 - 4A_1C_1}}{2A_1} \tag{87}$$

The zero shearing stress condition at the bubble surface, equation (50), will be satisfied by making the usual finite difference approximations and then solving for $S_{2,j}$ from the resulting algebraic equations. Thus we obtain

$$\left\{\frac{1}{DiD}[SYX + 2H\,G_y(-3S_{1,j} + 4S_{2,j} - S_{3,j}) + 4G(2S_{i,j} - 5S_{2,j} + 4S_{3,j} - S_{4,j})] - \frac{H\cdot SX}{DiB} + \right.$$

$$\left. - \frac{HG}{DiB}(-3S_{i,j} + 4S_{2,j} - S_{3,j})\right\} \frac{dFB}{dX} \tag{88}$$

$$- [(\frac{1}{DiD^2} - G\,)(2S_{1,j} - 5S_{2,j} + 4S_{3,j} - S_{4,j})$$

$$- \frac{H}{2}(\frac{1}{DiD\cdot DiB} + G_x + G_yG)(-3S_{i,j} + 4S_{2,j} - S_{3,j}) +$$

$$- SXX - \tfrac{1}{2} G \cdot SYX][1 - (\frac{dFB}{dX})^2] = 0 \tag{88}$$

and from this,

$$S_{2,j} = - B_2/A_2 \tag{89}$$

where

$$A_2 = [\frac{8G_yH}{DiD} - \frac{20G}{DiD} - \frac{4HG}{DiB}]\frac{dFB}{dX} + [5(\frac{1}{DiD^2} - G^2)$$

$$+ 2H(\frac{1}{DiY \cdot DiD} + G_x + G_yG)][1 - (\frac{dFB}{dX})^2]$$

$$B_2 = [\frac{SYX}{DiD} + \frac{2G_yH}{DiD}(-3S_{1,j} - S_{3,j}) +$$

$$\frac{4G}{DiD}(2S_{1,j} + 4S_{3,j} - S_{4,j}) - \frac{H \cdot SX}{DiY}$$

$$- \frac{H \cdot G}{DiY}(-3S_{1,j} - S_{3,j})] + \frac{dFB}{dX}$$

$$- [(\frac{1}{DiD^2} - G^2)(2S_{1,j} + 4S_{3,j} - S_{4,j})$$

$$- \frac{H}{2}(\frac{1}{DiY \cdot DiD} + G_x + G_yG)(-3S_{1,j} - S_{3,j})$$

$$- SXX + \tfrac{1}{2} G \cdot SYX][1 - (\frac{dFB}{dX})^2].$$

The vorticity at the bubble surface can be calculated using forward differences in equation (23).

$$W_{i,j} = -\frac{1}{H^2 DiB}\left\{\frac{SYY}{DiD^2} - \frac{H\ SY}{2(DiD)(DiB)} + SZZ\right\} . \qquad (90)$$

For a completely spherical bubble in which surface tension forces are very large, the pressure boundary condition (86) is not suitable and the pressure need not enter the calculations explicitly. The stream function distribution on the bubble surface is specified in terms of the translational velocity of the bubble according to equation (56). Therefore, for this case, equation (87) must be replaced by an integration along the bubble in the X,Y plane.

At grid points not at either end of the bubble

$$S_{1,j} = S_{1,j-1} + H\ V_T\ FB(Z-H/2)\ FB(Z-H/2), \qquad (91)$$

where $V_T$ is the translational velocity of the bubble. At each end of the bubble, special formulas are needed when the bubble does not end on a grid line. At the end of the bubble nearer the origin of the axes, for the first grid point on the bubble

$$S_{1,j} = \frac{(1-\alpha)^2}{\alpha(\alpha-2)}\ S_{1,j+1} + \frac{(1-\alpha)}{\alpha}\ H\ FB(X)\ \frac{dFB}{dX}\ V_T , \qquad (92)$$

where $(1-\alpha)$ is the fraction of one grid width between the point in question and the end of the bubble. Equation (92) takes into account the fact that on the centerline S=0. At the other end of the bubble, for the last grid point on the bubble,

$$S_{1,j} = \frac{(1-\beta)^2 S_{1,j-1}}{\beta(\beta-2)} - \frac{(1-\beta)}{\beta} H\, FB(X)\, \frac{dFB}{dX}\, V_T \,, \qquad (93)$$

where $(1-\beta)$ is the fraction of a grid width between the point in question and the end of the bubble. Again, equation (93) includes the effect of S=0 on the centerline.

# IV COMPUTER SOLUTIONS TO DIFFERENCE EQUATIONS

Three basic computer programs were used to solve the difference equations in Chapter III. These programs were written for (1) the steady state flow of liquid only, (2) the time-dependent flow of liquid only and (3) the time-dependent flow of liquid containing gas bubbles. Fortran IV coding was used and the programs run on the University of Alabama's IBM 360 Model 50 computer and the UNIVAC 1108 located at the University Research Institute in Huntsville, via the remote terminal at the Tuscaloosa campus.

## Steady State Program

Figure 5 is a flowchart for the steady state program. The calculations were started by reading the parameters governing the fluid flow, tube geometry and numerical grid and making an initial guess for S and W which was similar to that of fully developed laminar flow in a tube. Gauss-Seidel iteration with a relaxation factor was then used to iterate to a steady state solution when possible. With a converged solution for S and W, the pressure and velocities were calculated from subprograms. The data were then printed in tabular form and as plots drawn using special

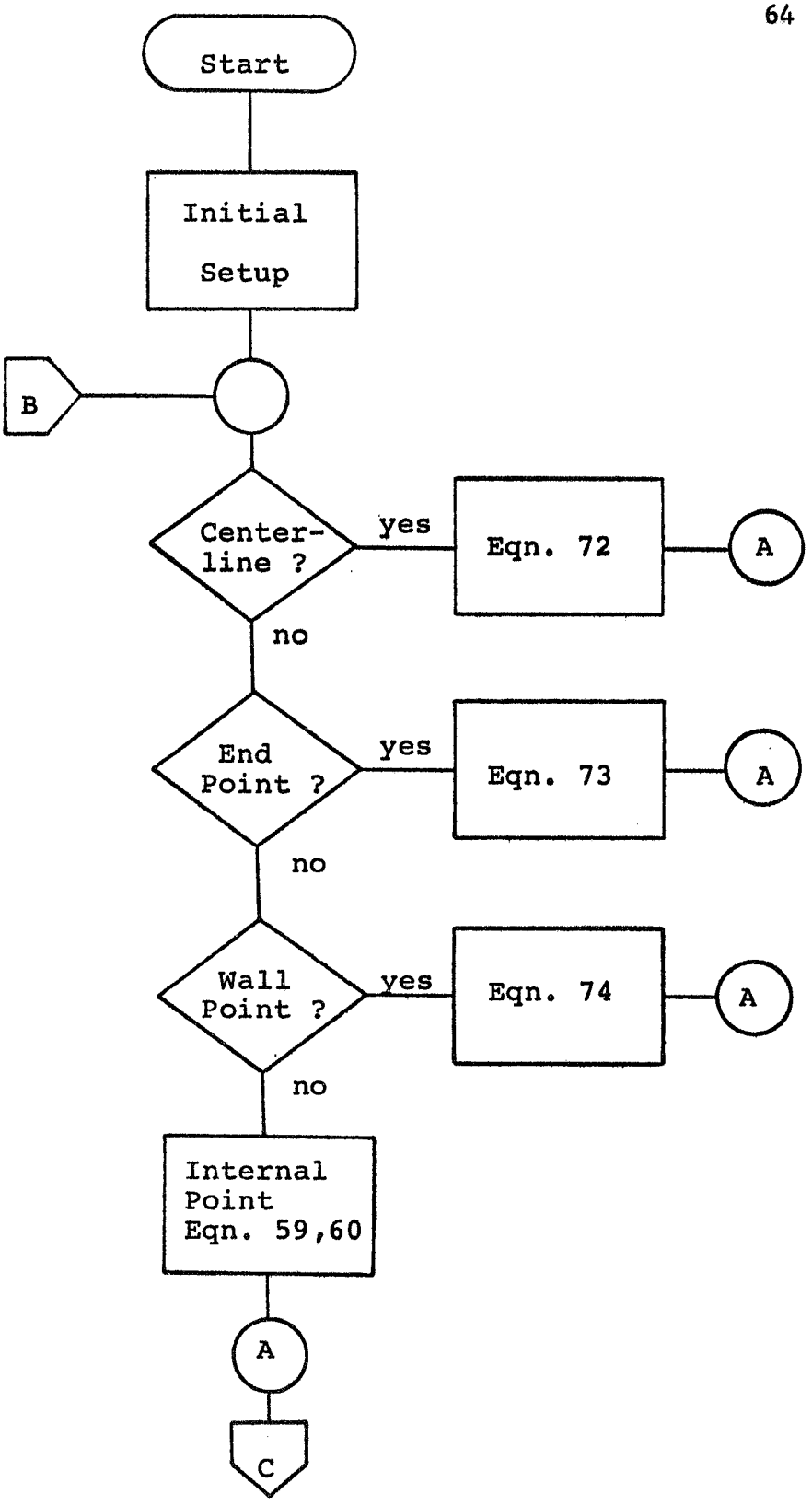


Figure 5a. Flowchart for Steady State Program

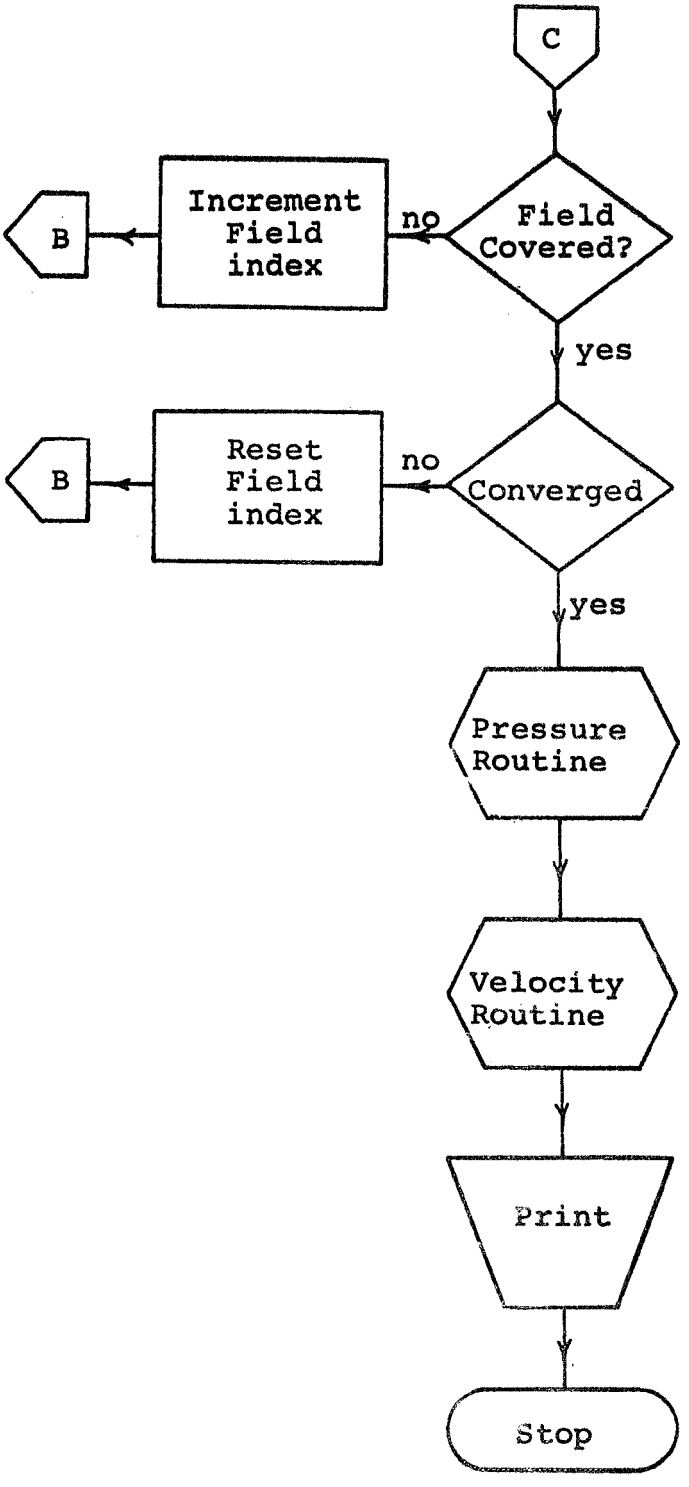


Figure 5b. Flowchart for Steady State Program (con't)

routines for the standard on-line printers. To improve the efficiency of the calculations, for a fixed tube geometry and grid size, calculations for several different Reynolds numbers were made during one computer run. For all Reynolds numbers after the first, the flow field for the previous Reynolds number was used as a guess for getting the next iteration started. Typical run times on the IBM machine for a particular solution with a grid mesh of 11 by 21 were from three to five minutes.

Time-Dependent Program

A flowchart for the program for time-dependent flow without gas bubbles is given in Figure 6. The usual method of starting the calculations in this case was to assume that for time less than zero the fluid was at rest and at time zero require the flowrate to be a constant. Since the fluid was initially at rest, the flow was everywhere irrotational at time zero, except at the wall. This means that the initial vorticity would be everywhere zero except at the wall where a region of concentrated vorticity would exist due to the no slip condition. In this type of start-up, the main flow field is potential with a viscous boundary layer near the wall which grows until a fully developed viscous flow fills the entire tube. The advantage of this type of initial condition is that it is physically reasonable and that in the computer program one

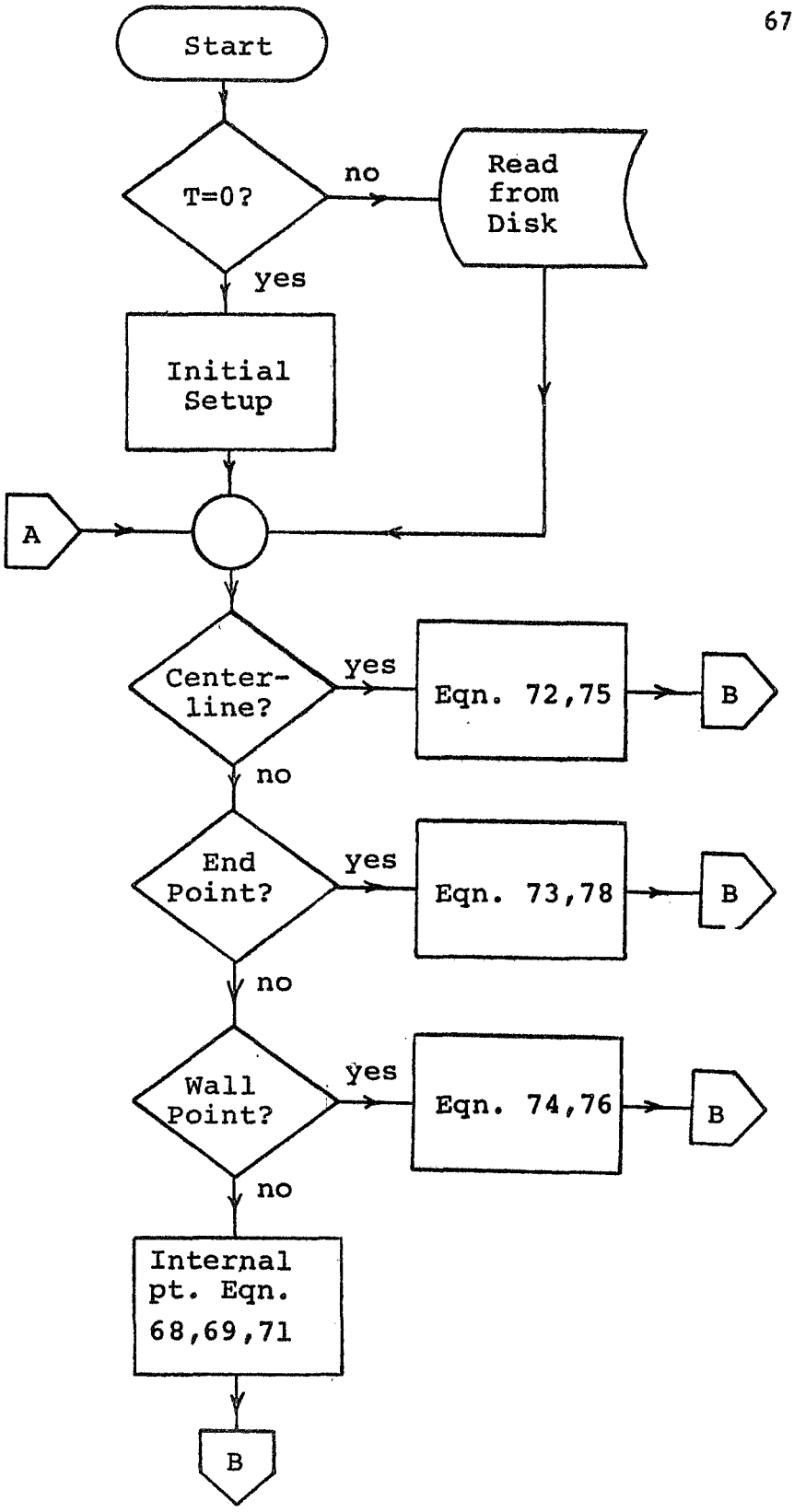


Figure 6a. Time-Dependent Program for Liquid Flow Only

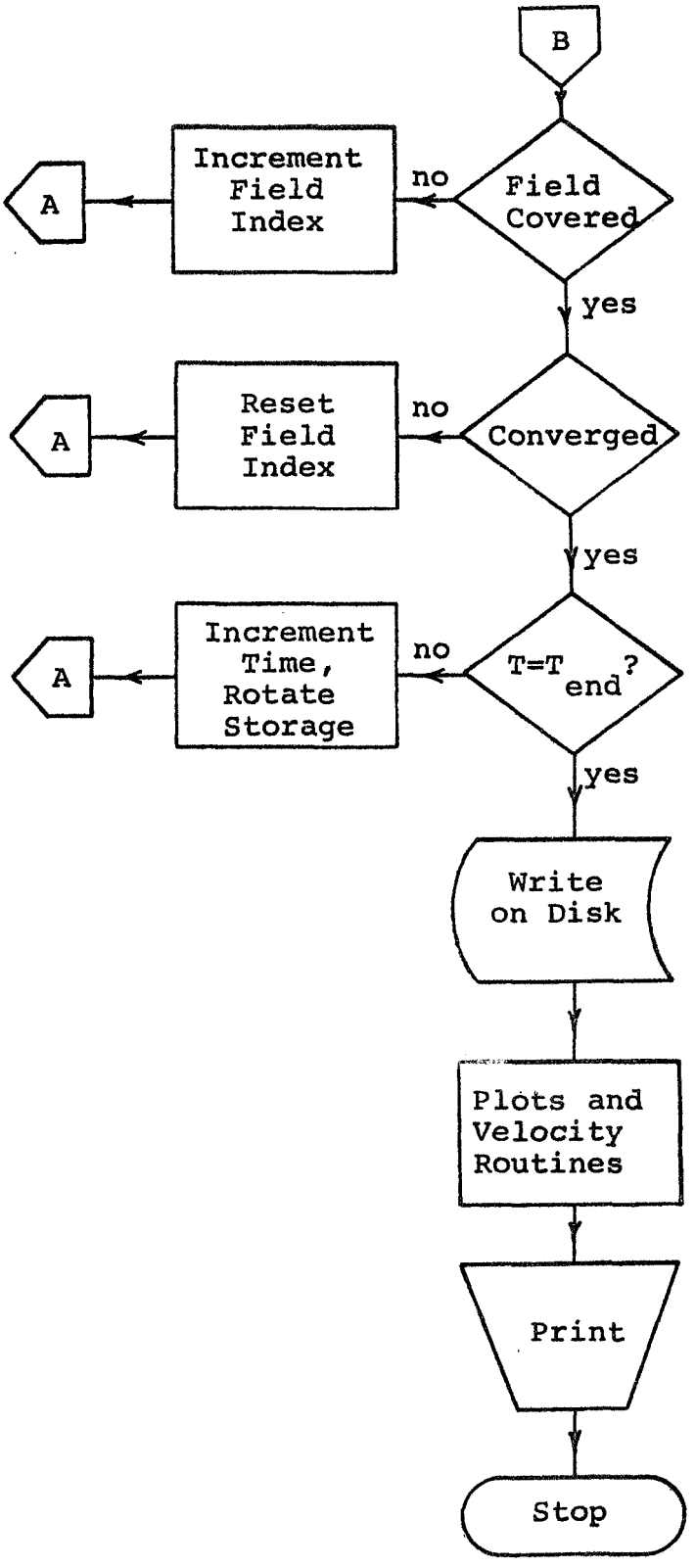


Figure 6b. Time-Dependent Program for Liquid Flow Only (con't)

simply sets the vorticity to zero in the main field and at the wall calculates the vorticity by equation (80).

Iteration on the time integration as well as the spatial integration was required because the difference equations were implicit on time. To speed up the convergence process, Gauss-Seidel iteration with a relaxation parameter was used. Also a variable time step was used [5]. When the number of iterations required for convergence at a given time step were less than an arbitrary number, usually two, the time step was doubled. When it was greater than an arbitrary number, usually twenty-five, the time step was halved.

Since the IBM machine was more accessible than the UNIVAC, although considerably slower, these runs were made on the IBM machine in short blocks of approximately twenty minutes by storing the data at the end of one run on a direct access disk and restarting at that point with the next run. Using this method, approximately one hour of running time was needed to reach a reasonably steady state with 11 by 21 grid mesh. The data were printed at selected times in the form of tabulated data, streamline and velocity plots.

## Bubble Program

The calculation of flows with gas bubbles includes all of the features of the time-dependent calculations described in the previous section with the additional

requirements that the bubble boundary conditions be satisfied and the location of the bubble be determined by integrating the velocity in time. For the calculations in which the pressure boundary condition was used for the bubble, the pressure field was calculated along with the stream function and vorticity. Figure 7 is a flow-chart of the computer program to perform the calculations. As indicated in Figure 7, the calculations for points away from the bubble are the same as for time-dependent flow without bubbles.

The calculations on the bubble surface were performed from separate subprograms. Figure 8a is a flowchart for the calculations using the pressure boundary condition. The pressure inside was calculated from equation (86), using the pressure in the liquid at the tail of the bubble which was known from the integration of equation (81). At the nose a reverse process was used, since the pressure inside the bubble was constant, to obtain the pressure in the liquid at the centerline so that the integration of equation (81) could continue. The pressure, stream function and vorticity near the bubble were calculated from equations (86), (87), (89) and (90) as described in Chapter III.

Figure 8b is a flowchart for the bubble surface subprogram using the velocity boundary condition for a spherical bubble. The translational velocity of the

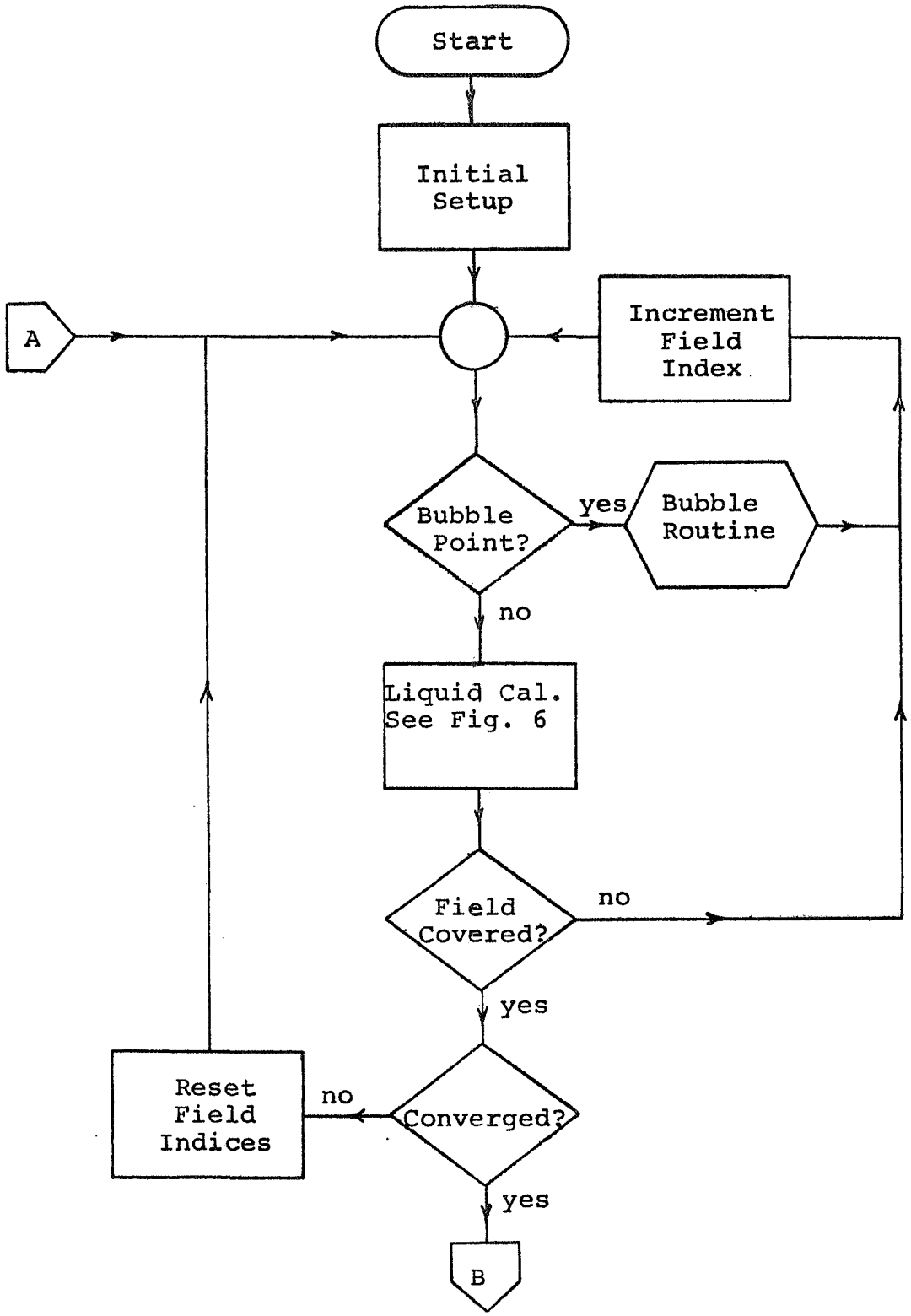


Figure 7a. Flowchart for Main Bubble Program

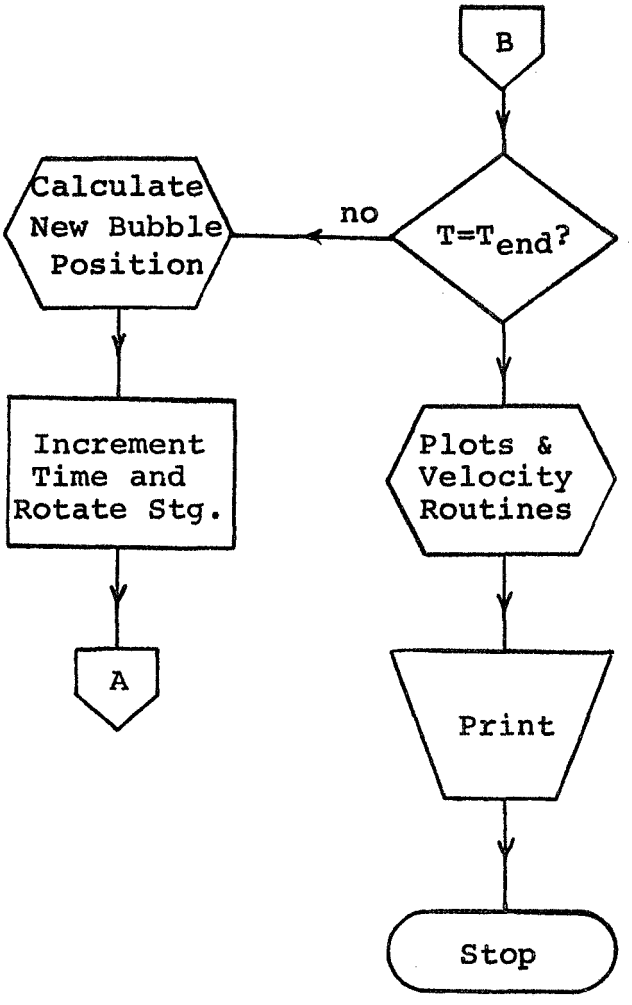


Figure 7b. Flowchart for Main Bubble Program (con't)

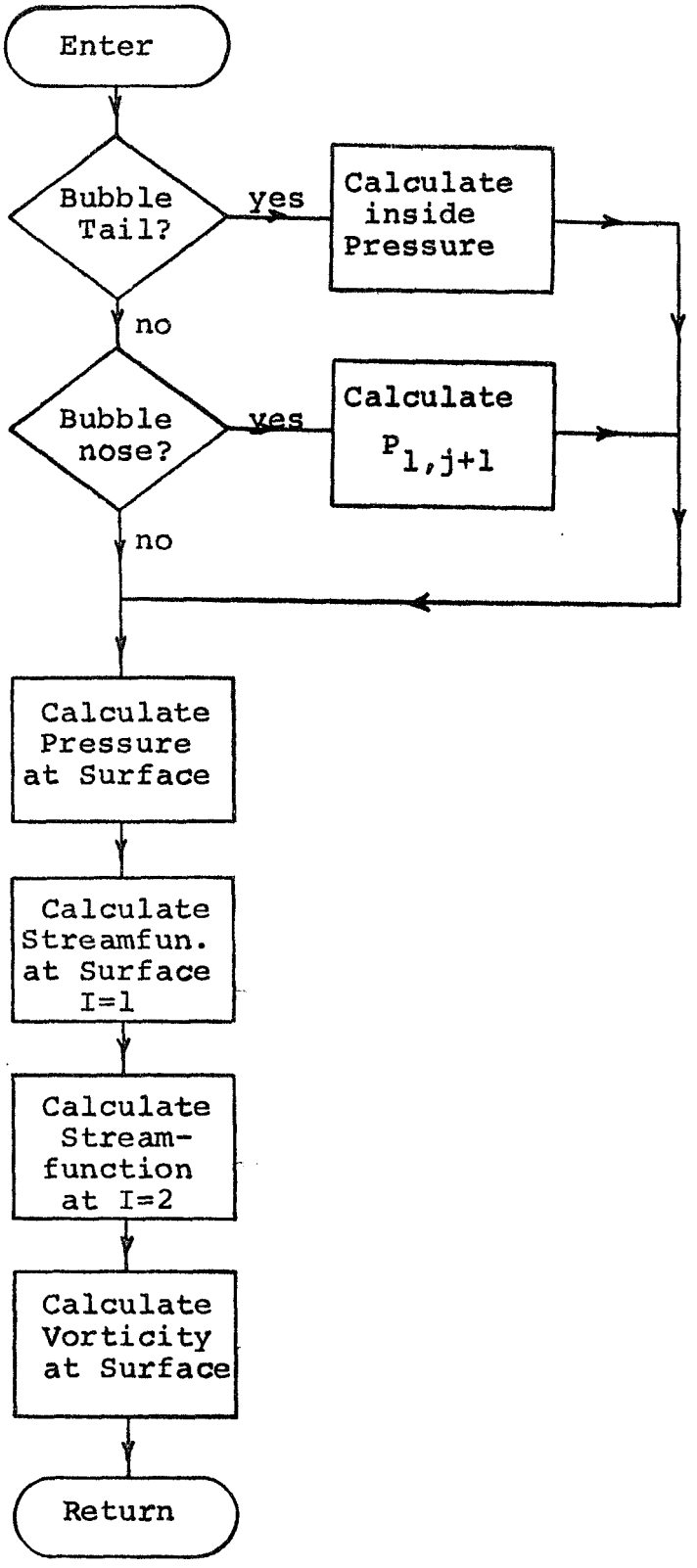


Figure 8a. Flowchart for Bubble Surface Subprogram with Pressure Boundary Condition

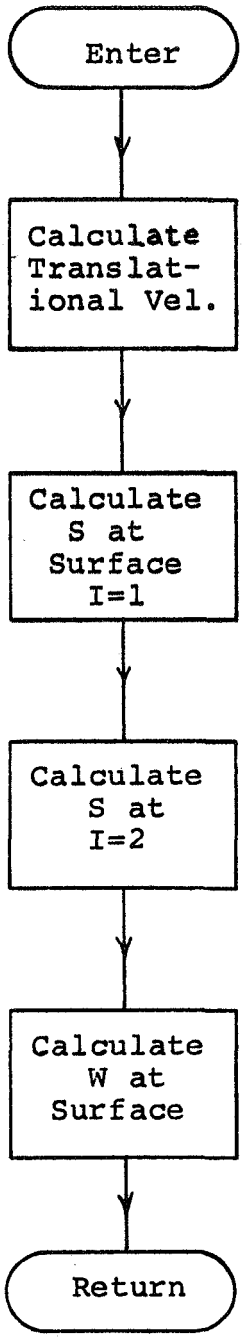


Figure 8b. Flowchart for Bubble Surface Sub-program with Velocity Boundary Condition

bubble was obtained by taking the average of the velocity calculated at the end of the bubble. The stream function distribution in the liquid flow one grid width away from the centerline was linearly extrapolated to each end of the bubble to determine these velocities. Since the flow pattern was quite different at the two ends of the bubble, these velocities did not agree in general. This is a limitation of the finite difference approximations and the translational velocity was assumed to be the average of the two. From this value of the translational velocity, the stream function on the bubble surface was obtained. The iterations were carried out until agreement between the bubble boundary conditions, the translational velocity, and the liquid flow was obtained.

Because of the nature of the transformation used, it was necessary to keep a bubble positioned so that neither end was very close to a grid line. This was accomplished in the computer programs by letting the bubble move only in specified increments and choosing the bubble radius correctly. Best results were obtained by taking the increment as one grid width. The bubble was not allowed to move until the integral of the velocity in time became equal to or greater than the specified increment. After the bubble was moved to a new position, the integral or displacement function was reduced by the bubble increment and allowed to build up again until the next bubble increment. The number

of time steps between bubble increments varied from three to seven, depending upon the translational velocity.

To improve the convergence of the calculations for the case of the pressure boundary condition on the bubble a special iteration procedure was used. The method used was that at the beginning of a given time increment, including the first, the values for stream function, S, on the bubble surface were held fixed until the rest of the field converged by iteration. Then the values of S on the bubbles were relaxed to be compatible with the rest of the flow field. Finally, the standard Gauss-Seidel iteration method was used until convergence was obtained. Then time was advanced, and the above procedure repeated.

# V RESULTS

The function which describes the shape of the tube has been assumed to be a general continuous periodic function of the distance along the tube axis. However, for the numerical computations in this study the particular function used was

$$FB(Z) = 1-A \cos(\pi Z/C)$$

with the value of C taken to be one. By varying the value of A, different degrees of "waviness" could be obtained. Although data were obtained for values of A from zero to one-half, that presented in this chapter are for A=0.25, except for some bubble results for A=0. This degree of waviness was chosen arbitrarily since the qualitative aspects of the flows do not change with variations of A in the region investigated and more meaningful comparisons can be made by using the same value of A.

## Steady State Flow

Figures 9, 10 and 11 are streamline plots from a standard digital printer with streamlines drawn in by

hand. The subroutine which generated this output used linear interpolation to find the location of specified values of stream function. A unique digit was used for each streamline although the digit does not necessarily have any relation to the value of stream function.

Figures 9, 10 and 11 show the effect of increasing Reynolds number on steady state solutions for a fixed tube geometry. For sufficiently low Reynolds number, the flow is completely attached everywhere in the tube as shown in Figure 9. Although the Reynolds number is only 5 in this case, the flow pattern is slightly unsymmetrical, showing the effect of fluid inertia.

In Figure 10 a separated flow region has developed in the diverging section of the tube, indicated by the closed streamline for S=0.5. Since this is a steady state solution, this corresponds to a ring vortex standing in the diverging cross sections of the tube.

In Figure 11, for Reynolds number 20 and the same tube geometry, the separated flow region has grown to fill almost all of the "valley" formed by the diverging section. From the streamline pattern, it is seen that the effective flow area is determined by the minimum radius of the tube.

Figure 12 is a plot of dimensionless axial pressure gradient times Reynolds number versus Reynolds number for three values of A. The dotted line is the pressure drop

relationship predicted analytically for A=0, that is, Poiseuille flow. This plot shows that the effect of increased tube "waviness" is a rather large increase in pressure loss.

It was found that in order to obtain convergent steady state solutions, it was necessary to reduce the relaxation parameter $\omega$ as the Reynolds number was increased. The values plotted on Figure 12 include the maximum Reynolds number for which solutions were obtained by using values of $\omega$ from 1.0 to a minimum of 0.5 Most of these calculations were made with a grid width H of 0.1.

Time-Dependent Flow of Liquid Only

Figure 13, 14 and 15 are streamline plots for a Reynolds number of 25 and A=0.25 for three different values of dimensionless time, with time measured from the impulsive start described in Chapter II. These plots were drawn using the same technique as for the steady state case.

Figure 13 is for T=0.02, which is very soon after start-up. The flow pattern is symmetrical with respect to the center of the section since the main flow is potential flow at this time, with a thin viscous boundary layer near the wall. At a later time, T=0.50, in Figure

14 the flow has become separated in the diverging section with a corresponding shift in the other streamlines. In Figure 15, the flow has approached a steady state pattern for T=5.0. Concerning the dimensionless time scale, a value of T=1.0 corresponds to the physical time required for a particle moving with the average fluid velocity to move a distance of one tube radius.

Exact quantitative correspondence between the steady state solutions and time-dependent solutions for large values of time was not obtained. This can be seen by comparing Figures 11 and 15. Although the Reynolds number is 25 for the time-dependent solution shown in Figure 15, a comparison can be made with the steady state solution of Figure 11 which is for a Reynolds number of 20. The vortex in Figure 15 is smaller than the one in Figure 11, but a decrease in the Reynolds number from 25 to 20 would result in a still smaller vortex. This difference is expected since the time-dependent solutions were not carried to a steady state due to the excessive computer time required. However, another source of difference is that the iteration procedures and equations for steady state and time-dependent solutions were completely different. The intermediate iterations to a steady state solution have no physical significance whereas the time-dependent solution models

the physical flow at each time step. Also, after dropping the time derivatives from the time-dependent equations, algebraic manipulations were performed to yield suitable iteration equations for the steady state case. The resulting equations were of a rather different form than the differential equations, as was pointed out in Chapter III. However, the steady state solutions and time-dependent solutions for large values of time do agree qualitatively for the results obtained.

Figure 16 shows velocity profiles in the X,Y plane for four cross sections in the tube. These data correspond to the streamline plots of Figure 14. The effect of convergence and divergence of the tube and the fluid inertia may be seen by the different shapes of the velocity profiles for the four cross sections chosen. For flow with no inertia effects identical profiles would exist for X=C/2 and X=3C/2.

Time-Dependent Flow with Bubbles

Although numerical solutions for arbitrary bubble shapes were not obtained and only limited solutions for spherical bubbles with the pressure boundary condition were obtained, the case of spherical bubbles with the velocity boundary condition for several values of the parameters was numerically solved. In this section some

of the solutions are presented and in the following section the principal difficulties encountered in the bubble calculations are discussed.

For the case of spherical bubbles using the pressure boundary condition, the Weber number was taken to be numerically very small and the bubble assumed to be spherical. These results presented here are for a straight wall tube, and the extension to a wavy wall tube is straight forward. The parameters governing the flow were systematically varied in seeking convergent solutions. Although solutions for more than the first few fime steps were not obtained, it was found that best results were obtained for Reynolds numbers of from 10 to 50 and for dimensionless body force values for from 2 to 5. These values of body force would decrease the velocity of a bubble relative to the average fluid velocity.

Figure 17 is a streamline plot of time T=0 with a Reynolds number of 50, a bubble radius of 0.275, a Weber number of 0.005, and a body force of 3. Because the plots from the digital printer could not be drawn to the same scale in the horizontal and vertical directions the bubble does not appear as a true semicircle. Figure 18 is a streamline plot at T=0.01, after ten time steps, with the other parameters remaining the same. For later time steps the calculations began to diverge as was typical of the cases using the pressure boundary condition. Since

convergent solutions could not be obtained for more than ten time steps the solution was not extended to a wavy wall tube.

Using the velocity boundary condition, solutions were obtained for a bubble moving near one end of a typical tube section to near the other end. Since it was desired to study the motion of bubbles in a viscous flow, an approximation to a fully deveolped viscous flow pattern for the liquid was used as an initial condition. However, only the solutions for the smaller bubbles and Reynolds numbers can be considered to have approached a steady state. As the bubble size increases, the initial guess to a fully developed viscous flow is less accurate. Also, for the wavy wall cases, the above effect is combined with the effect of a bubble moving through the changing cross section of the tube. The bubbles shown in Figures 19 through 26 are all spherical, but do not appear so due to the differences in the vertical and horizontal scales of the computer plots. All of the results are for a grid of 21 by 41 with H=0.05 and E=0.002.

Figure 19 is a streamline plot for a bubble of radius 0.1375 moving with a velocity of 3.2 at this instant with the average fluid velocity being 1.0 as it is for all of the flows considered. The tube wall is

straight, that is A=0, and the Reynolds number of the liquid flow is 10. Sixty four time steps have elapsed since starting the calculations. For fully developed flow in a straight wall tube, the dimensionless velocity at the centerline is 2 so that the bubble has a velocity approximately 50% greater than the neighboring fluid particles would have if the bubble were not present. As can be seen by the streamline pattern, the general flow far away from the bubble is not greatly disturbed by the presence of the bubble.

Figure 20 is a streamline plot for flow in a straight wall tube with a liquid Reynolds number of 10 and a bubble radius of 0.1875. The bubble velocity is 7.0 and 84 time steps have elapsed since beginning the calculations. At later time steps these calculations diverged as the flow pattern became more disturbed. Perhaps a smaller grid size would have allowed the calculations to converge for the more disturbed flow, but current computer storage capacity and speed made this unfeasible. However, this flow pattern is of interest because it shows the marked change in the flow with the increase in the bubble size and Reynolds number.

Figures 21, 22 and 23 are streamline plots for a bubble of radius 0.1375 in a wavy wall tube with A=0.25. The liquid Reynolds number is 1.0. In Figure 21, the

bubble is centered at Z=0.55 and 29 time steps have elapsed since beginning the calculations. The bubble velocity at this instant is 4.0. In Figure 22, the bubble is centered at Z=1.0 and has a velocity of 2.8. At this point 94 total time steps have been taken. In Figure 23 the bubble is centered at Z=1.75 and has a velocity of 4.4. The total number of time steps at this point is 214. At this low Reynolds number and small bubble radius the general flow pattern is not greatly disturbed by the motion of the bubble as was the case for the straight wall tube with Reynolds number of 10, shown in Figure 19.

Figures 24, 25 and 26 are streamline plots for a bubble of radius 0.1875 in a wavy wall tube with A=0.25 and a Reynolds number of 10. In Figure 24 the bubble is centered at Z=0.65 and has a velocity of 5.5. Thirty four time steps have been taken at this point since the beginning of the calculations. In Figure 25 the bubble is centered at Z=1.0 and has a velocity of 6.1. The total number of time steps at this point is 64. In Figure 26 the bubble is centered at Z=1.35 and has a velocity of 7.7. Eighty nine total time steps have been taken at this point. For later times these calculations also diverged as those described in the discussion of Figure 20.

Convergent solutions were not obtained for bubbles

of larger size or for Reynolds numbers of 25 or greater except for a few time steps.

Problems Encountered in the Bubble Calculations

Three principal areas of difficulty may be identified for the case of time-dependent flow including bubbles: (1) the discontinuous derivatives of the coordinate transformation at each end of the bubble, (2) the difficulty in obtaining accurate numerical values of curvature for an arbitrary bubble shape, and (3) divergence of the calculations using the pressure boundary condition. These will be discussed separately in some detail.

Coordinate system singularity. At each end of the bubble where the tube centerline intersects the bubble surface, the derivative of the bubble radius with respect to the axial coordinate becomes infinite due to the axial symmetry. Due to the nature of the coordinate transformation used the angle between the X and Y coordinate lines in the R,Z plane at this point becomes zero and both are parallel to the R direction. Therefore, the expression for derivatives with respect to Z becomes useless. However, for numerical approximations, this singularity may be avoided if it can be arranged to have the bubble positioned so that a grid line in the Y

direction never gets very close to these critical X coordinates. This was accomplished for a spherical bubble by choosing the initial position and radius correctly and allowing the bubble to move with a constant step as described in Chapter IV. For changing bubble shape such a procedure might not be possible.

This problem would not arise if the bubble shape were not transformed to a segment of the centerline. However, using finite differences, the difficulties of the coordinate system not matching the bubble boundary lead to a tedious group of algebraic equations for the boundary conditions. This method was tried in the course of the study and because of the amount of algebraic labor involved it was rejected.

Calculations of bubble curvature. The nature of the boundary condition on pressure, equation (46), requires an accurate determination of the bubble curvature. For the case of a general bubble shape this was found to be a major problem in seeking numerical solutions. The bubble shape and position at given time can be determined by numerically integrating the velocity in time. This yields the location of a set of points on the bubble surface. From these points, the first and second derivatives of the bubble boundary with respect to the axial direction must be calculated. It is well known that the

determination of second derivatives from discrete data is subject to large error. This inaccuracy would then magnify any error in the location of points on the surface. If the bubble shape does not change and may be specified by a continuous function such as the equation of a sphere this is no longer a problem. Although other difficulties exist for the case of a general bubble shape this was the initial reason for restricting the calculations to the case of spherical bubbles.

Divergence of calculations using pressure boundary condition. If the Weber number in the pressure boundary condition (46) is made very small, the resulting bubble shape should approach that of a sphere. Because of the problems encountered in calculating curvatures, attempts were made to obtain solutions for spherical bubbles by making the Weber number in equation (46) very small with the hope of showing that the velocities obtained would result in an approximately spherical bubble. These calculations were well behaved for a number of iterations. However, after a certain number they began to diverge, Slowly at first but finally becoming meaningless. The divergence usually could be seen to begin between 50 and 100 total iterations. The cause of the divergence was not determined.

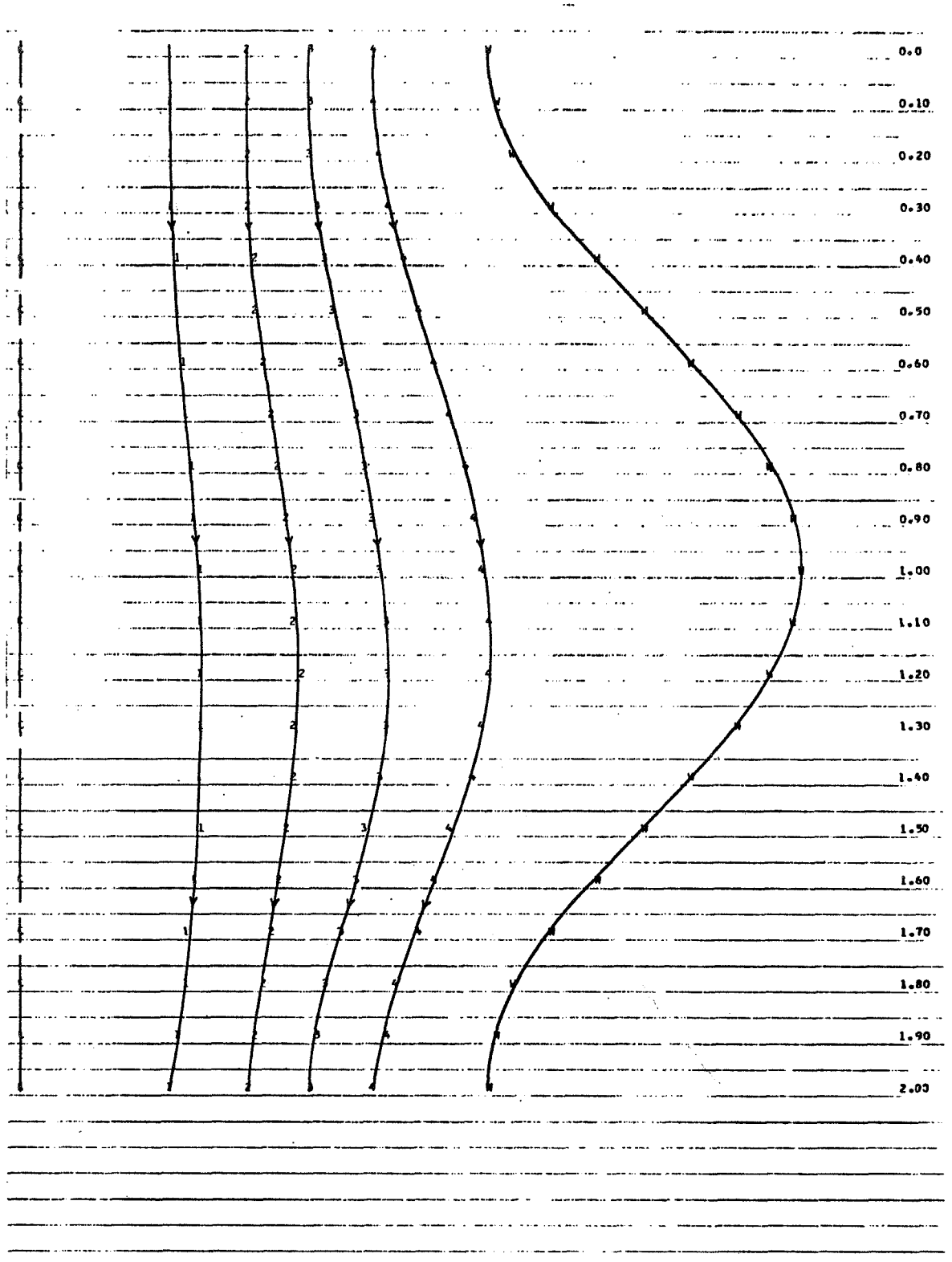


Figure 9. Streamlines for Steady State Flow
RN=5, A=0.25, C=1.0

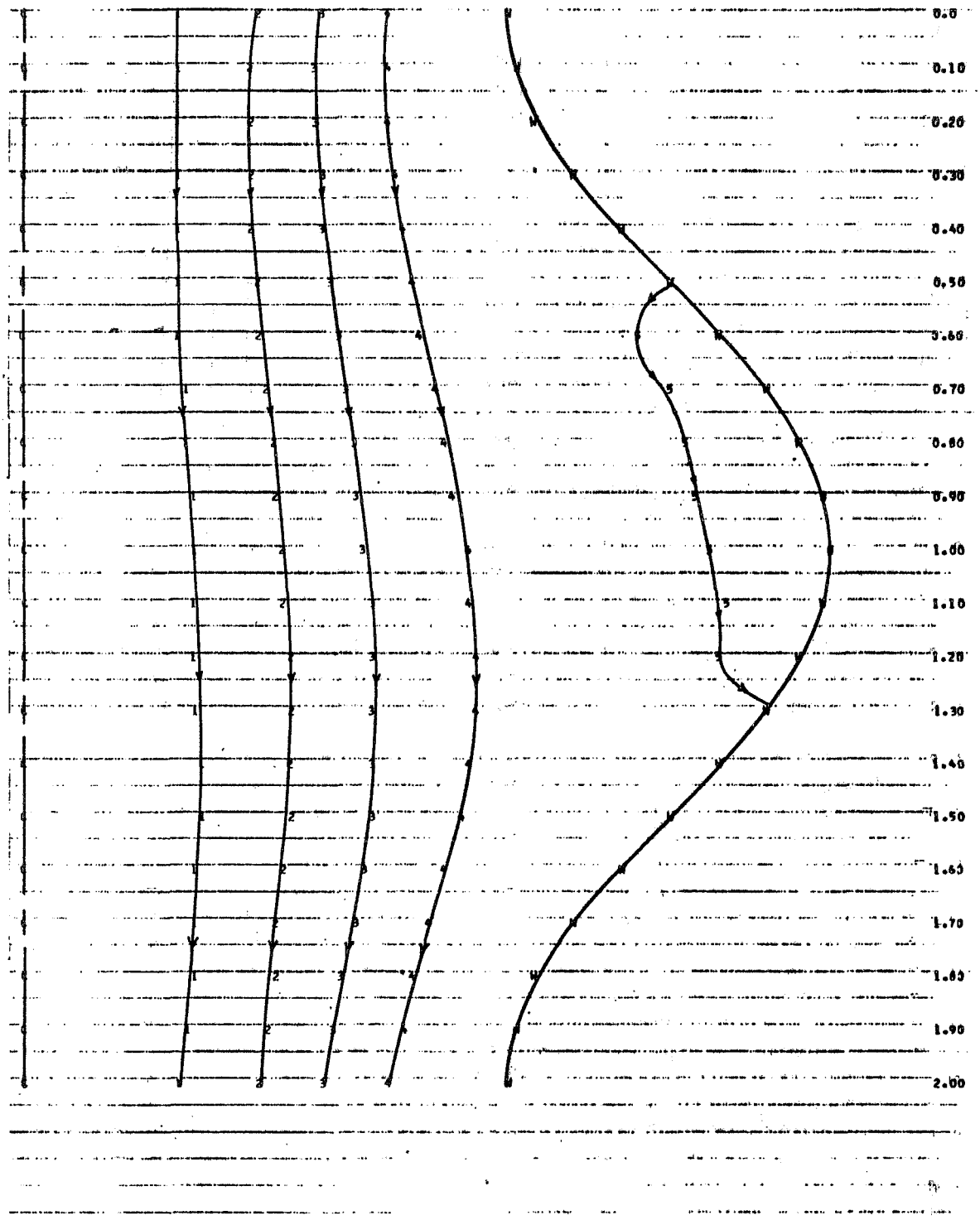


Figure 10. Streamlines for Steady State Flow
RN=10, A=0.25, C=1.0

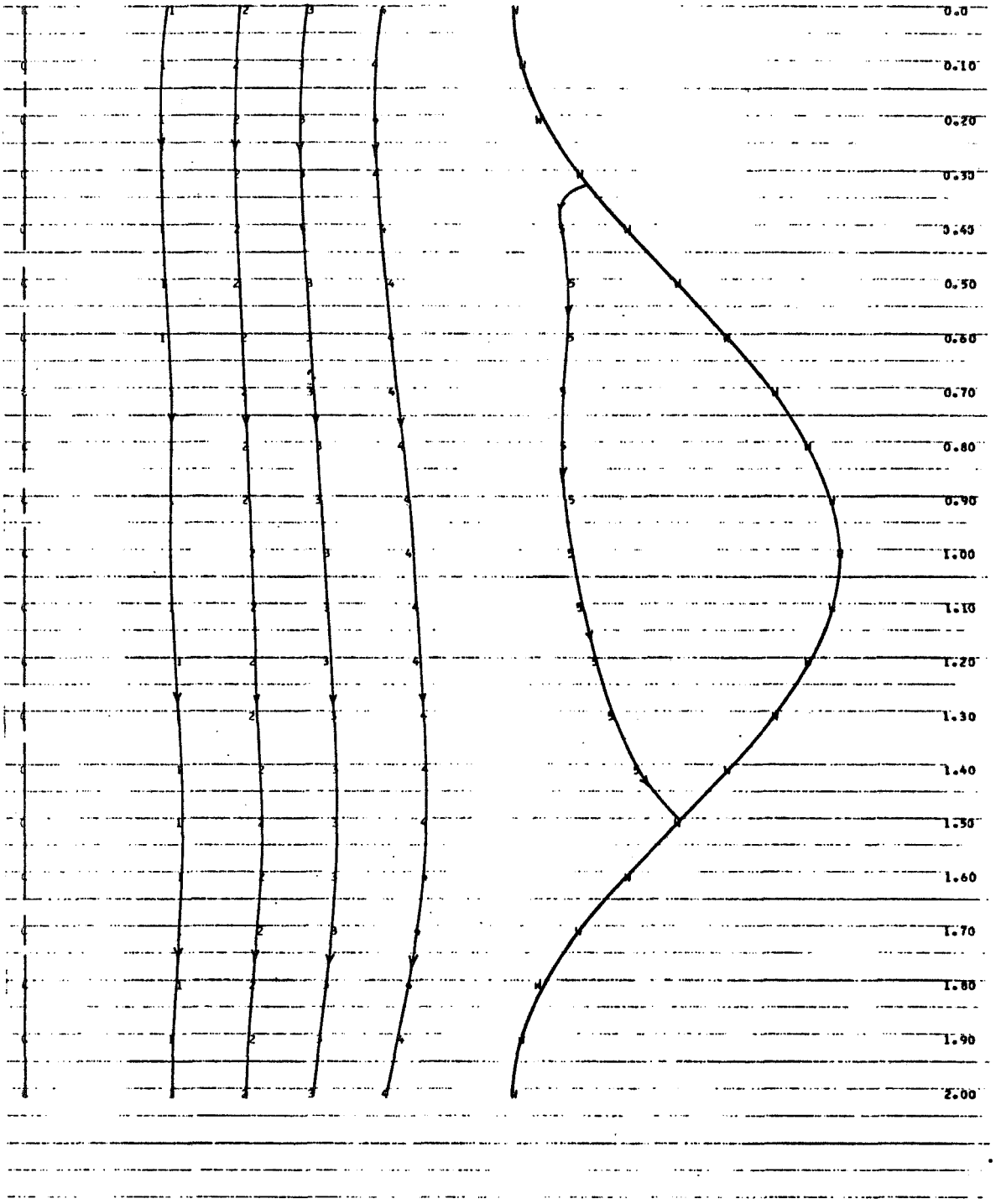


Figure 11. Streamlines for Steady State Flow
RN=20, A=0.25, C=1.0

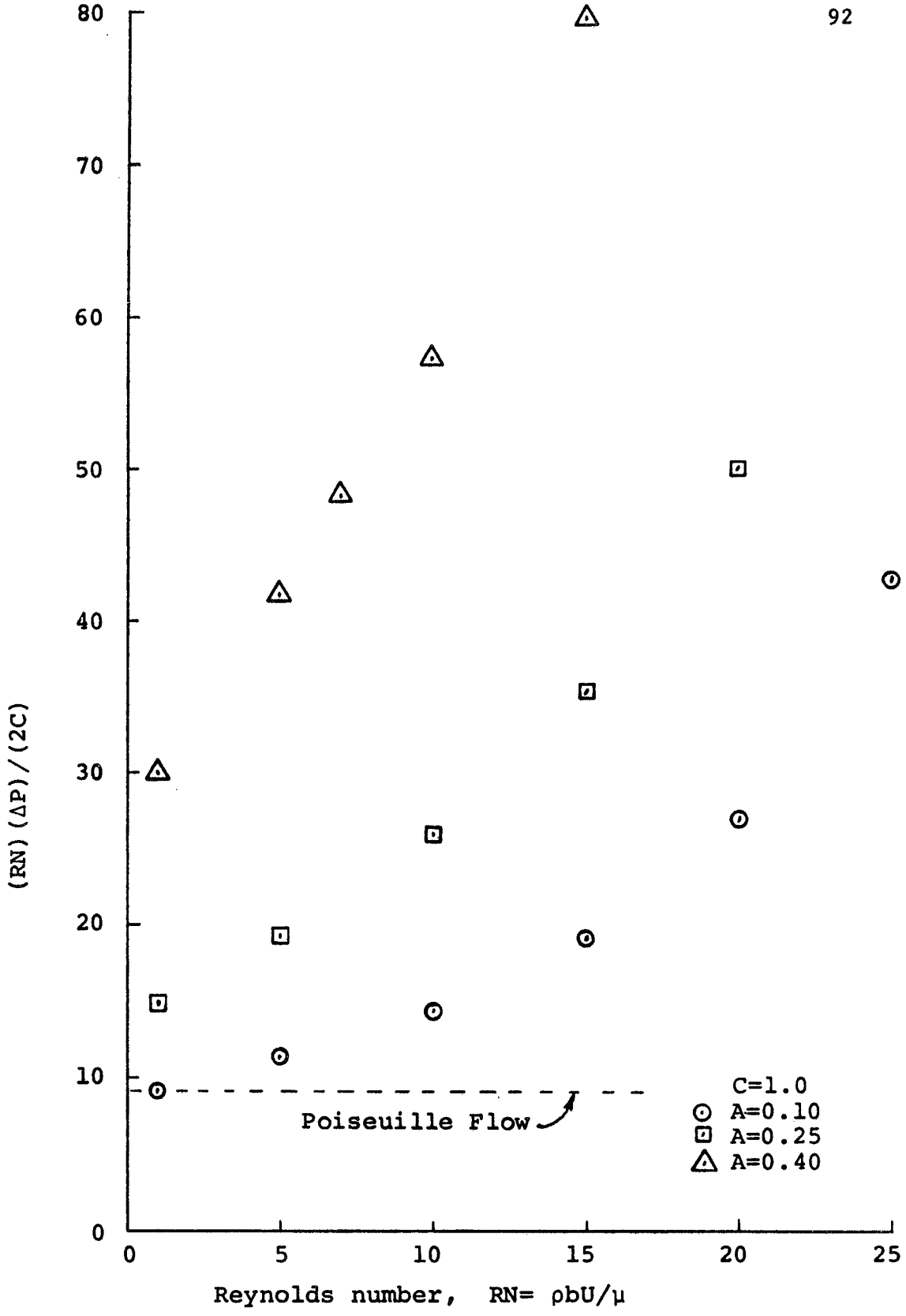


Figure 12. Pressure Drops from Steady State Solutions

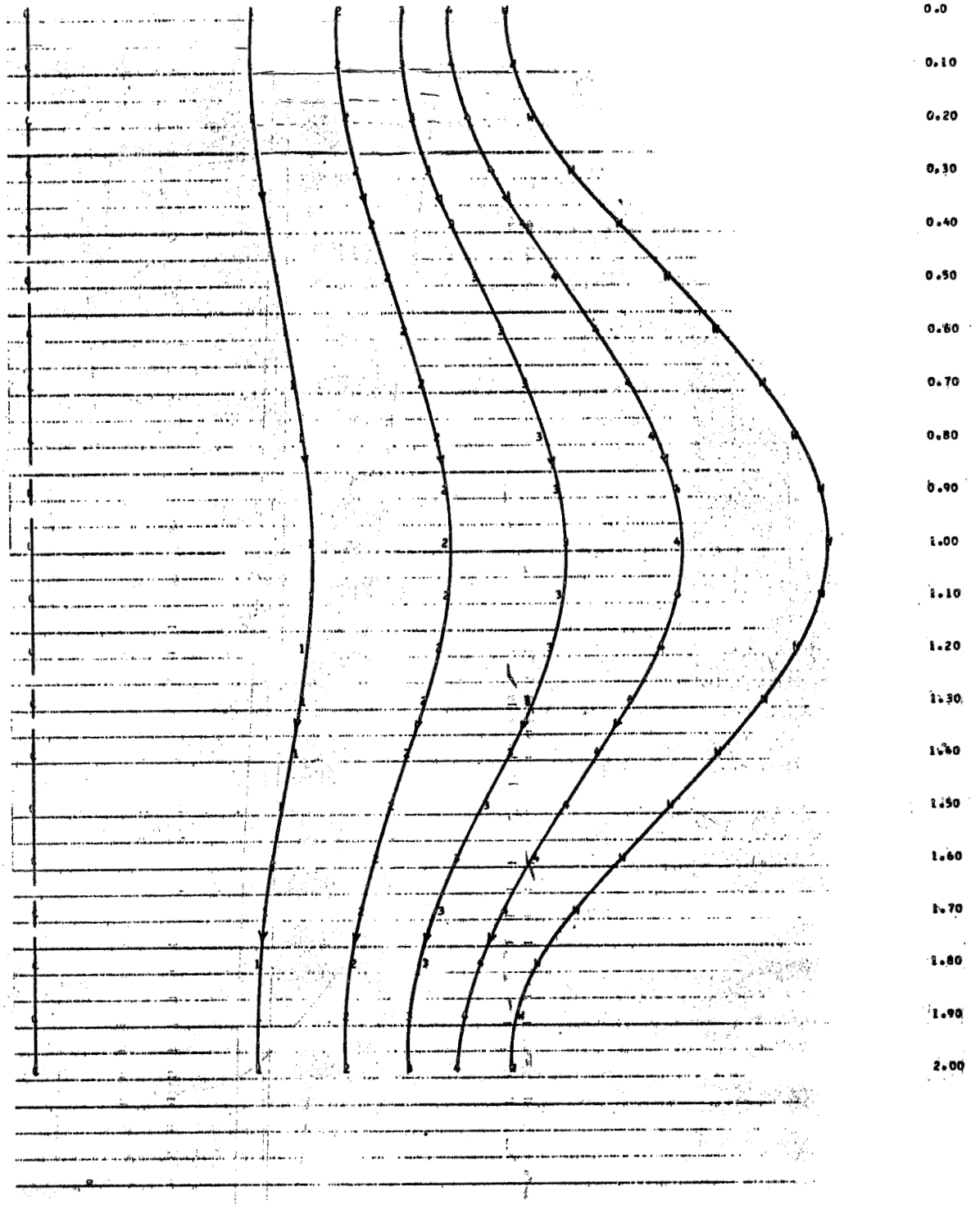


Figure 13. Streamlines for Time-Dependent Flow
RN=25, A=0.25, C=1.0, T=0.02

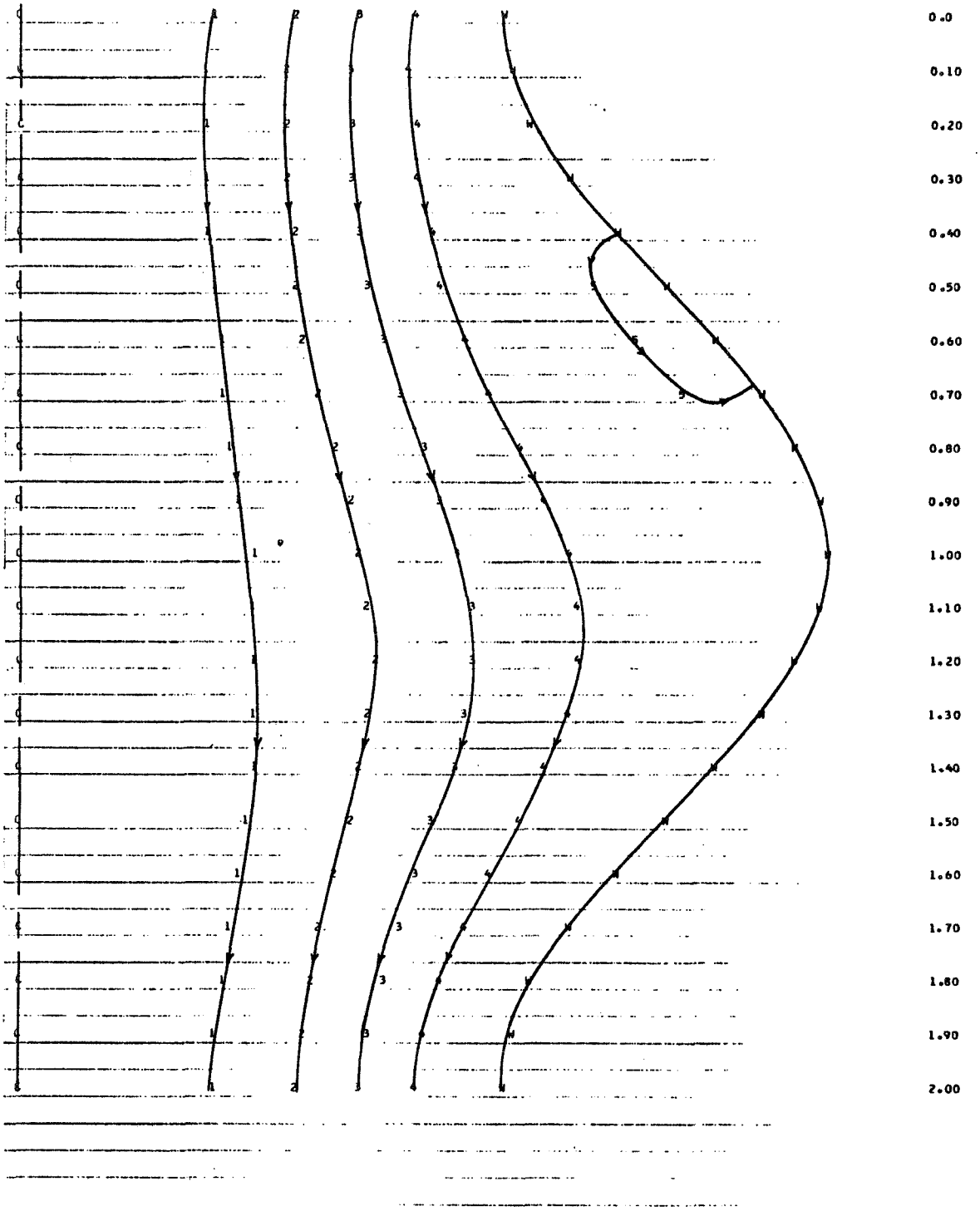


Figure 14. Streamlines for Time-Dependent Flow RN=25. A=0.25, C=1.0, T=0.50

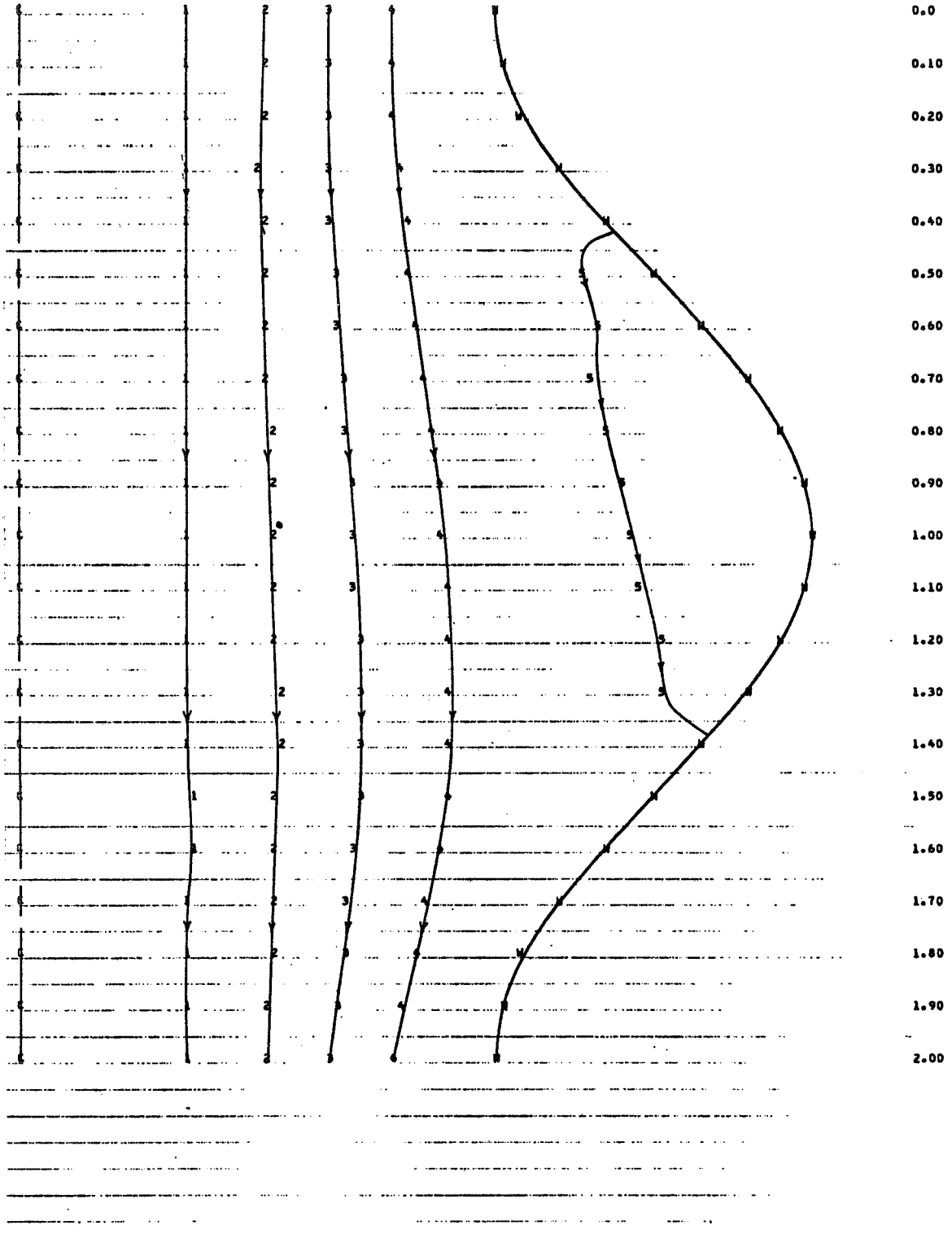


Figure 15. Streamlines for Time-Dependent Flow
RN=25, A=0.25, C=1.0, T=5.00

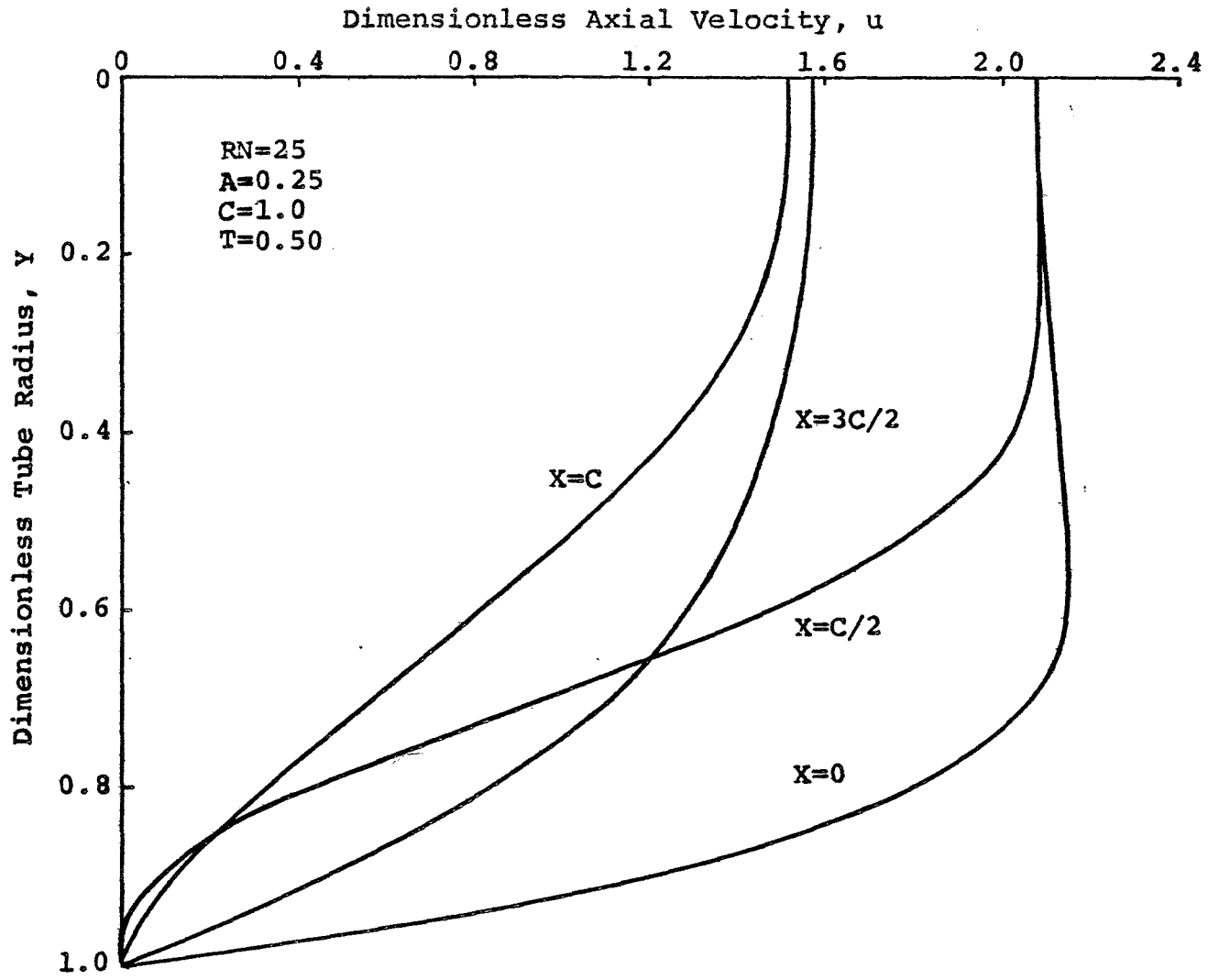


Figure 16. Velocity Profiles for Time-Dependent Flow without Bubbles

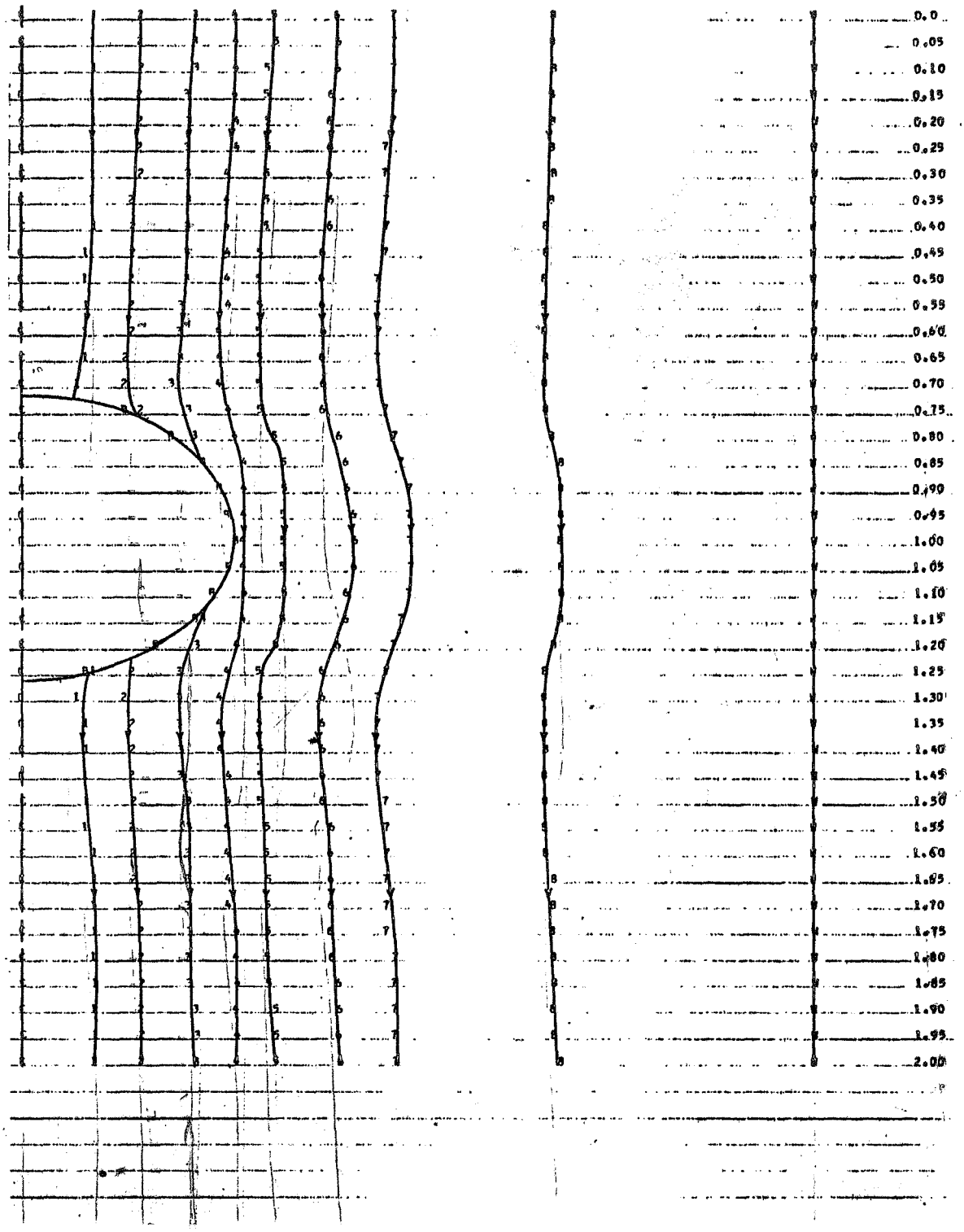


Figure 17. Streamlines for Flow with Bubbles using Pressure Boundary Condition RN=50, A=0.0, C=1.0, Bubble Radius=0.275 $Z_0$=1.0, T=0.0

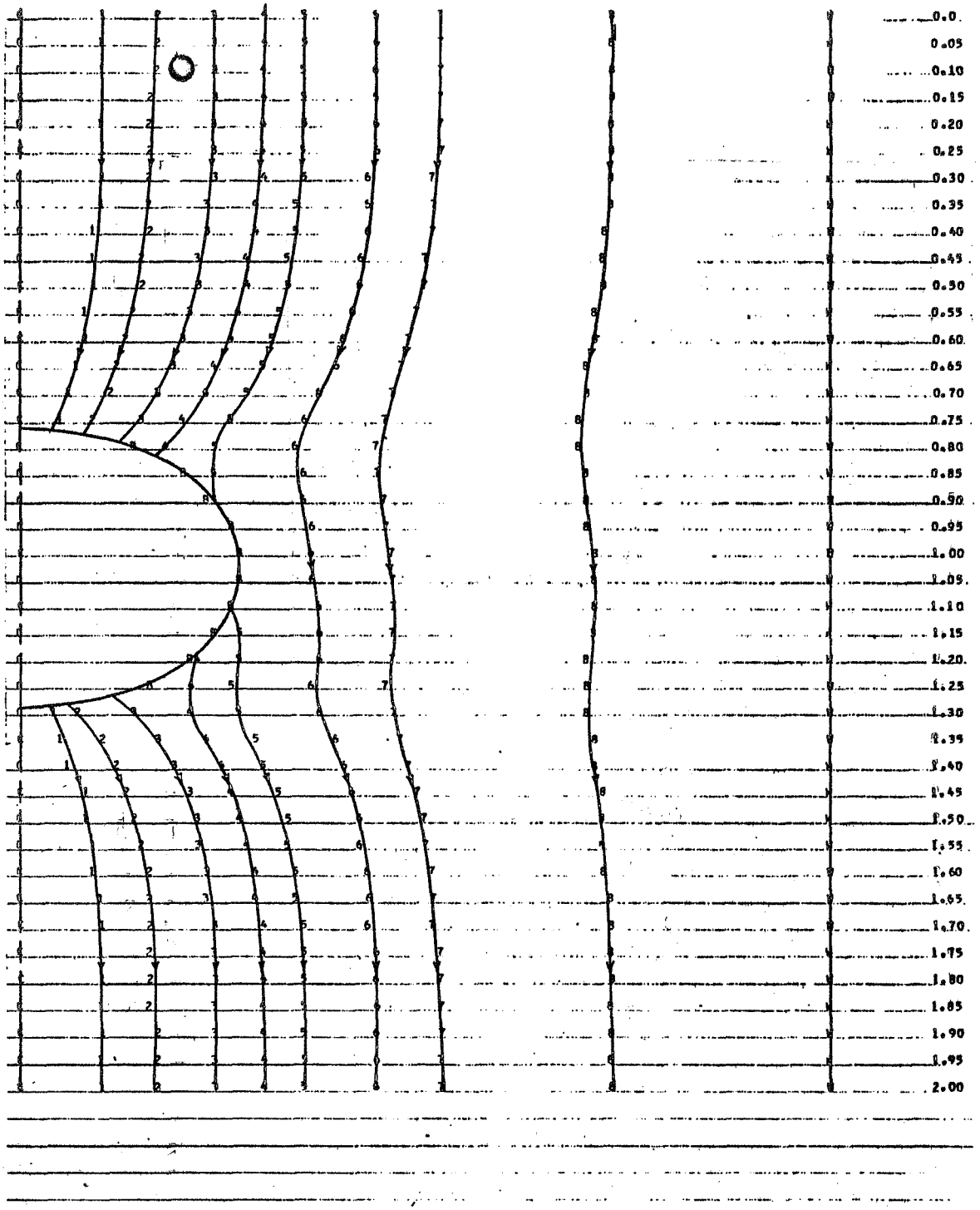


Figure 18. Streamlines for Flow with Bubbles using Pressure Boundary Condition RN=50, A=0.0, C=1.0, Bubble Radius=0.275 $Z_0$=1.025, T=0.01

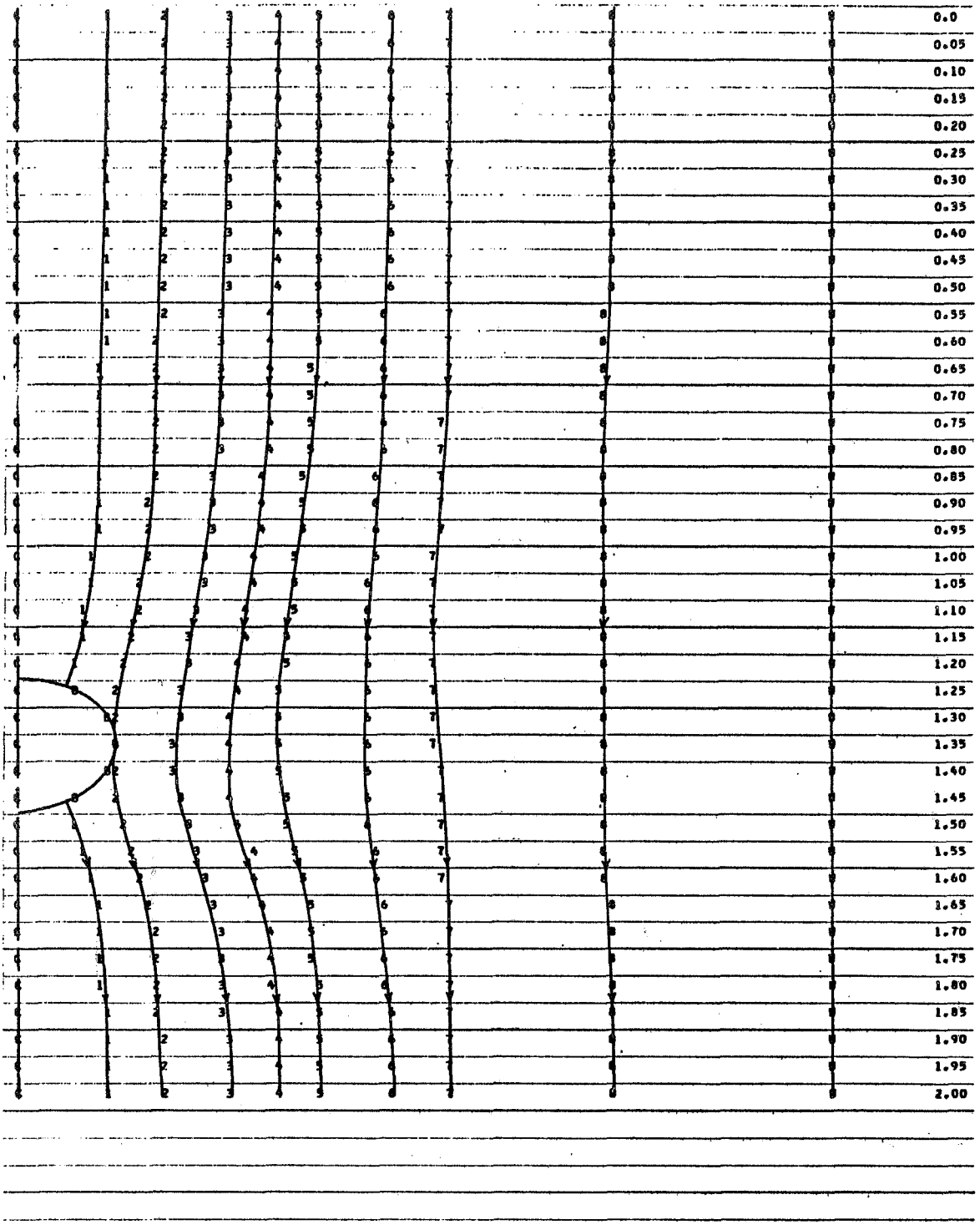


Figure 19. Streamlines for Flow with Bubbles using Velocity Boundary Condition RN=10, A=0.0, C=1.0, Bubble Radius=0.1375 $Z_0$=1.35, $V_T$=3.15, T=0.124

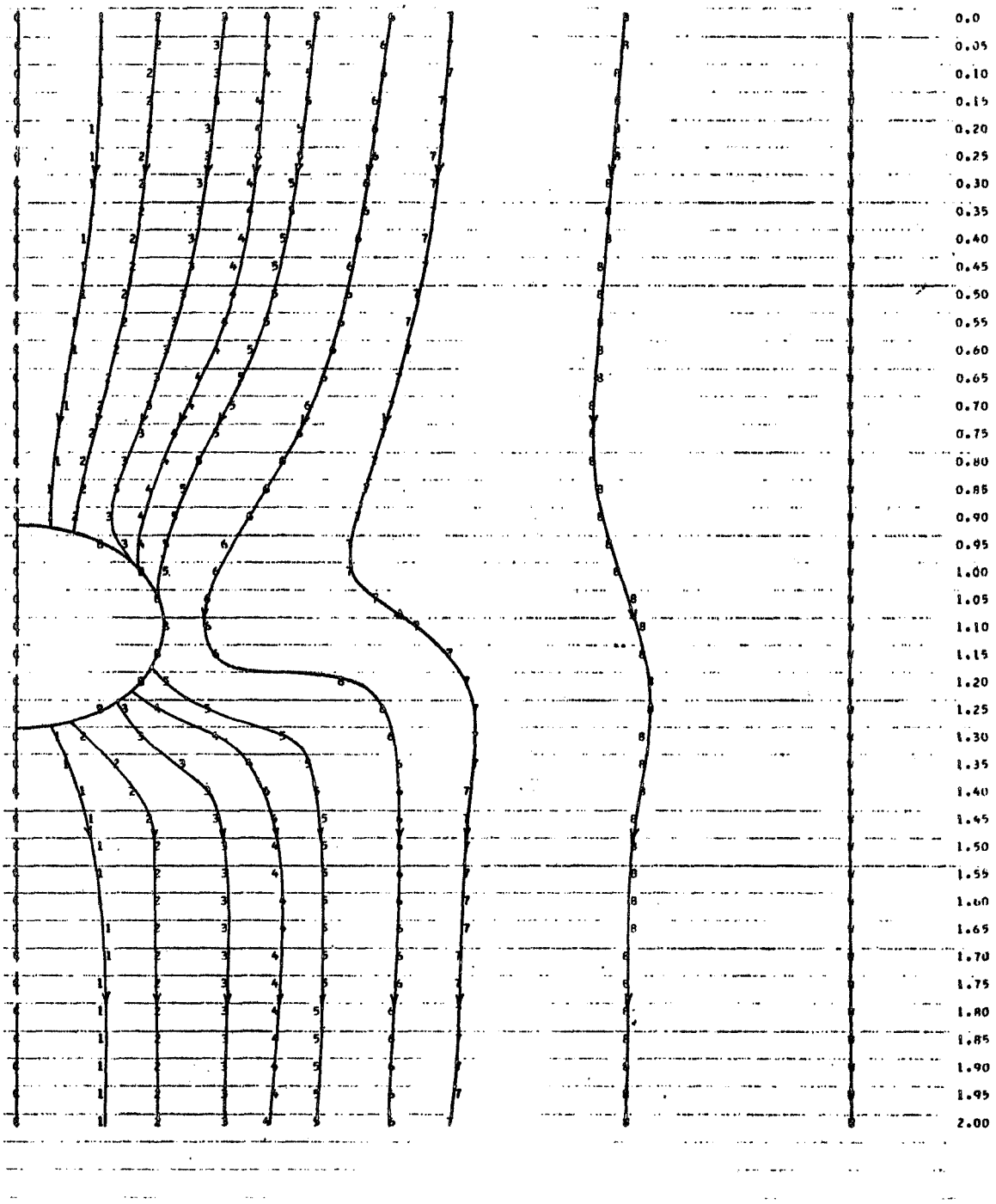


Figure 20. Streamlines for Flow with Bubbles using Velocity Boundary Condition RN=10, A=0.0, C=1.0, Bubble Radius=0.1875 $Z_0$=1.10, $V_T$=7.0, T=0.168

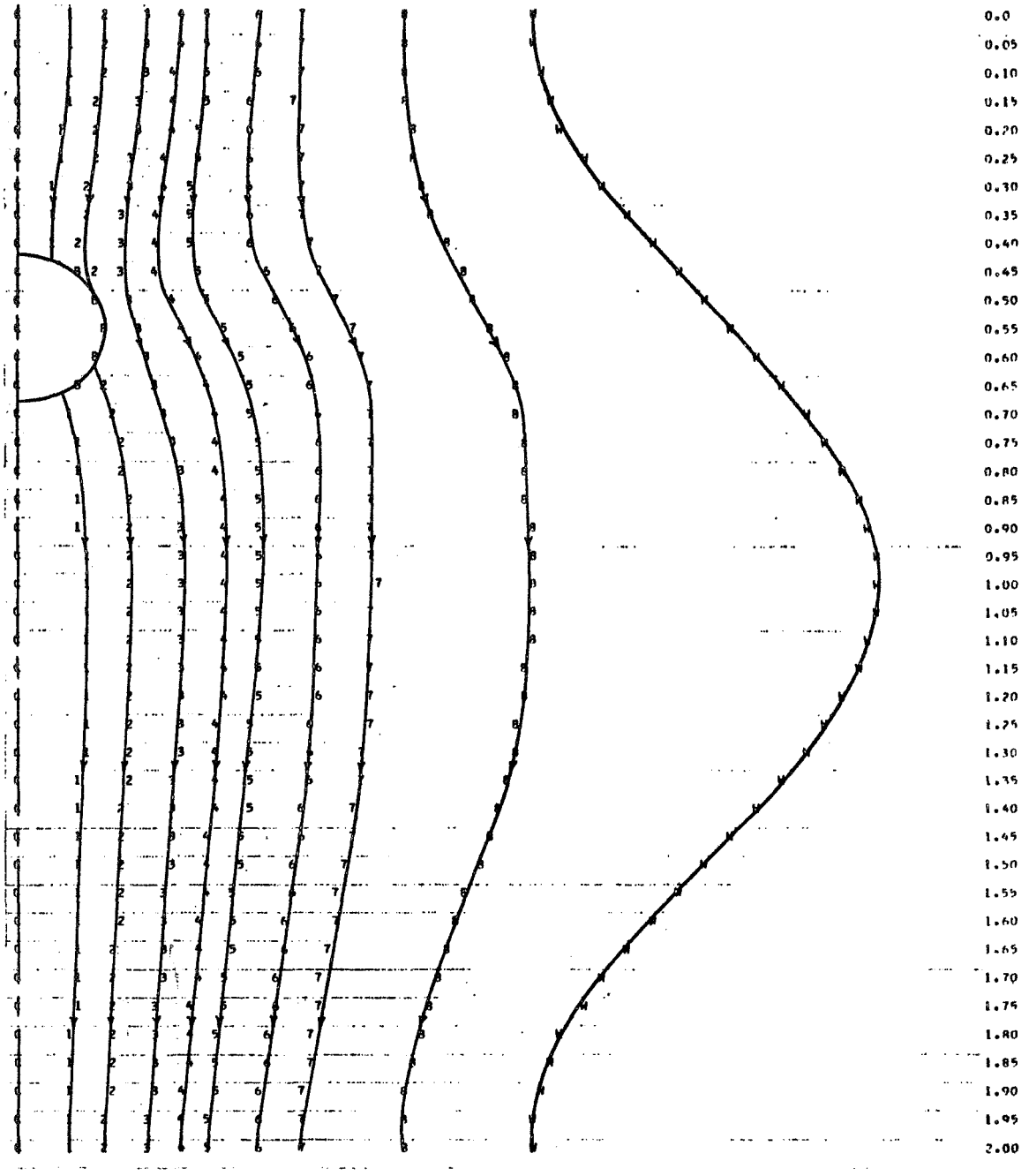


Figure 21. Streamlines for Flow with Bubbles using Velocity Boundary Condition RN=1.0, A=0.25, C=1.0, Bubble Radius=0.1375 $Z_0$=0.55, $V_T$=4.0, T=0.058

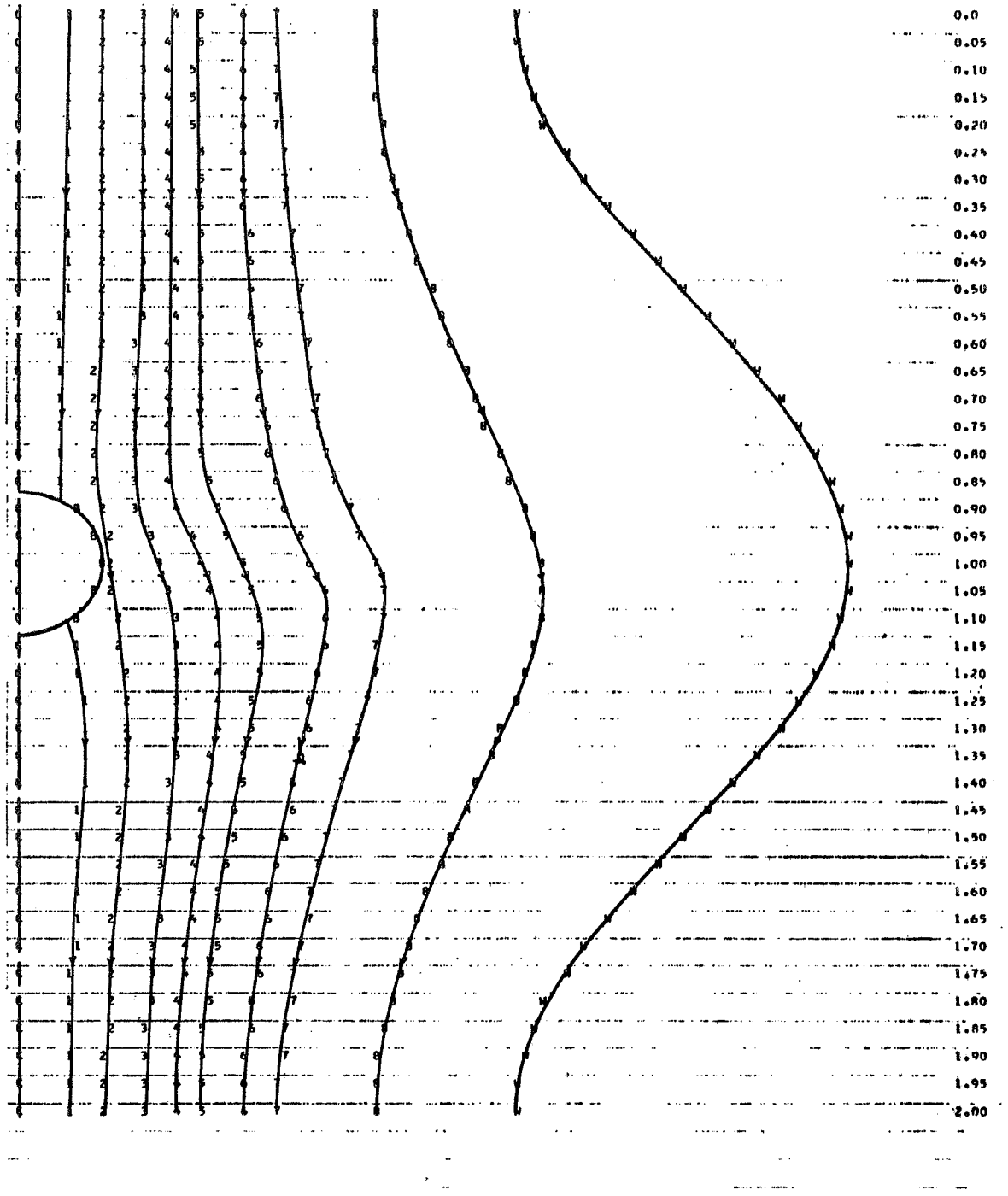


Figure 22. Streamlines for Flow with Bubbles using Velocity Boundary Condition RN=1.0, A=0.25, C=1.0, Bubble Radius=0.1375 $Z_0$=1.00, $V_T$=2.8, T=0.188

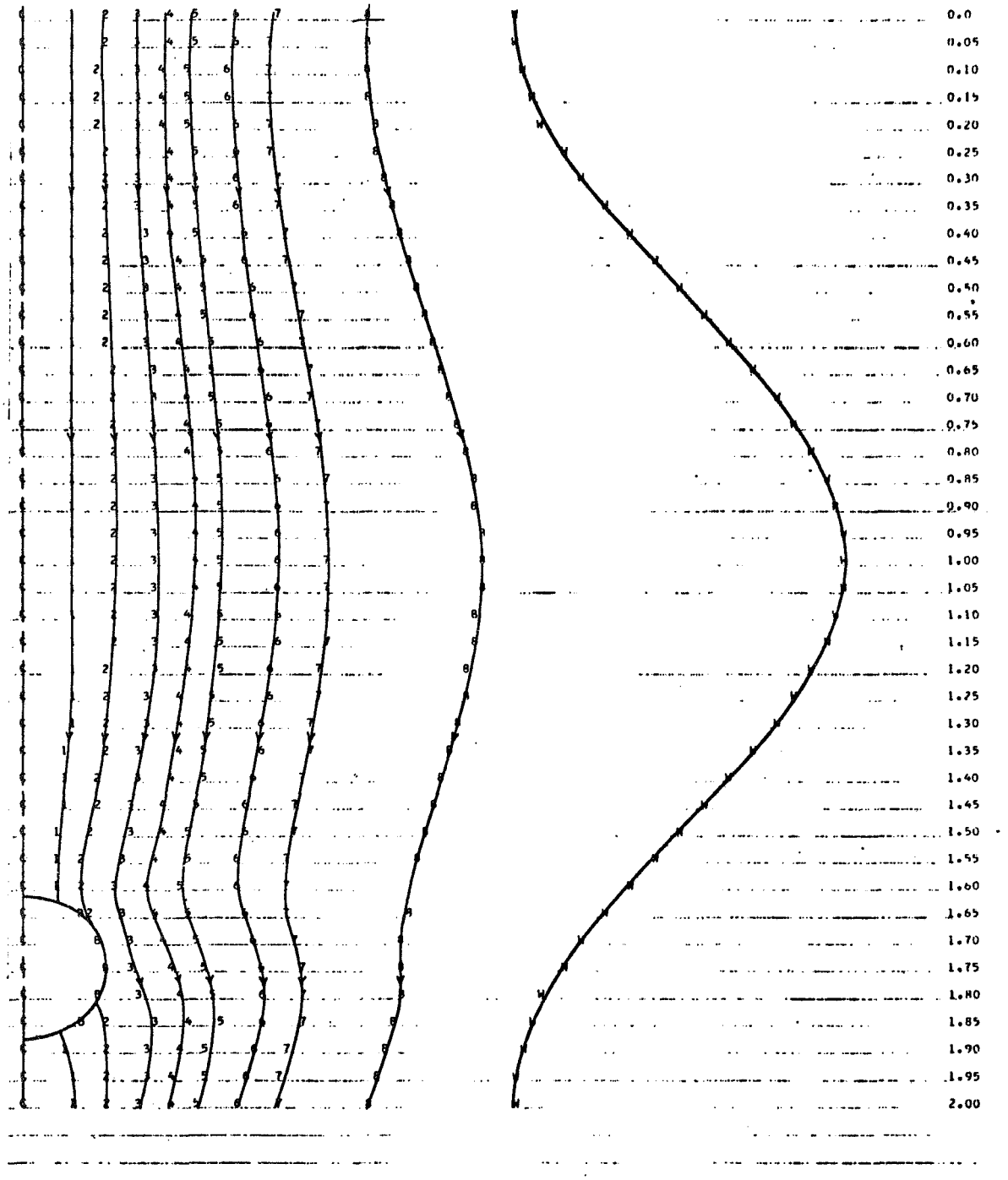


Figure 23. Streamlines for Flow with Bubbles using Velocity Boundary Condition RN=1.0, A=0.25, C=1.0, Bubble Radius=0.1375 $Z_0$=1.75, $V_T$=4.4, T=0.428

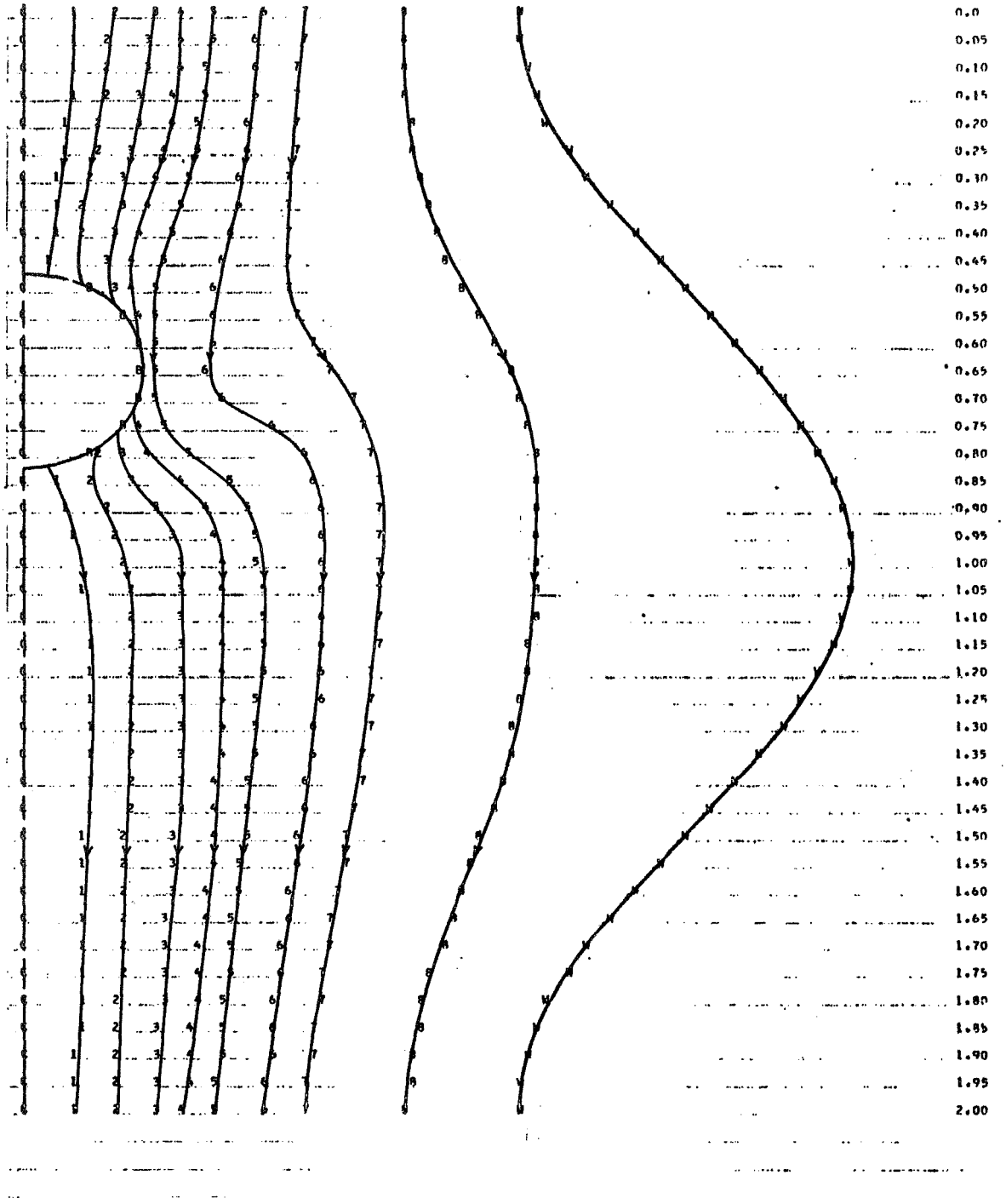


Figure 24. Streamlines for Flow with Bubbles using Velocity Boundary Condition RN=10, A=0.25, C=1.0, Bubble Radius=0.1875 $Z_0$=0.65, $V_T$=5.5, T=0.068

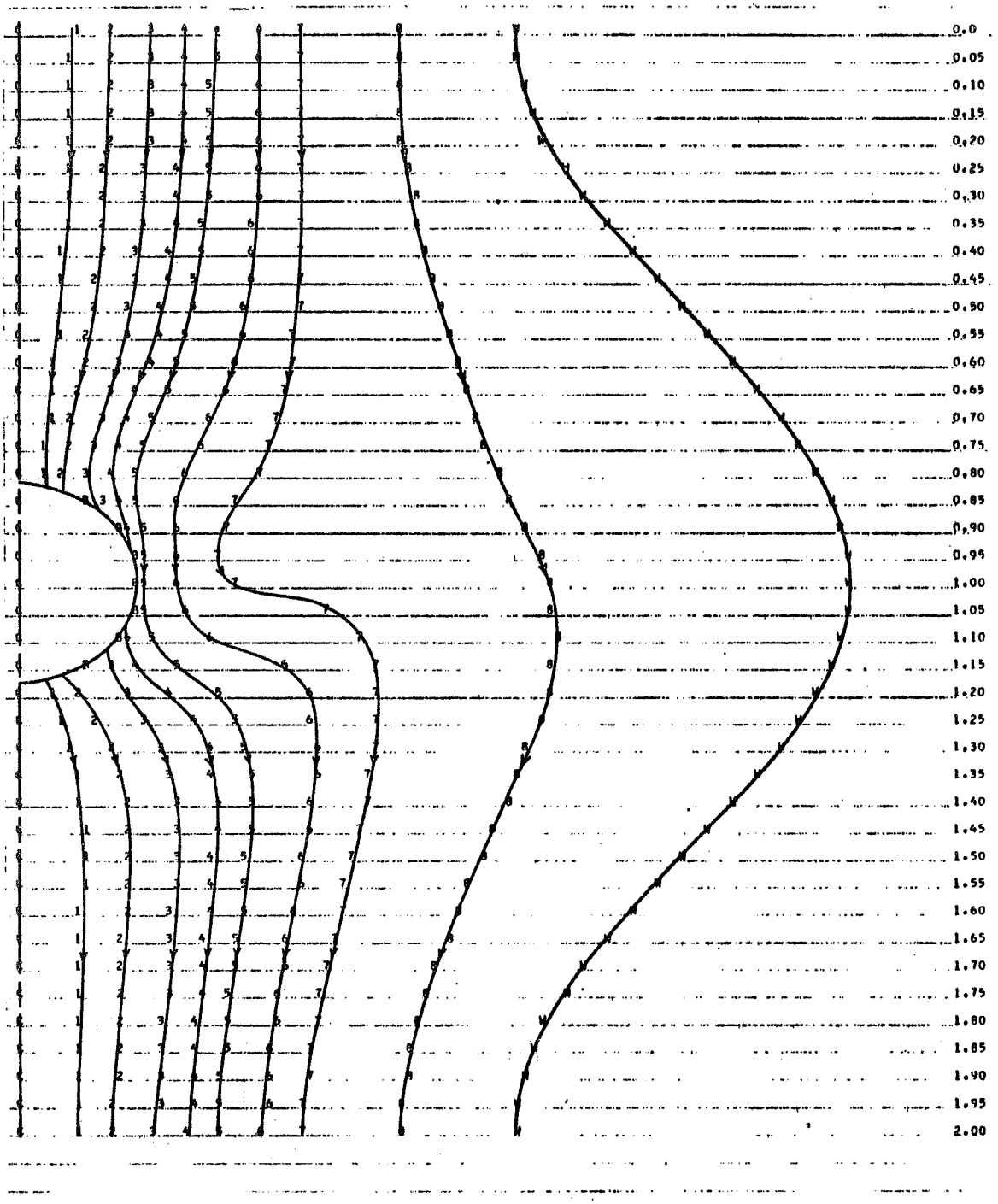


Figure 25. Streamlines for Flow with Bubbles using Velocity Boundary Condition RN=10, A=0.25, C=1.0, Bubble Radius=0.1875 $Z_0$=1.00, $V_T$=6.1, T=0.128

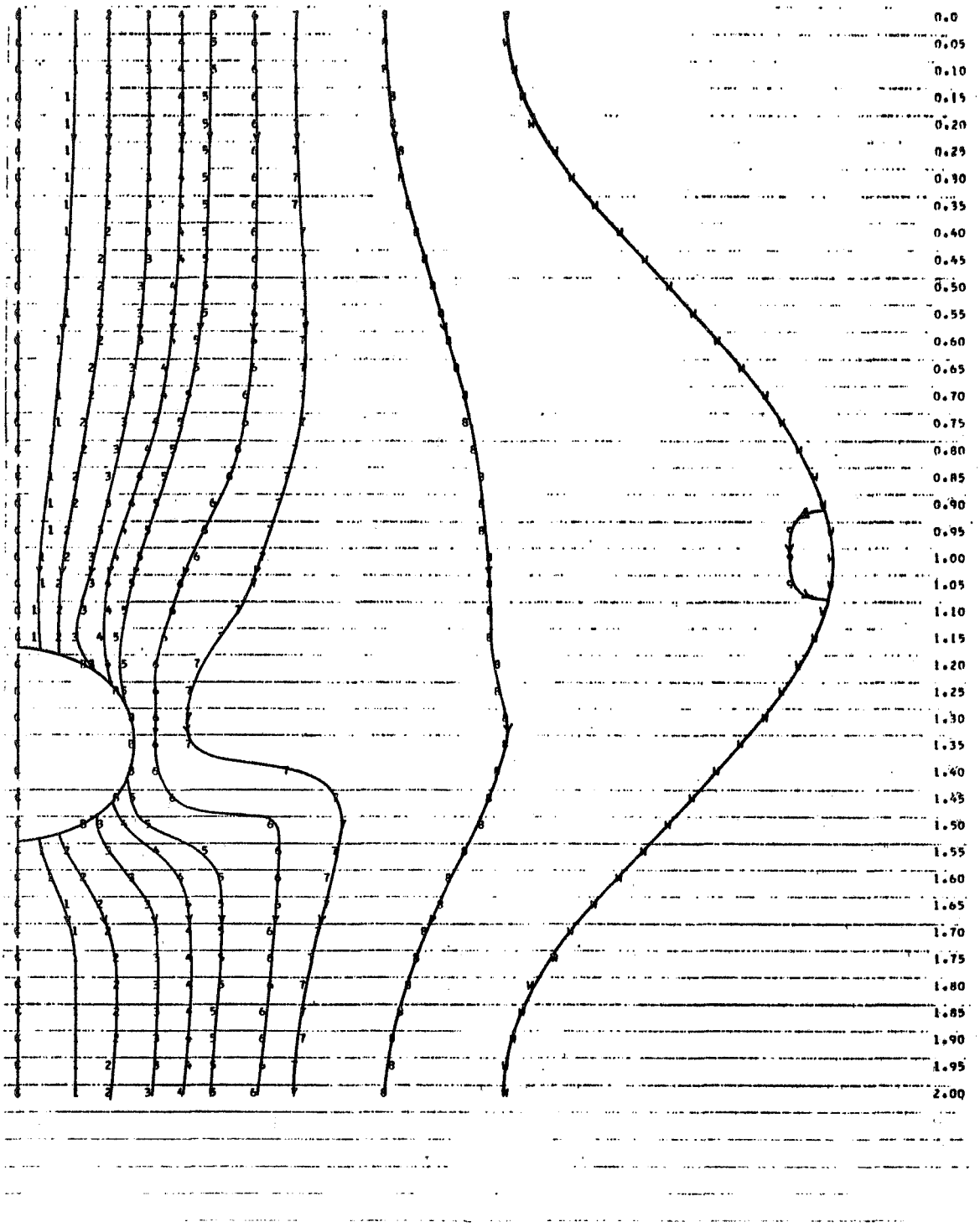


Figure 26. Streamlines for Flow with Bubbles using Velocity Boundary Condition RN=10, A=0.25, C=1.0, Bubble Radius=0.1875 $Z_0$=1.35, $V_T$=7.7, T=0.178

# VI CONCLUSIONS AND RECOMMENDATIONS

The problem of the flow of a viscous liquid with gas bubbles in an infinitely long, wavy wall tube has been formulated. Numerical solutions were determined for the steady state flow of the liquid in the absence of gas bubbles and for time-dependent flow both with and without gas bubbles.

The coordinate transformation used simplified the geometry and made the application of boundary conditions much easier. Because of a singularity in the transformed coordinate system at each end of a bubble, a specialized technique for repositioning a bubble during its motion was used. However, overall the transformation was found to reduce the labor in obtaining numerical solutions. This general type of transformation should be useful for numerical solutions to other types of problems with boundaries which do not coincide to standard coordinate systems.

The steady state solutions showed the presence of ring vortices standing in the divergent sections of the tube for sufficiently large Reynolds numbers. Also, an increase in waviness of the tube resulted in a large increase in pressure loss. The time-dependent solutions in the absence of gas bubbles showed the development of the

viscous flow pattern with time and the production and growth of vortices in the divergent sections. These solutions approached a steady state for large values of time and were in qualitative agreement with the steady state solutions obtained. For a straight wall tube the numerical solutions were in good agreement with Poiseuille flow in a pipe.

The time-dependent solutions for flow with gas bubbles using the velocity boundary condition showed that the velocity of relatively small spherical bubbles was from two to eight times the average velocity of the liquid. Even for very low Reynolds numbers, large velocities of bubbles relative to the liquid were found with corresponding large disturbances in the liquid flow pattern.

Although the problem of the motion of arbitrarily shaped gas bubbles was formulated, numerical difficulties made it possible to obtain solutions for spherical bubbles only. The limited solutions using the pressure boundary condition should not be considered conclusive since the calculations diverged after a few time steps.

To make a general study of the motion of gas bubbles moving in a viscous liquid which flows in a tube, with either changing or constant cross section, the bubble shape should be allowed to vary according to the liquid flow. However, unless some means can be found to express the bubble shape in terms of analytical expressions, the

inherent error in numerically calculating the bubble curvature will be a major problem. A possible technique would be to assume the shape as a sum of a series of ellipses with undetermined parameters. With logical criteria for determining these parameters, this could be combined with a finite difference solution for the liquid flow, which is well suited to solving the equations of motion for the liquid.

Since a coordinate system which does not coincide to the bubble boundary causes the application of the boundary conditions to be very tedious, some type of transformation should be used. If the bubble shape were constrained to be constant, then perhaps a coordinate transformation could be found which left the bubble shape unchanged but caused the wall to coincide to a coordinate line. This would avoid the difficulty encountered in this work with the discontinuous derivatives at the ends of the bubble. However, the type of transformation used in this study can be used with a bubble of changing shape.

For arbitrary bubble shapes, pressure appears explicitly in the boundary conditions. Therefore, it would be advantageous to have the equations for the liquid flow written with pressure as a fundamental variable, rather than an auxiliary variable. Also, this would allow the boundary conditions at the ends of a finite tube to be specified in terms of pressure.

The use of a larger and faster computer would allow the use of a smaller grid size in the solutions for the motion of bubbles using the velocity boundary condition. This could improve the accuracy in determining the translational velocity of the bubbles and allow the calculations to converge for more disturbed flow patterns. Also, the motion of a bubble could be followed through more than one wavelength of the tube. The calculation of a drag coefficient for a bubble would allow more meaningful comparisons to be made with other results.

## APPENDIX

In order to determine the stream function at a particular point on the bubble surface using the pressure boundary condition a finite difference form of equation (24) is used with forward differences for Y derivatives Let

$$SX = S_{1,j+1} - S_{1,j-1}$$

$$SYX = -3(S_{1,j+1} - S_{1,j-1}) + 4(S_{2,j+1} - S_{2,j-1}) - (S_{3,j+1} - S_{3,j-1}) \qquad \text{(A-1)}$$

$$BY = -3B_{1,j} + 4B_{2,j} - B_{3,j}$$

$$BYY = 2B_{1,j} - 5B_{2,j} + 4B_{3,j} - B_{4,j}$$

$$BXX = B_{1,j+1} + B_{1,j-1} - 2B_{1,j}.$$

Then from (24) we get

$$\left(\frac{1}{DiD^2} + G^2\right)BYY + \frac{H}{2}\left(\frac{1}{DiY \cdot DiD} + G_x + GG_y\right)BY$$

$$+ BXX + \tfrac{1}{2}\, G \cdot BYX + \frac{1}{2(DiB)^4}\left\{(SX)^2 + 2G \cdot SX \cdot \right. \qquad \text{(A-2)}$$

$$\left.(-3S_{1,j} + 4S_{2,j} - S_{3,j}) + G^2(-3S_{1,j} + 4S_{2,j} - S_{3,j})^2\right\} +$$

$$- \frac{2}{(DiD)(DiB)^3}\left\{\frac{(SX)(SYX)}{8H} + \frac{G_y \cdot SX}{4}(-3S_{1,j} + 4S_{2,j} - S_{3,j}) + \frac{SX \cdot G}{2H}(2S_{1,j} - 5S_{2,j} + 4S_{3,j} - S_{4,j}) + \frac{SYX \cdot G}{8H}(-3S_{1,j} + 4S_{2,j} - S_{3,j}) + \frac{GG_y}{4}(3S_{1,j} + 4S_{2,j} - S_{3,j})^2 + \frac{G^2}{2H}(-3S_{1,j} + 4S_{2,j} - S_{3,j})(2S_{1,j} - 5S_{2,j} + 4S_{3,j} - S_{4,j})\right\} + \frac{2}{(DiB)^2(DiD)^2}\left\{\frac{(SYX)^2}{16\,H^2} + \frac{G_y^2}{4}(-3S_{1,j} + 4S_{2,j} - S_{3,j})^2 + \frac{G^2}{H^2}(2S_{1,j} - 5S_{2,j} + 4S_{3,j} - S_{4,j})^2 + \frac{SYX \cdot G_y}{4H}(-3S_{1,j} + 4S_{2,j} - S_{3,j}) + \frac{G \cdot SYX}{2H^2}(2S_{1,j} - 5S_{2,j} + 4S_{3,j} - S_{4,j}) + \frac{GG_y}{H}(-3S_{1,j} + 4S_{2,j} - S_{3,j})(2S_{1,j} - 5S_{2,j} + 4S_{3,j} - S_{4,j})\right\} \quad \text{(A-2)}$$

$$+ \frac{2}{(DiB)^3(DiD)}\left\{\frac{1}{2H}(S_{1,j+1} + S_{1,j-1} - 2S_{1,j})(-3S_{1,j} + 4S_{2,j} - S_{3,j}) + \frac{G_x + GG_y}{4}(-3S_{1,j} + 4S_{2,j} - S_{3,j})^2 + \frac{G \cdot SYX}{4H}(-3S_{1,j} + 4S_{2,j} - S_{3,j}) + \frac{G_x + GG_y}{4}(-3S_{1,j} + 4S_{2,j} - S_{3,j})^2 + \frac{G \cdot SYX}{4H}(-3S_{1,j} + 4S_{2,j} - S_{3,j}) +$$

$$+\frac{G^2}{2H}(-3S_{1,j}+4S_{2,j}-S_{3,j})(2S_{1,j}-5S_{2,j}+4S_{3,j}$$

$$-S_{4,j})\Big\}-\frac{2}{(DiB\cdot DiD)^2}\Big\{\frac{1}{H^2}(S_{1,j+1}+S_{1,j-1}-2S_{1,j})\times$$

$$(2S_{1,j}-5S_{2,j}+4S_{3,j}-S_{4,j})+\frac{G_x+GG_y}{2H}(-3S_{1,j}$$

$$+4S_{2,j}-S_{3,j})(2S_{1,j}-5S_{2,j}+4S_{3,j}-S_{4,j}) \qquad \text{(A-2)}$$

$$+\frac{G\cdot SYX}{2H^2}(2S_{1,j}-5S_{2,j}+4S_{3,j}-S_{4,j})$$

$$+\frac{G^2}{H^2}(2S_{1,j}-5S_{2,j}+4S_{3,j}-S_{4,j})^2\Big\}=0.$$

Equation (A-2) is a quadratic algebraic equation for $S_{i,j}$. Therefore,

$$S_{1,j}=\frac{-B_1+\sqrt{B_1^2-4A_1C_1}}{2A_1} \qquad \text{(A-3)}$$

where

$$A_1=\frac{4.5\,G^2}{(DiB)^4}+\frac{4.5\,G_y^2}{(DiB)^2(DiD)^2}+\frac{6(G_x-GG_y)}{H(DiB)^2(DiD)^2}$$

$$+\frac{6}{H(DiB)^3(DiD)}+\frac{8}{H^2(DiD)^2(DiB)^2}+\frac{4.5\,G_x}{(DiB)^2(DiD)}$$

$$B_1=-\frac{3\,G\cdot SX}{(DiB)^4}-\frac{3\,G^2(4S_{2,j}-S_{3,j})}{(DiB)^4}+\frac{1.5\,G_y\cdot SX}{(DiD)(DiB)^3}+$$

$$- \frac{2\ G\cdot SX}{H(DiD)(DiB)^3} - \frac{0.75\ G\cdot SYX}{H(DiD)(DiB)^3} - \frac{3\ G_y^2}{(DiB)^2(DiD)^2} \times$$

$$(4S_{2,j} - S_{3,j}) - \frac{1.5\cdot SYX\cdot G_y}{H(DiB)^2(DiD)^2} + \frac{1}{H(DiB)^3(DiD)} \times$$

$$(-3S_{1,j+1} - 3S_{1,j-1} - 8S_{2,j} + 2S_{3,j})$$

$$- \frac{4}{H^2(DiB)^2(DiD)^2} (S_{1,j+1} + S_{1,j-1} + 5S_{2,j} -$$

$$4S_{3,j} + S_{4,j}) - \frac{3G_x}{(DiB)^3(DiD)} (4S_{2,j} - S_{3,j})$$

$$- \frac{(G_x - GG_y)}{H(DiB)^2(DiD)^2} (23S_{2,j} - 14S_{3,j} + 3S_{4,j}),$$

$$C_1 = (\frac{1}{DiD^2} + G^2)BYY + \tfrac{1}{2} H(\frac{1}{DiB\cdot DiD} + G_x + GG_y)BY + BXX$$

$$+ \tfrac{1}{2} G\ BYX + \frac{1}{2(DiB)^4} \left\{ (SX)^2 + 2G\cdot SX\ (4S_{2,j} - S_{3,j}) \right.$$

$$\left. + G^2(4S_{2,j} - S_{3,j})^2 \right\} - \frac{SX\cdot SYX}{4H(DiD)(DiB)^3}$$

$$- \frac{G_y\cdot SX}{2(DiD)(DiB)^3} (4S_{2,j} - S_{3,j}) - \frac{G\cdot SX}{H(DiB)^3(DiD)} \times$$

$$(-5S_{2,j} + 4S_{3,j} - S_{4,j}) + \frac{SYX\cdot G}{4H(DiD)(DiB)^3} (4S_{2,j}$$

$$- S_{3,j}) + \frac{(SYX)^2}{8H^2(DiB)^2(DiD)^2} + \frac{G_y^2}{2(DiB)^2(DiD)^2} \times$$

$$(4S_{2,j} - S_{3,j})^2 + \frac{SYX\cdot G_y}{H(DiB)^2(DiD)^2} (4S_{2,j} - S_{3,j}) +$$

$$- \frac{(G_x - GG_y)}{H(DiB)^2(DiD)^2} (4S_{2,j} - S_{2,j})(-5S_{2,j} + 4S_{3,j} - S_{4,j})$$

$$+ \frac{1}{H(DiB)^3(DiD)} (S_{1,j+1} + S_{1,j-1})(4S_{2,j} - S_{3,j})$$

$$- \frac{2}{H^2(DiB)^2(DiD)^2} (S_{1,j+1} + S_{1,j-1})(-5S_{2,j} + 4S_{3,j}$$

$$- S_{4,j}) + \frac{G_x}{2(DiB)^3(DiD)} (4S_{2,j} - S_{3,j})^2.$$

## REFERENCES CITED

### Books


1. Aris, Rutherford. Vectors, Tensors, and the Basic Equations of Fluid Mechanics. Englewood Cliffs, N. J.: Prentice-Hall, Inc., 1962.

2. Donnelly, Russell J., Herman, Robert, and Prigogine, Ilya (ed.). Non-Equilibrium Thermodynamics, Variational Techniques, and Stability. Chicago: University of Chicago, 1966.

3. Happel, John, and Bremmer, Howard. Low Reynolds Number Hydrodynamics. Englewood Cliffs, N. J.: Prentice-Hall, Inc., 1965.

4. Salvadori, Mario G. and Baron, Melvin L. Numerical Methods in Engineering. Englewood Cliffs, N. J.: Prentice-Hall, Inc., 1961.

5. Saul'yev, V. K. Integration of Equations of Parabolic Type by the Method of Nets. Trans. G. J. Tee. Ed. K. L. Steward. New York: MacMillan, 1964.

6. Schechter, R. S. The Variational Method in Engineering. New York: McGraw-Hill, 1967.

7. Schlichting, Hermann. Boundary Layer Theory. New York: McGraw-Hill, 1960.

8. Smith, G. D. Numerical Solutions of Partial Differential Equation. New York: Oxford Press, 1965.

Articles and Reports

9. Collins, R. "The Effect of a Containing Cylindrical Boundary on the Velocity of a Large Gas Bubble in a Liquid." Journal of Fluid Mechanics, Vol. 28, 1967, pp. 97-112.

10. Davenport, W. G., Bradshaw, A. V., and Richardson, F. D. "Behavior of Spherical Cap Bubbles in Liquid Metals." Journal of the Iron and Steel Institute, October, 1967, pp. 1034-1042.

11. Davies, R. M. and Taylor, Geoffrey. "The Mechanics of Large Bubbles Rising Through Extended Liquids and Through Liquids in Tubes." Proceedings of the Royal Society (London), Series A, February, 1950, pp. 375-390.

12. Douglas, J., Jr. "On the Numerical Integration of Quasi-Linear Parabolic Differential Equations." Pacific Journal of Mathematics, Vol. 6, 1956, pp. 35-42.

13. Evers, James L. An Investigation of Two Phase Flow through Porous Media. Ph.D. Dissertation. University of Alabama, 1969.

14. French, James V., Jr. An Investigation of Metering Two-Phase Flow Using Porous Cartridges. M.S. Thesis. University of Alabama, 1968.

15. Fromm, Jacob E. A Method for Computing Nonsteady, Incompressible, Viscous Fluid Flows. LA 2910. Los Alamos, N. M.: The University of California, 1963.

16. Fromm, J. E. and Harlow, F. H. "Numerical Solution of the Problem of Vortex Street Development." The Physics of Fluids, Vol. 6, 1963, pp. 975-982.

17. Haberman, W. L. and Morton, R. K. An Experimental Study of the Motion of Gas Bubbles in Various Liquids. Rep. No. 802. David Taylor Model Basin, 1952.

18. Harlow, Francis H. and Fromm, Jacob E. "Dynamics and Heat Transfer in the von Karman Wake of a Rectangular Cylinder." The Physics of Fluids, Vol. 7, 1964, pp. 1147-1156.

19. Harlow, F. H. and Welch, J. E. "Numerical Calculation of Time-Dependent Viscous Incompressible Flows of Fluid with Free Surface." The Physics of Fluids, Vol. 8, 1965, pp. 2182-2189.

20. Harlow, F. H. and Welch, J. E. "Numerical Study of Large-Amplitude Free-Surface Motions." The Physics of Fluids, Vol. 9, 1966, pp. 842-859.

21. Harper, J. F., Moore, D. W. and Pearson, J. R. A. "The Effect of the Variation of Surface Tension with Temperature of the Motion of Bubbles and Drops." Journal of Fluid Mechanics, Vol. 27, 1967, pp. 361-366.

22. Harper, J. F. and Moore, D. W. "The Motion of a Spherical Liquid Drop at High Reynolds Number." Journal of Fluid Mechanics, Vol. 32, 1968, pp. 367-391.

23. Hartunian, R. A. and Sears, W. R. "On the Instability of Small Gas Bubbles Moving Uniformly in Various Liquids." Journal of Fluid Mechanics, Vol. 3, 1957, pp. 27-47.

24. Jenson, V. G. "Viscous Flow Round a Sphere at Low Reynolds Numbers (<40)." Proceedings of the Royal Society (London), A249, 1959, pp. 346-366.

25. Kawaguti, M., "Numerical Solution of the Navier-Stokes Equations for the Flow Around a Circular Cylinder at Reynolds Number 40." Journal of the Physical Society of Japan, Vol. 8, 1953, p. 747.

26. Moore, D. W. "The Rise of a Gas Bubble in a Viscous Liquid." Journal of Fluid Mechanics, Vol. 6, 1959, pp. 113-130.

27. Moore, D. W. "The Boundary Layer on a Spherical Gas Bubble." Journal of Fluid Mechanics, Vol. 16, 1963, pp. 161-176.

28. Moore, D. W. "The Velocity of Rise of Distorted Gas Bubbles in a Liquid of Small Viscosity." Journal of Fluid Mechanics, Vol. 23, 1965, pp. 747-766.

29. Proudman, I. and Pearson, J. R. A., "Expansions at Small Reynolds Numbers for the Flow Past a Sphere and a Circular Cylinder." Journal of Fluid Mechanics, Vol. 2, 1957, p. 237.

30. Rhodes, John M. and Peebles, Fred N. "Local Rates of Mass Transfer from Spheres in Simple Cubic Packing and a Numerical Solution of the Navier-Stokes Equations for Viscous Flow Past a Single Sphere." Report EM 66-8-2. University of Tennessee

31. Saffman, P. G. "On the Rise of Small Air Bubbles in Water." Journal of Fluid Mechanics, Vol. 1, 1956, pp. 249-275.

32. Taylor, T. D. and Acrivos, Andreas, "On the Deformation and Drag of a Falling Viscous Drop at Low Reynolds Number." Journal of Fluid Mechanics, Vol. 18, 1964, pp. 466-476.

33. Thompson, Joe F. "Computer Experimentation with an Implicit Numerical Solution of the Navier-Stokes Equations for an Oscillating Body." AIAA Paper No. 69-185. New York, 1969.

34. Walters, J. K. and Davidson, J. F. "The Initial Motion of a Gas Bubble Formed in an Inviscid Liquid, Part 1. The Two-Dimensional Bubble." Journal of Fluid Mechanics, Vol. 12, 1962, pp. 408-416.

35. Walters, J. K. and Davidson, J. F. "The Initial Motion of a Gas Bubble formed in an Inviscid Liquid, Part 2. The Three-Dimensional Bubble and the Toroidal Bubble." Journal of Fluid Mechanics, Vol. 17, 1963, pp. 321-336.